Examining the Role and Regulation of Cell-Cell Adhesion in Aggressive Prostate Cancer

Alison G. Barber

Submitted in partial fulfillment of the
requirements for the degree of
Doctor of Philosophy
in the Graduate School of Arts and Sciences

COLUMBIA UNIVERSITY

2011

Abstract

Examining the Role and Regulation of Cell-Cell Adhesion in Aggressive Prostate Cancer

Alison G. Barber

Prostate cancer is the second leading cause of cancer death in American men, yet despite the prevalence of this disease, there is a distinct lack of prognostic biomarkers for estimating the likelihood of prostate cancer aggressiveness. The loss of cell-cell adhesion is frequently associated with the progression of prostate cancer to a metastatic state. While both adherens junctions and desmosomes are involved in establishing and maintaining this adhesion, previous studies of cell-cell adhesion in prostate cancer have focused solely on the role of adherens junctions, leaving the role of desmosomal adhesion unexplored. The goals of this thesis were to perform a functional analysis of the role and regulation of adherens junctions and desmosomes in aggressive prostate cancer, and to examine the efficacy of classical and desmosomal cadherins as prognostic biomarkers of aggressive prostate cancer.

I began this study by characterizing the expression profile of desmosomal cadherins in normal human prostate and metastatic prostate cancer cell lines. This study revealed that DSG2, DSC2, and DSG4 were consistently expressed

at a high level in the luminal cells of the prostate. Further, analysis of metastatic prostate cancer cell lines showed that the expression of DSG2 is present in most cell lines examined, while the expression of DSG4 is absent.

Following this characterization, I examined the role of E-cadherin and DSG2 in metastatic prostate cancer cell lines. Interestingly, the loss of E-cadherin resulted in the inhibition of extensive primary and metastatic tumor formation, suggesting that E-cadherin may have a role in promoting the progression of prostate cancer in addition to its well-established role as a tumor suppressor. Additionally, the loss of E-cadherin based adherens junctions was not associated with the reciprocal loss of DSG2 based desmosomes, challenging the common belief that the formation of adherens junctions is a prerequisite for the formation of desmosomes.

I then examined the regulatory effects of PI3K/AKT signaling on E-cadherin and DSG2 expression in metastatic prostate cancer cell lines. The expression of activated AKT was found to be associated with the inhibition of *E-cadherin* expression, while the expression of DSG2 was relatively unperturbed in the presence of activated AKT expression. These results suggest that aberrantly activated PI3K/AKT signaling in prostate cancer may result in the loss of E-cadherin expression, and that the loss of E-cadherin and DSG2 expression in prostate cancer may be regulated by separate pathways.

Finally, I examined the expression of E-cadherin and DSG2 in a large cohort of patients with prostate cancer to determine whether these cadherins were associated with prostate cancer aggressiveness. Interestingly, the loss of

these cadherins was found to be significantly associated with biochemical recurrence demonstrating their potential utility as prognostic markers of aggressive prostate cancer.

Table of Contents

Chapter 1: General Introduction…… 1

1. Anchoring Junctions: Adherens Junctions and Desmosomes…… 2

2. Assembly of Adherens Junctions…….. 5

3. Assembly of Desmosomes……. 6

4. Regulation of Anchoring Junction Assembly……... 8

5. Adherens Junctions and Desmosomes in Development……. 10

6. EMT and Development…….. 12

7. The PI3K/AKT Signaling Pathway……... 14

8. Prostate Cancer…….. 15

9. E-cadherin and Cancer…….. 19

10. Desmosomes in Disease and Cancer……... 22

11. EMT and Cancer……... 25

12. The PI3K/AKT Signaling Pathway and Cancer…… 28

13. The PI3K/AKT Signaling Pathway in EMT and Cancer…….. 31

14. Work Described in this Thesis……. 32

Chapter 2: Expression of Desmosomal Cadherins in Normal Human Prostate and Human Prostate Cancer Cell Lines……. 36

1. Overview……... 37

2. The Expression of Desmosomal Cadherins in Normal Human Prostate……... 42

3. The Expression of DSG2 and DSG4 in Human Prostate Cancer Cell Lines……. 47

4. Discussion……... 51

5. Materials and Methods…….. 53

Chapter 3: Functional Analysis of Cell-Cell Adhesion in Prostate Cancer……. 58

1. Overview…….. 59

2. *In Vitro* Analysis of Desmosomes and the Loss of Adherens Junctions in Prostate Cancer…….. 61

3. *In Vivo* Tumorigenesis Analysis of Cell-Cell Adhesion in Prostate Cancer……... 68

4. *In Vivo* Analysis of Cell-Cell Adhesion in Extravasation and Metastatic Tumor Colony Formation…… 72

5. Discussion……. 76

6. Materials and Methods…… 81

Chapter 4: Functional Analysis of the Regulation of Cell-Cell Adhesion by PI3K/AKT Mediated Signaling in Prostate Cancer…… 87

1. Overview…… 88

2. *In Vitro* Analysis of Anchoring Junctions and Activated AKT Signaling……. 91

3. *In Vitro* Analysis of EMT and Adherens Junctions…… 100

4. *In Vivo* Tumorigenesis Analysis of Cell-Cell Adhesion in Prostate Cancer…….. 105

5. *In Vivo* Analysis of Cell-Cell Adhesion in Extravasation and Metastatic Tumor Colony Formation……... 115

6. Discussion…… 120

7. Materials and Methods…….. 127

Chapter V: Examining the Role of E-cadherin, DSG2, pAKT, and Snail in Aggressive Prostate Cancer……. 132

1. Overview……. 133

2. Immunofluorescence analysis of E-cadherin, DSG2, pAKT, and Snail on Primary Prostate Cancer Tissue Microarrays and Descriptive Statistics of the Cohort .....……. 136

3. Descriptive Statistics and Expression of E-cadherin, DSG2, pAKT, and Snail in Primary Prostate Cancer……. 140

4. Discussion……... 156

5. Materials and Methods…….. 158

Chapter VI: General Discussion…… 160

References…….. 178

List of Abbreviations:

In general, human genes and RNA are written in italicized capital letters, while human proteins are written in non-italicized capital letters (e.g. *DSG2* refers to the human gene or RNA while DSG2 refers to the human protein). Mouse genes and RNA are italicized with only the first letter capitalized, while murine proteins are non-italicized with only the first letter capitalized (e.g. *Dsg2* refers to the murine gene or RNA while Dsg2 refers to the murine protein).

AKT — v-akt murine thymoma viral oncogene homolog 1
Arp2/3 — Actin related protein 2/3 complex
ARVC — Arrhythmogenic right ventricular cardiomyopathy
BPH-1 — Benign prostatic hyperplasia 1
BSA — Bovine Serum Albumin
Cdc42 — Cell division cycle 42 (GTP binding protein, 25kDa)
ChIP — Chromatin immunoprecipitation
CK8/18 — Cytokeratin 8/18
C-RAF — v-raf-1 murine leukemia viral oncogene homolog 1
DAPI — 4',6-diamidino-2-phenylindole
DP — Desmoplakin
DSC — Desmocollin
DSG — Desmoglein
EcadKD — E-cadherin knock down
EGF — Epidermal growth factor
EGFR — Epidermal growth factor receptor
EMT — Epithelial-mesenchymal transition
ER — Estrogen Receptor
ErbB2 — v-erb-b2 erythroblastic leukemia viral oncogene homolog 2, neuro/glioblastoma derived oncogene homolog (avian); also known as HER2
FBS — Fetal Bovine Serum
FFPE — Formalin-fixed paraffin-embedded
FGF — Fibroblast growth factor
FGFR1 — Fibroblast growth factor receptor 1
Foxo3a — Forkhead Box O3a
GDP — Guanosine Diphosphate
GEF — Guanine Nucleotide Exchange Factor
GFP — Green Fluorescent Protein
Gli — GLI family zinc finger
GRB2 — Growth factor receptor-bound protein 2
GSK3β — Glycogen synthase kinase 3 beta
GTP — Guanosine 5' Triphosphate
HA-tag — Hemagglutinin tag
H&E — Hematoxylin and eoisin

HER2 — v-erb-b2 erythroblastic leukemia viral oncogene homolog 2, neuro/glioblastoma derived oncogene homolog (avian); also known as ERBB2
HF — Hair follicle
HGF/SF — Hepatocyte growth factor/scatter factor
HGMA2 — High mobility group A2
Hh — Hedgehog
IGF2 — Insulin-like growth factor 2
IGF-IR — Insulin-like Growth Factor I Receptor
INPP4B — Inositol polyphosphate-4-phosphatase, type II, 105kDa
IQGAP1 — IQ motif containing GTPase activating protein 1
IRS — Inner root sheath
K14 — Keratin 14
LOH — Loss of Heterozygosity
MAH — Myristoylated AKT HA-tagged
MAPK — Mitogen activated protein kinase
MDCK — Madin Darby Canine Kidney
MET — Mesenchymal-epithelial transition
MPAKT — Murine prostate restricted Akt kinase activaty transgenic
mTOR — Mammalian target of rapamycin
myrAkt — Myristoylated AKT
NICD — Notch intracellular domain
N-WASP— Neuronal Wiskott Aldrich sydrome protein
ORS — Outer root sheath
pAKT — Phosphorylated AKT
PBS — Phosphate Buffered Saline
PCR — Polymerase chain reaction
PDGF — Platelet-derived growth factor
PDK1 — Phosphatidylinositol-dependent kinase 1
PIK3CA — Phosphatidylinositol 3-kinase, catalytic, alpha polypeptide
PG — Plakoglobin
PH domain — Pleckstrin homology domain
PHLLP — PH domain and leucine rich repeat protein phosphatase
PIN — Prostatic Intraepithelial Neoplasia
PI3K — Phosphatidylinositol 3-Kinase
PIP — Phosphatidylinositol (3) phosphate; also known as PI(3)P
PIP2 — Phosphatidylinositol (3, 4) biphosphate; also known as $PI(3,4)P_2$ **or** Phosphatidylinositol (4, 5) biphosphate; also known as $PI(4,5)P_2$
PIP3 — Phosphatidylinositol (3, 4, 5) triphosphate; also known as $PI(3, 4, 5)P_3$
PKP — Plakophilin
PPKS — Striate palmoplantar keratoderma
PR — Progesterone Receptor
PSA — Prostate Specific Antigen
PTEN — Phosphatase and tensin homolog
qRT-PCR — quantitative real-time polymerase chain reaction

Rac1 — Ras-related C3 botulinum toxin substrate 1 (rho family, small GTP binding protein Rac1)
Ras — Rat sarcoma viral oncogene homolog
Rho — Rhodopsin
RNAi — RNA interference
RTK — Receptor Tyrosine Kinase
RT-PCR — Reverse Transcription Polymerase Chain Reaction
SDS — Sodium dodecyl sulfate
SDS-PAGE— Sodium dodecyl sulfate polyacrylamide gel electrophoresis
SH2 — Src Homology 2
shRNAmir — microRNA adapted short hairpin RNA
siRNA — small interfering RNA
SOS — Son of sevenless
Src — v-src sarcoma (Schmidt-Ruppin A-2) viral oncogene homolog (avian)
TCF — T cell factor
TGFβ — Transforming growth factor β
Tiam1 — T-cell lymphoma invasion and metastasis 1
TMA —Tissue Microarray
TNM —Tumor, Nodes, Metastases
VEGF — Vascular endothelial growth factor
VEGFR-3 — Vascular endothelial growth factor receptor 3
Wnt — Wingless-related MMTV integration site

Acknowledgements

I would like to thank all those who contributed to my graduate training as well as the subject matter addressed in this thesis. While most graduate students generally have a single mentor for the duration of their thesis work, I had the distinct pleasure of being mentored by two truly remarkable scientists. I would like to thank my co-mentor Dr. Carlos Cordon-Cardo for welcoming me into his lab and for providing me with the time, scientific insight, and resources to complete my thesis work. I am grateful for the opportunity to have been mentored by such a positive, enthusiastic, and generous individual. I would also like to thank my co-mentor Dr. Angela Christiano for tirelessly guiding me in the early years of my thesis work. I am grateful for the dedication, wisdom, and patience she pours into developing well-rounded graduate students.

I would also like to thank members of the Cordon-Cardo and Christiano labs past and present. In the Cordon-Cardo lab, I am especially thankful for the privilege of working with Dr. Mireia Castillo-Martin, an amazing pathologist and outstanding human being. Having the opportunity to learn about cancer pathology from such a talented individual was invaluable to my development as a researcher. I am also thankful for the technical assistance and friendship of Dennis Bonal and Joslyn Mills. I thank Elizabeth Charytonowicz, Nataliya Gladoun, Dr. Josep Domenech, Todd Hricik, and Dr. Orit Schmidt-Karni for the scientific discussion, assistance, and camaraderie. I thank Angela Yuanyuan Jia, Sara Siddiqi, and Dr. Filemon Dela Cruz — the original learning corner crew —

for being sounding platforms for the constant stream of ideas that tend to run through my mind, and for the fun times that allowed me to maintain sanity. In the Christiano lab I thank Dr. Ana Kljuic, Dr. Hisham Bazzi, and Dr. Yoshiyuki Ishii for their assistance with the early DSG4 project as well as their generous spirits. I thank the much-adored Ming Zhang for always keeping me well stocked and well fed. I thank Dr. Hyunmi Kim, Dr. Katherine Fantauzzo, and Lynn Petukhova for the scientific discussions and assistance, but perhaps most especially for the discussions and assistance which fell well outside of the scientific sphere.

I thank the members of my thesis committee Dr. Michael Shen, Dr. Dorothy Warburton, and Dr. Ramon Parsons. I am grateful to Dr. Shen for acting as my second reader and providing me with his objective insight, for his participation on my TRAC committee, as well as for the many discussions that were instrumental in shaping my final thesis project. I also thank Dr. Warburton for assiduously attending every committee meeting I have ever had as a graduate student, and for inviting me into her lab to learn cytogenetic techniques. I thank my qualifier examiners Dr. Frank Costantini and Dr. Eric Shon for their time and participation. I thank Dr. Jean Gautier and Dr. Timothy Bestor for allowing me to rotate in their labs as a first year student. I had an amazing experience in each lab, and greatly value the ideas and techniques I was able to acquire. I thank Dr. Lawrence Shapiro for allowing me to explore the biochemical aspects of DSG4 in his laboratory. I thank Dr. Cory Abate-Shen for the scientific discussions, reagents, and protocols regarding the study of desmosomal cadherins in mouse models of prostate cancer.

I am especially grateful for Dr. Virginia Papaioannou for working so hard to ensure that we graduate students get the most out of our experience at Columbia. I would have been lost without her diligence, patience, and generosity. I thank the administrative officers in the Department of Genetics and Development, the Department of Dermatology, and the Cordon-Cardo lab for keeping things running smoothly over the years.

Finally I would like to thank my family and friends. I am eternally grateful for my amazing parents who have always put their children before themselves and who taught us to value our education. I thank my grandmother for being a model of generosity and empathy. I thank my siblings for being such wonderful people and always laughing at my jokes. I thank my amazing husband for standing by my side throughout this entire journey, and for never letting me take myself too seriously. I thank Charlie for being the best four-legged friend a girl could have. I thank all my west coast friends who make it so hard to leave home, and all my east coast friends who have made living in New York such a unique pleasure.

Dedication

To my parents, for their endless love and support. To my husband, for making every day the best day of my life. To our little Jelly Bean, for whom I always hope to set a good example.

Chapter I

General introduction

1. Anchoring Junctions: Adherens Junctions and Desmosomes

Multicellular organisms rely on cell-cell adhesion for the development, differentiation, and maintenance of their tissues. A variety of cell-cell junctions serve this purpose, with functions ranging from establishing a physical connection between cells to establishing a channel of communication between cells. Cell-cell anchoring junctions are an example of a junction that functions to establish a physical connection between cells by anchoring cells via the cytoskeleton. Cell-cell anchoring junctions are comprised of two subtypes that differ in the cytoskeletal filaments to which they attach. The first subtype is the adherens junction which forms a physical connection to actin microfilaments. The second subtype is the desmosome which forms a physical connection to intermediate filaments, thereby conferring an additional degree of strength to tissues that undergo a high level of mechanical stress. These junctions are interdependent with respect to their assembly and regulation, and the significance of this interdependence is evidenced by the multitude of both developmental aberrations and human diseases resulting from their disregulation.

The core of the adherens junction is comprised of members of two protein families—cadherins and catenins. The cadherin family is represented by the “classical” cadherins, so named because they were the first type of cadherin within the cadherin superfamily to be discovered. The first three classical cadherins discovered were named according to the main cell type in which they were originally identified; E-cadherin is the predominant cadherin in epithelial

tissues, N-cadherin is the predominant cadherin in neurons, and P-cadherin is the predominant cadherin in the placenta (Nagafuchi et al., 1987; Nose et al., 1987; Hatta et al., 1988). The catenin family is represented by members of the armadillo superfamily including p120-catenin, β-catenin, and plakoglobin (γ-catenin); as well as the structurally unrelated α-catenin (Meng and Takeichi, 2009). The assembly of adherens junctions is initiated via a calcium-dependent, homophilic interaction of the extracellular regions of cadherins in the extracellular space between opposing cells. This interaction then leads to the binding of the cadherin cytoplasmic tails to p120-catenin as well as β-catenin or plakoglobin, followed by the binding of β-catenin to α-catenin (Stepniak et al., 2009). This core complex is then linked to the actin cytoskeleton via interactions between α-catenin and actin binding proteins such as eplin, formin, and vinculin (Fig. 1) (Abe and Takeichi, 2008; Kobielak et al., 2004; Watabe-Uchida et al., 1998).

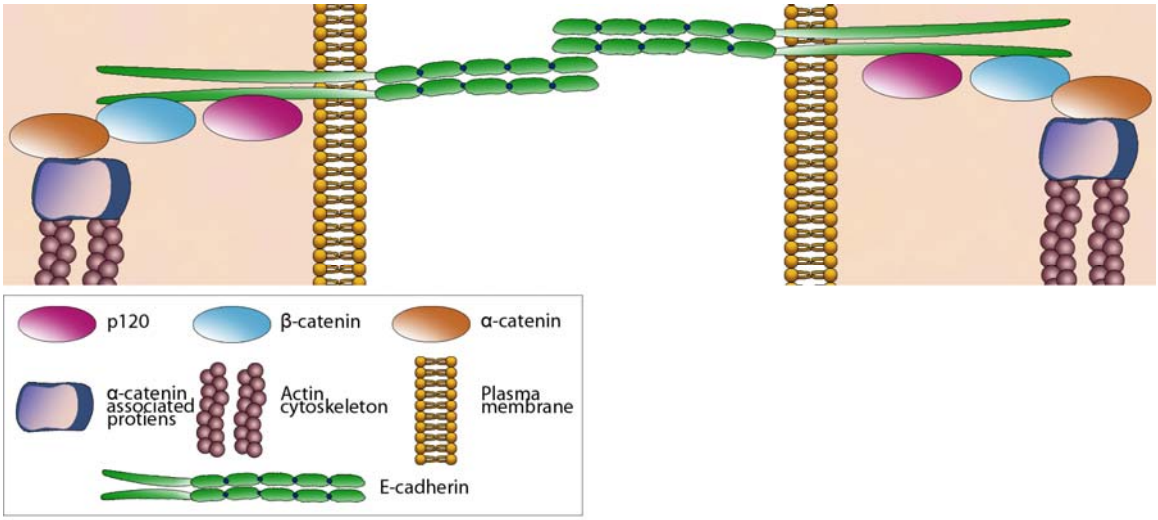

Figure 1: Adherens junction (Adapted from Perez-Moreno and Fuchs, 2006)

Desmosomes are comprised of members from three protein families—the cadherin family, the armadillo family, and the plakin family. In the desmosome, the cadherin family is represented by “non-classical” cadherins which include desmogleins (DSG 1-4) and desmocollins (DSC1-3), while the armadillo family is represented by plakoglobin (PG) and plakophilins (PKP 1-4), and the plakin family is represented by desmoplakin (DP) (Getsios et al., 2004). Desmogleins and desmocollins play a dual role in the formation of desmosomes. In the extracellular space, desmogleins and desmocollins on opposing cells interact in a heterophilic calcium-dependent manner via their cadherin repeat domains. Intracellularly, the cadherins bind to plakoglobin and plakophilin, which in turn bind to desmoplakin. Desmoplakin then binds to intermediate filaments, thereby securing the entire structure to the cytoskeleton (Fig. 2) (Tselepis et al., 1998; Delva et al., 2009). Unlike classical cadherins which preferentially bind to β-catenin, but are also able to substitute plakoglobin for β-catenin in cases where β-catenin is unavailable, desmosomal cadherins cannot substitute β-catenin for plakoglobin and the affinity of plakoglobin for desmosomal cadherins is much greater than its affinity for E-cadherin (Lewis et al., 1997; Chitaev et al., 1996).

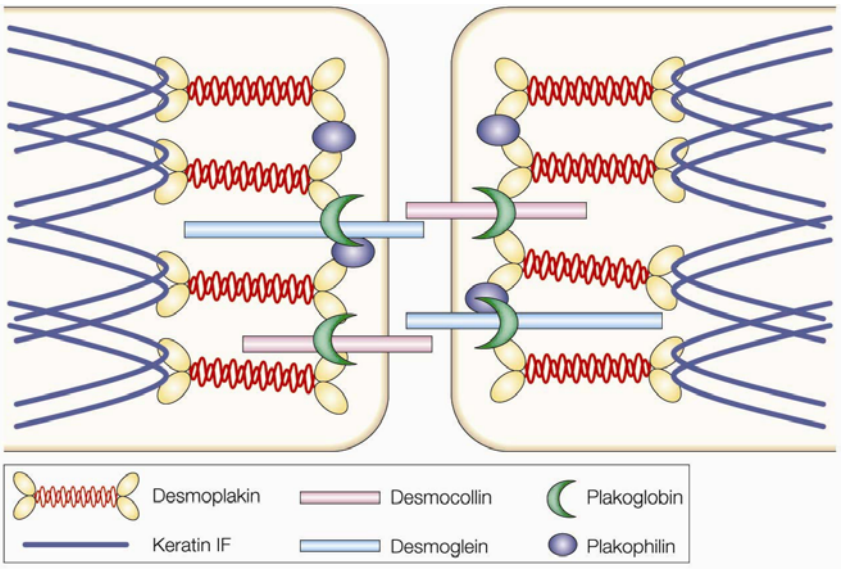

Figure 2: The desmosome (Adapted from Fuchs and Raghavan, 2002)

2. Assembly of Adherens Junctions

Cell-cell adhesion is initiated when cells contact one another through the extension of either lamellipodia or filopodia. These projections are formed when actin microfilaments are organized perpendicular to the leading edge of the cell in either a web-like branched actin network or in linear bundles thereby forming lamellipodia or filopodia, respectively (Pollard and Borisy, 2003; Vasioukhin et al., 2000). E-cadherin has been shown to coassemble with β-catenin and α-catenin, in a complex referred to as a "puncta", at sites of cell-cell contact (Adams et. al, 1996). *In vitro* analysis of GFP-tagged E-cadherin in Madin Darby Canine Kidney (MDCK) epithelial cells has shown that the contact of lamellipodia on opposing cells initiates the spontaneous clustering and immobilization of puncta at the site of cell-cell contact, followed by an interaction between the cadherin-catenin complex and actin microfilaments that have branched from the cortical actin network. These puncta then accumulate along the contact region and form

plaques at either end of the developing contact (Adams et al., 1998). With the maturation of this intercellular adhesion, cortical actin is replaced by circumferential actin bundles attached to the interface of adhering cells, thereby forming the belt-like band of adherens junctions typical of a polarized epithelial cell (Yonemura et al., 1995). *In vitro* analysis of freshly isolated primary mouse keratinocytes has shown that opposing cells extend filopodia, and upon contact with a neighboring cell, the filopodia slide along each other until they finally project into the membrane of the neighboring cell, a process which forces the membranes of opposing cells together. Puncta then form at the tips of the embedded filopodia, resulting in a double row of puncta referred to as an "adhesion zipper", which serves to stabilize the interaction site of the neighboring cells. As a result of this stabilization, the opposing surfaces of the neighboring cells are further drawn together. These filopodial projectiles were also identified in epidermal cells of mouse skin, suggesting that this process of intercellular adhesion exists *in vivo* as well as *in vitro* (Vasioukhin et al., 2000).

3. Assembly of Desmosomes

The formation of adherens junctions has been shown to precede that of desmosomes. In the *in vitro* analysis of primary mouse keratinocytes conducted by Vasioukhin et al., desmosomes were first detected at the flanking ends of the adhesion zipper. As filopodia contain actin microfilaments, and not keratin intermediate filaments, the formation of desmosomes in the early stages of filopodial penetration and adhesion zipper formation is not possible. The strength

of desmosomes may serve to stabilize the newly formed intercellular contact site.

The details of desmosome assembly are not as fully understood, though key studies have provided critical insight into the possible mechanism. Calcium switch experiments, in which cells grown in low calcium conditions (less than 0.1mM) that do not favor cadherin based adhesion are switched to high calcium conditions (greater than 0.1mM) which allow for cadherin based adhesion, have shown that all desmosomal proteins are continuously expressed in a low calcium state (Duden et al., 1988). Under these low calcium conditions, desmosomal proteins transiently assemble into “half-desmosomes”— plaques that contain desmosomal proteins and localize to the cell membrane but do not attach to desmosomal plaques on an opposing cell surface. These half-desmosomes are continuously recycled via endocytosis in the absence of cell-cell contact and accumulate in cytoplasmic endocytic vesicles (Demlehner et al., 1995). Further *in vitro* analysis of GFP-tagged DP in the human epidermoid carcinoma A431 cell line has shown that cell-cell contact initiates the *de novo* appearance of punctate fluorescence at the contact site, followed by the colocatization of DP and PKP2 into cytoplasmic particles, and the rapid translocation of these particles to the maturing contact in an actin microfilament dependent manner (Godsel et al., 2005). The link between the assembly of adherens junctions and that of desmosomes is thought to lie with the desmosomal representatives of the armadillo family, plakoglobin and plakophilin. *In vitro* analysis of A431D — a derivative of the A431 cell line that expresses all desmosomal proteins except PKP1, but lacks the expression of E- and P-cadherin — has shown that

desmosomes are only able to form in the presence of a classic cadherin, and when sufficient levels of PG are expressed to accommodate association with both desmosomal and classic cadherins (Lewis et al., 1997). Further analysis of A431D cells has shown that the expression of PKP1 and a classic cadherin also results in the assembly of desmosomes at the cell-cell border (Wahl III, 2005). Taken together these studies suggest that the formation of adherens junctions triggers the accumulation of desmosomal proteins at the cell border and that this process may be regulated by PG and PKP.

4. Regulation of Anchoring Junction Assembly

The assembly of anchoring junctions is regulated in part by the Rho family of small GTPases. These small GTPases serve as molecular switches within the cell, and are themselves subject to tight temporal and spatial regulation. Small GTPases are present in either a GDP-bound inactive or GTP-bound active state, and the exchange of GDP for GTP is mediated by guanine nucleotide exchange factors (GEFs) (Watanabe et al., 2009). Upon initiation of E-cadherin based cell-cell adhesion, Rac1 and Cdc42 — members of the Rho family of small GTPases — translocate from the cytosol to the sites of cell-cell junctions and become active (Jou and Nelson, 1998; Nakagawa et al., 2001; Kim et al., 2000). This accumulation of Rac1 and Cdc42 may be mediated by phosphatidlyinositol 3-kinase (PI3K) which is thought to function upstream of Rac1 as inhibiting the activity of PI3K has been shown to inhibit the activation of Rac1 (Kotani et al., 1994; Nakagawa et al., 2001). It has been shown that PI3K and Rac1 are

recruited to sites of E-cadherin mediated cell-cell adhesion, and that PI3K is activated as a result of this adhesion (Perez et al., 2008; Pece et al., 1999). Through the use of *in vitro* calcium-switch experiments, Pece et al. demonstrated that the formation of adherens junctions leads to the activation of AKT, a downstream effector of PI3K. This activation of AKT was dramatically reduced in the presence of wortmannin, an inhibitor of PI3K. When E-cadherin mediated adhesion was interrupted in high calcium conditions using antibodies that target E-cadherin and block its capacity for homophilic interaction, the activation of AKT was also dramatically reduced. The physical association of PI3K and E-cadherin via coimmunoprecipitation was also demonstrated. These results suggest that PI3K interacts directly with E-cadherin at sites of cell-cell adhesion, and that this interaction leads to the activation of PI3K which may then lead to the accumulation of small GTPases at sites of cell-cell adhesion.

Much like Rac1 and Cdc42, GEFs, such as Tiam1, also accumulate at sites of adherens junctions (Hordijk et al., 1997). This accumulation may be mediated by the interaction of the Tiam1 PDZ domain with the PDZ consensus sequence found in β-catenin, which could account for the activation of Rac1 and Cdc42 at adherens junctions (Songyang et al., 1997; Michiels et al., 1995; Dobrosotskaya et al., 2000). Additionally, Tiam1 contains a PH domain which allows it to bind to phosphatidlyinositol lipids, products of PI3K, thereby allowing it to dock at sites of PI3K activity and serving as a means by which Tiam1 is recruited to sites of cell-cell adhesion in a PI3K dependent manner (Rameh et al., 1997; Fleming et al., 2000).

Once active at sites of cell-cell adhesion, small GTPases play a regulatory role in the formation of adherens junctions by enhancing the formation of these junctions through inhibition of a negative regulator of E-cadherin based adhesion and through modifications of the actin cytoskeleton that serve to reinforce cadherin-mediated adhesion. Overexpression of constitutively active mutant of Rac1 has been shown to induce the accumulation of E-cadherin, β-catenin, and actin filaments at sites of cell-cell contact, while the overexpression of a dominant negative mutant of Rac1 has been shown to reduce this accumulation (Takaishi et al., 1997). Rac1 and Cdc42 have also been shown to bind to and inactivate IQGAP1, a negative regulator of adherens junction formation that interacts with β-catenin and dissociates α-catenin from β-catenin (Kuroda et al., 1998; Fukata et al., 1999). Additionally, Cdc42 and PIP2 have been shown to interact with N-WASP thereby enhancing the ability of N-WASP to interact with the Arp2/3 complex. The Arp2/3 complex is required for the nucleation of actin microfilament assembly, and by interacting with N-WASP in a Cdc42 dependent manner, the Arp2/3 complex is able to initiate this actin microfilament assembly at sites of cell-cell adhesion (Rohatgi et al., 1999; Rohatgi et al., 2000).

5. Adherens Junctions and Desmosomes in Development

The formation of anchoring junctions is crucial in embryonic development. In the preimplantation embryo, E-cadherin is initially provided maternally, and at the 8-cell stage of embryonic development, E-cadherin is critical for compaction — the process by which blastomeres go from being rounded and loosely

adherent to highly polarized and flattened with a significant increase in adherens junctions along the maximized contact surface between cells (Ohsugi et al., 1996). Subsequent asymmetric cell division gives rise to a 16-cell morula that contains inner daughter cells surrounded by an outer cell layer which preferentially contributes to the trophectoderm. E-cadherin expression by the embryo at the morula stage is critical for the formation of the trophectoderm, as mutant mice that lack E-cadherin expression die at E4 due to defects in trophectoderm formation (Fleming et al., 1987; de Vries et al., 2004; Larue et al., 1994).

Much like *de novo* anchoring junction formation between the cells of adult tissues, the formation of adherens junctions precedes the formation of desmosomes in the preimplantation embryo. Desmosomes initially form in the mature trophectoderm at the 32-cell stage. While the expression of PG can be detected as early as the 8-cell stage, the expression of most desmosomal cadherins is not detected until the 32-cell stage (Jackson et al., 1980; Fleming et al., 1991). The importance of desmosomes in early development is underscored by the phenotypes of mutant mice lacking desmosomal protein expression. Mutant mice that lack the expression of DP are able to form a trophectoderm, however these mice die after implantation at E6.5. The DP null embryos show a dramatic reduction in cell proliferation and fragility upon mechanical dissection, suggesting that the mutant embryos are unable to handle the increased proliferation and tissue reorganization that occurs between E5.0 and E7.0 (Gallicano et al., 1998). Mutant mice lacking the expression of Dsc3 and Dsg2

die at E3.5 or at the time of implantation, respectively. Interestingly, in both cases the formation of trophectoderm appears normal, indicating a possible role for desmosomal cadherins beyond that of desmosomal architecture (Den et al., 2006; Eshkind et al., 2002).

6. EMT and Development

Epithelial-mesenchymal transition (EMT) is essential in early embryonic developmental processes such as gastrulation. In EMT, cells lose epithelial characteristics such as apical-basal polarity and cell-cell adhesion, and acquire mesenchymal characteristics such as motility. Prior to implantation, the mouse embryo is effectively a ball of cells consisting of an inner cell mass and the trophectoderm. Following implantation, the embryo undergoes dramatic changes in size and shape that result in the formation of a trophoblast, hypoblast, epithelialized epiblast, and amniotic cavity (Tam and Behringer, 1997). During gastrulation, the cells of the epiblast (embryonic ectoderm) undergo complex morphogenetic rearrangements that result in the formation of the three primary germ layers, basic body plan, and primitive gut (Tam et al., 1987).

Gastrulation is initiated by the formation of the primitive streak. Prior to the formation of the primitive streak, cells of the epiblast are tightly packed and express E-cadherin (Damjamov et al., 1986). The primitive streak is formed when cells of the epiblast undergo ingression and de-epithelialization thereby losing contact with neighboring cells (Bellairs et al., 1986; Hashimoto and Nakatsuji, 1989). This loss of epithelialization allows the prospective mesodermal and

endodermal cells to migrate along the streak, and is concomitant with the loss of E-cadherin expression (Burdsal et al., 1993; Damjanov et al., 1986). FGF signaling plays a critical role in gastrulation as mouse embryos lacking the expression of FGF Receptor 1 (Fgfr1) die before or during gastrulation (Deng et al., 1994). In vitro analysis of *Fgfr1* $^{-/-}$ embryonic tissue explants from the primitive streak shows that in the absence of Fgfr1 expression cells have defects in migration and aberrantly accumulate beneath the primitive streak while maintaining E-cadherin expression (Ciruna et al., 2001). Ciruna and colleagues went on to show that while Snail was expressed in the early primitive streak, there was a subsequent loss of Snail expression in the late primitive streak of *Fgfr1* $^{-/-}$ mutant explants, suggesting that the expression of Fgfr1 is required for the maintenance of Snail expression. Snail is a zinc finger transcription factor that binds to E-boxes in the promoters of target genes and acts as a transcriptional repressor (Nieto, 2002). Snail has been shown to be a direct repressor of E-cadherin expression (Cano et al., 2000). Mice that lack the expression of Snail die at E8.5 and show defects in gastrulation and mesoderm formation. These mutant mice form an abnormal mesoderm layer that expresses mesodermal markers but retains epithelial features such as adherens junctions due to maintained E-cadherin expression (Carver et al., 2001). Thus the loss of E-cadherin expression via the EMT effector Snail is critical in early developmental processes such as gastrulation.

7. The PI3K/AKT Signaling Pathway

The PI3K/AKT signaling pathway is involved in a variety of cellular processes that regulate metabolism, protein synthesis, cell cycle, and cell survival. This pathway is activated when growth factors bind to their respective growth factor receptor tyrosine kinases (RTKs). A variety of growth factors have been shown to activate the PI3K/AKT signaling pathway including insulin, PDGF, EGF, and FGF (Burgering and Coffer, 1995). The ligand bound RTKs are then activated via autophosphorylation thereby creating a docking site that allows for the binding of adaptor proteins containing phosphotyrosine-binding domains such as SH2 domains. Class IA PI3Ks can either bind directly to the activated RTKs through their SH2 domain, or can bind via adaptor proteins, and in both cases this leads to activation of PI3K. Activated PI3K then phosphorylates inositol phospholipids at the 3 position to generate PI(3)P, PI(3,4)P_2, or PI(3, 4, 5)P_3 (PIP, PIP2, PIP3, respectively). These phosphorylated inositol phospholipids then interact with the lipid binding domains of PI3K effector proteins leading to their activation. PI3K signaling can be inactivated at this point in the pathway by PTEN, a phosphatase that dephosphorylates PI(3, 4, 5)P_3 converting it to PI(4,5)P_2 (Maehama and Dixon, 1998). In the presence of PIP3, the serine/threonine kinase AKT serves as a major effector of PI3K signaling. The production of PIP3 recruits AKT and PDK1 to the membrane via their PH domains. At the membrane, AKT is activated when PDK1 phosphorylates AKT at threonine 308 (Thr308) in its activation loop while the rictor-mTOR complex phosphorylates AKT at serine 473 (Ser473) in its C-terminal tail. Activated AKT

then goes onto phosphorylate and inhibit a variety of proteins thereby promoting glucose metabolism, protein synthesis, cell proliferation, and survival (Fig. 3) (Vanhaesebroeck et al., 2010; Engelman et al., 2006; Cully et al., 2006; Sarbassov et al., 2005).

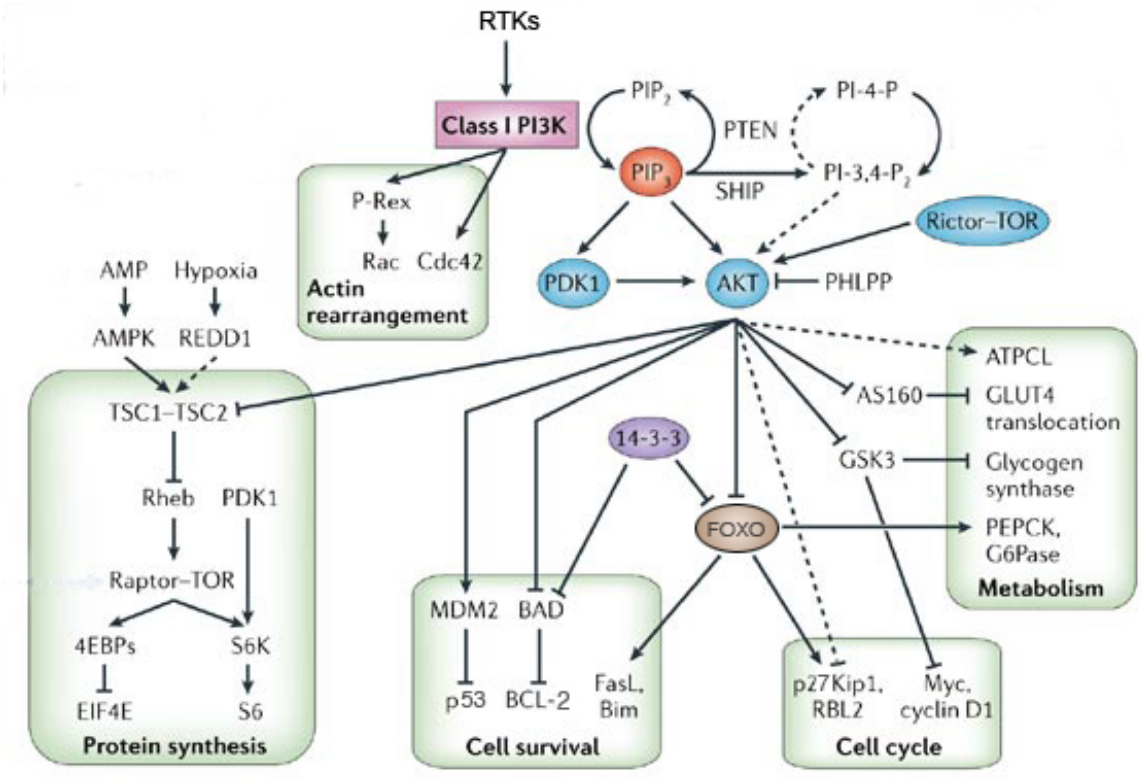

Figure 3: PI3K/AKT signaling pathway (Adapted from Engelman et al., 2006)

8. Prostate Cancer

Prostate cancer is the most frequently diagnosed cancer in American men as well as the second leading cause of cancer death. In 2009, The American Cancer Society estimates over 190,000 new cases of prostate cancer and over 27,000 prostate cancer related deaths (American Cancer Society, 2009). Prostate cancer is generally diagnosed using a core needle biopsy, a method by which a needle is inserted into the prostate gland to procure small cylinders of

prostate tissue. These core biopsies are submitted to a pathologist who then determines if cancer cells are present, and assigns a Gleason score in the event of cancer. This Gleason score is the result of the sum of two Gleason grades. The Gleason grades range from 1-5 with low Gleason grades corresponding to cancers that are well differentiated and high Gleason grades corresponding to cancers that are poorly differentiated. Well differentiated cancers are composed of glands which architecturally resemble normal prostate glands, while poorly differentiated cancers lack the shape and architecture of normal prostate glands. As prostate cancers are often comprised of areas with different grades, the Gleason score is obtained by adding the predominant grade (primary) and the second most predominant grade (secondary) when present. The Gleason score is divided into 3 categories: low (≤6), intermediate (7) and high (≥8), and has been shown to be a critical prognostic factor for patients with prostate cancer. Once prostate cancer has been graded it must then be staged to determine whether the cancer is confined to the prostate capsule, or whether it has spread to nearby tissues or distant sites. A clinical stage is assigned based on the results of a digital rectal exam, serum prostate specific antigen (PSA), and Gleason Score. As prostate cancer is generally a slow growing cancer, low-grade cases confined to the prostate capsule are often treated with “watchful waiting”. With watchful waiting the patient is closely monitored with regular PSA screenings, physical exams, and in some cases, biopsies, to determine if the cancer is growing. Cases of prostate cancer that remain confined to the prostate capsule, but have a high Gleason grade, high PSA level, or both, are generally

treated with local therapy such as prostatectomy or radiation. In most cases this treatment is curative; however there are cases of aggressive prostate cancer, which evade treatment. Prostate cancer recurrence is often detected by routine PSA screenings following treatment. A serum PSA result of 0.4ng/mL is indicative of biochemical recurrence and therefore disease relapse (American Joint Committee on Cancer, 2010; American Cancer Society, 2005). The challenge of prostate cancer diagnosis and treatment lies in predicting the potential of a given cancer to be an aggressive cancer. Unlike breast cancer, for which the presence or absence of HER2, ER, and PR serve as prognostic factors, there are no biomarkers that have been established as prognostic factors for prostate cancer beyond serum PSA determination. Therefore, there is a great need for prognostic biomarkers that can assist in estimating the likelihood of prostate cancer aggressiveness.

The glandular tissue of the prostate is comprised of ducts and acini that are lined by a simple cuboidal epithelium facing the lumen of the glands. In addition to this secretory component, two other specialized cells are an integral part of the prostate glandular structures, namely the basal cells and the neuroendocrine cells (Abate-Shen et al., 2000; Bonkhoff, 1996). The luminal cells secrete prostate specific antigen (PSA) and represent the functional unit of the organ. These cells form a continuous layer which lies on top of the basal cells. The basal cells are characterized by the expression of high molecular weight cytokeratins and p63. Dispersed throughout the acini is the third cell population, the neuroendocrine cells, the origin and function of which are ill defined.

Tumor initiation in the prostate is thought to be generated by the transformation of an epithelial cell precursor that develops into a premalignant lesion known as prostatic intraepithelial neoplasia (PIN) (Brawer, 1992). PIN is characterized by dysplasia — loss of normal cellular architecture — and proliferation of the transformed cells which usually display the luminal phenotype, namely they secrete PSA (Brawer, 1992). In PIN, which can be classified as low grade or high grade, the basal cell layer is usually lost or presents as a discontinuous layer (Brawer, 1992; Bostwick et al., 1993). Low-grade PIN lesions are described as having relatively "normal" appearing cells, being on some occasions difficult to distinguish from hyperplastic epithelium (Eble et al., 2004). High-grade PIN lesions, which are sometimes regarded as carcinoma *in situ*, display abnormal nuclei with prominent nucleoli, similar to those found in prostatic adenocarcinomas (Brawer, 1992; Bonkoff et al., 1996). Tumors derived from high grade PIN lesions have been reported to be more aggressive in nature (Wilcox et al., 1998). The progression from PIN to an invasive adenocarcinoma is marked by the percolation of tumor cells from well-defined glandular structures into the surrounding stroma (Eble et al., 2004; Bonkhoff, 1996). Further tumor progression is marked by the spread of malignant cells locally to seminal vesicles and perineural invasion, followed by metastatic disease to lymph nodes and later to distant sites, most commonly the axial skeleton (Fig. 4) (Logothetis et al, 2005).

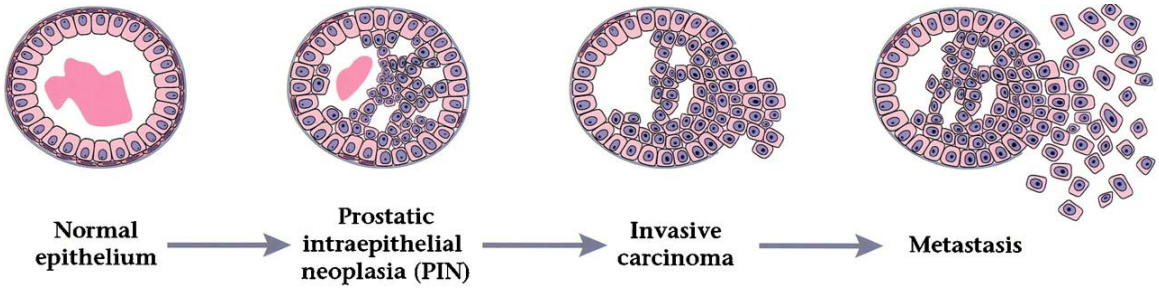

Figure 4: The progression of prostate cancer (Adapted from Abate-Shen and Shen, 2000)

9. E-cadherin and Cancer

While in many cases organ confined cancers are associated with a high survival rate, metastatic cancers are responsible for the vast majority of all cancer related deaths. This is clearly illustrated in the case of prostate cancer where there is a reported 100% five-year survival rate for prostate cancer that is confined to the prostate, while the five-year survival rate drops dramatically to 31.7% for prostate cancer that has metastasized to a distant site (American Cancer Society, 2009). As mentioned previously, the first step in metastasis is local invasion, where malignant cells first invade the surrounding stroma and then progressively move into local tissues. In order to travel to distant sites, malignant cells must enter into the circulatory system by undergoing intravasation, survive in the circulation, undergo extravasation upon reaching the distant site, and successfully establish a tumor colony at the distant site (Nguyen et al., 2009). The metastatic pathway presents a malignant cell with enormous challenges; accordingly there are relatively few cells that can survive all stages of the pathway. Those malignant cells that do survive must rapidly adopt properties

that will allow for their continued survival in a variety of new cellular environments.

In order to initiate the process of invasion, a cancer cell must detach itself from the primary tumor and adopt migratory properties that allow it to move into the surrounding stroma. In tumors of an epithelial origin, this initial detachment from the primary tumor is thought to be largely mediated by the downregulation or loss of E-cadherin based adherens junctions. The downregulation or loss of E-cadherin itself is a common feature of a variety of cancers, including prostate cancer, and can be caused by loss of heterozygosity (LOH), mutations, epigenetic silencing, transcriptional silencing, or increased endocytosis and proteolysis (Rubin et al., 2001; Berx and van Roy, 2009). Germline mutations of *E-cadherin* have been reported in familial gastric cancer, and in many cases these mutations are accompanied by promoter hypermethylation of the remaining allele thereby leading to a loss of E-cadherin expression (Guilford et al., 1998; Machado et al., 2001). Additionally, somatic genetic aberrations of *E-cadherin*, including LOH and mutations, have been identified in a variety of human cancers including diffuse gastric cancer, lobular breast cancer, bladder cancer, and prostate cancer (Becker et al., 1994; Berx et al., 1995; Taddei et al., 2000; Latil et al., 1997; Elo et al., 1997; Strathdee, 2002).

Several *in vitro* and *in vivo* studies have demonstrated a role for E-cadherin in the progression of cancer to an invasive and metastatic state. *In vitro* analysis shows that the introduction of E-cadherin expression in cancer cell lines leads to a diminished invasive capacity of the cell lines. This invasive capacity

was restored in the presence of anti-E-cadherin antibodies that block E-cadherin mediated adhesion (Vleminckx et al., 1991). *In vivo* analysis of a transgenic mouse model of pancreatic β-cell cancer (*Rip1Tag2*) shows that E-cadherin is expressed in well-differentiated adenomas but lost in invasive carcinomas (Perl et al., 1998). When E-cadherin expression was maintained in double transgenic mice that expressed E-cadherin in pancreatic β-cells (*Rip1Tag2;Rip1E-cad*) the incidence of carcinoma was significantly reduced. Conversely, when E-cadherin expression was lost in double transgenic mice expressing a dominant negative form of E-cadherin (*Rip1Tag2;Rip1dnE-cad*), the incidence of carcinoma increased dramatically and 25% of the double transgenic mice developed metastatic lesions. Additionally, a compound mutant mouse model of invasive lobular carcinoma with conditional deletion of *E-cadherin* in combination with epithelium-specific knock-down of *p53* (*K14Cre;Cdh1*$^{F/F}$; *Trp53*$^{F/F}$) was found to develop invasive and metastatic mammary carcinomas (Derksen et al., 2006). Interestingly, the knock down of *p53* alone results in relatively large mammary carcinomas that are generally not invasive, while the conditional deletion of *E-cadherin* alone results in hyperproliferation, but not in tumor formation. These findings suggest that the loss of E-cadherin is not involved in tumor initiation, but is required for the progression to an invasive and metastatic state. Additionally, the tumor vasculature in the compound mutant mice was found to be significantly more extensive than that found in mutant mice expressing E-cadherin, and conditioned medium from cultured *K14Cre;Cdh1*$^{F/F}$; *Trp53*$^{F/F}$ cells induced sprouting of endothelial cells *in vitro*. These results suggest an additional role for

E-cadherin in tumor angiogenesis and imply that the loss of E-cadherin results in the secretion of a factor that contributes to angiogenesis. The findings of Derksen et al. are further supported by compound mutant mouse models of non-small-cell lung carcinoma with conditional deletion of *E-cadherin* or expression of dominant negative *E-cadherin* in combination with the overexpression of C-RAF in type II alveolar pneumocytes (*SP-C C-RAF BXB*/*SP-C rtTA/Tet-O-cre/cdh1*$^{flox/flo}$ or *SP-C C-RAF BXB*/*SP-C rtTA/Tet-O dn E-cadherin*) (Ceteci et al., 2007). These compound mutant mice develop invasive carcinomas that metastasize into regional lymph nodes and bone marrow. Much like the Derksen et al. mouse model of invasive lobular carcinoma, mice overexpressing *C-RAF* alone develop multiple lung adenomas that do not progress to an invasive state, while the loss of E-cadherin alone leads to hyperproliferation but not tumor formation, further supporting the role of E-cadherin in the progression to an invasive state. Additionally, increased tumor angiogenesis was observed in compound mutant mice and this increase was associated with β-catenin induced expression of VEGF-A, VEGF-C and VEGFR-3, further supporting the role of E-cadherin in tumor angiogenesis. Taken together, these results suggest that the loss of E-cadherin plays a causal role in the progression of tumors to a malignant and invasive state as well as in tumor angiogenesis.

10. Desmosomes in Disease and Cancer

The importance of desmosomal cadherins in adult tissues is highlighted by the genetic diseases that arise due to their mutation. These diseases target

tissues that undergo a high degree of mechanical stress and therefore rely on desmosomes for the maintenance of their integrity. Mutations in *DSG1* are associated with striate palmoplantar keratoderma (PPKS), a rare autosomal dominant disorder characterized by thickening of the skin on the palms and soles (Rickman et al., 1999; Barber et al., 2006). Mutations in *DSG2* and *DSC2* are associated with arrythmogenic right ventricular cardiomyopathy (ARVC), an autosomal dominant disorder characterized by progressive myocardial atrophy with fibrofatty myocardial replacement of myocytes by adipocytes in the right ventricle (Awad et al., 2006; Pilichou et al., 2006; Syrris et al., 2007; Heuser et al., 2006). *DSC2* is also associated with an autosomal recessive form of ARVC that is accompanied by PPKS and wooly hair (Simpson et al., 2009). Mutations in *DSG4* are associated with localized autosomal recessive hypotrichosis, a disorder in which compromised hair shaft integrity results in hypotrichosis of the scalp, chest, arms, and legs (Kljuic et al., 2003). Mutations in *DSG4* have also been associated with monilethrix-like hypotrichosis, a disorder in which affected hairs have a beaded appearance and break easily thereby resulting in alopecia (Schweizer, 2006; Shimomura et al., 2006; Zlotogorski et al., 2006; Schaffer et al., 2006). Additionally, the autoimmune blistering disorders pemphigus foliaceus and pemphigus vulgaris are caused by autoantibodies that target and block the function of DSG1 and DSG3, respectively (Amagai et al., 1999).

While clearly important in maintaining the integrity of adult tissues, the role of desmosomal cadherins in the progression of cancer is less well understood. LOH near the chromosomal region containing the desmosomal

cadherin gene cluster has been reported in esophageal cancer as well as head and neck squamous cell carcinoma (Karkera et al., 2000; Takebayashi et al., 2000). Alterations in the expression of desmosomal cadherins have been reported for a variety of cancers. Reduced expression of DSG2 has been reported in gastric cancer and pancreatic cancer (Biedermann et al., 2005; Yashiro et al., 2006; Ramani et al., 2008). Additionally, the hypermethylation of the *DSC3* promoter was associated with reduced expression of DSC3 in breast cancer (Oshiro et al., 2005). Conversely, overexpression of DSG2 and DSG3 has been reported in squamous cell carcinomas of the skin as well as head and neck cancer, respectively (Kurzen et al., 2003; Chen et al., 2007). Desmosomal cadherin switching has also been reported in colorectal cancer, where reduced expression of DSC2 was associated with *de novo* expression of DSC1 and DSC3 (Khan et al., 2006). There is a lack of functional evidence regarding the role of desmosomal cadherin based adhesion in cancer. However, *in vitro* analysis of a non-adhesive, invasive fibroblast cell line shows that the expression of desmosomal cadherins and plakoglobin was able to generate adhesion and reduce the invasive capacity of the cell line (Tselepis et al., 1998). Treatment of these cells with peptides that blocked the desmosomal cadherin adhesion site both blocked adhesion and restored invasive capacity, suggesting that the observed adhesion and reduced invasive capacity were desmosomal cadherin specific. These results illustrate the possibility that desmosomal adhesion may result in a similar impaired invasive capacity of cancer cells, and that the loss of this adhesion may be required for the progression of metastasis.

11. EMT and Cancer

While the first step in the metastatic cascade relies on the ability of malignant cells to detach themselves from a primary tumor before migrating into the surrounding stroma, ultimately these cancer cells must again form a tumor upon arrival at a distant site. Though the loss of adhesion is useful in the initial stages of metastasis, the permanent loss of adhesion may ultimately impair metastatic tumor formation. Indeed, while the loss of adherens junctions is a frequent occurrence in primary tumors, re-expression of adherens junction proteins is often found in metastatic tumors (Bukholm et al., 2000).

Maintaining a dynamic regulation of anchoring junctions as opposed to enforcing their permanent loss may therefore offer a selective advantage to the metastasizing cancer cell. Epithelial-mesenchymal transition followed by mesenchymal-epithelial transition (MET) is one such way a cancer cell could maintain a dynamic regulation of its anchoring junctions (Fig. 5). Though clearly essential in early development, the role of EMT in cancer remains controversial. This is mainly due to the difficulty of identifying a cancer cell that has undergone EMT in a primary human tumor sample. Most EMT markers are expressed in either epithelial or mesenchymal cells making it impossible to distinguish an epithelial cell that has undergone EMT and migrated into the surrounding stroma from normal stromal cells (Yang and Weinberg, 2008).

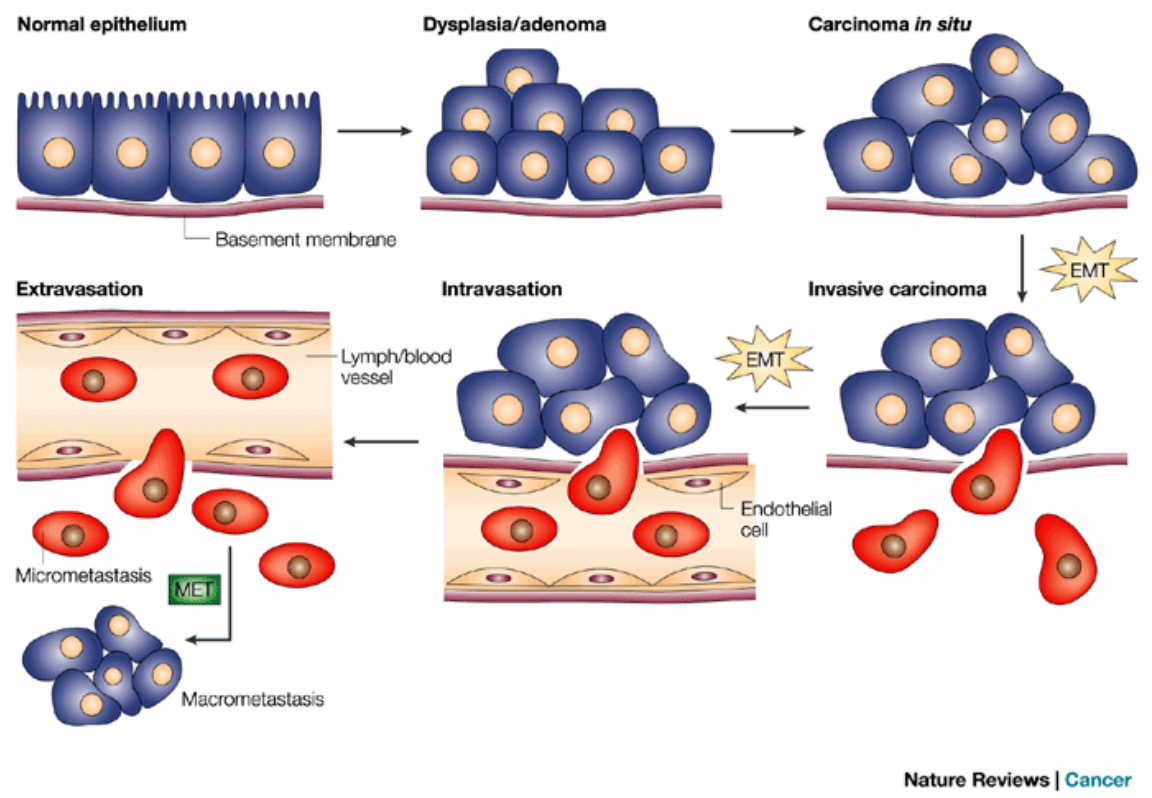

Figure 5: EMT in the progression of cancer (Thiery, 2002)

Despite the controversy, the loss of E-cadherin expression remains an underlying hallmark of both EMT and tumor progression. Additionally, much like EMT in early development, the loss of E-cadherin in the progression of cancer has been linked to transcriptional repression via effectors of EMT such as Snail, Slug, and Twist. The expression of Snail in breast cancer has been associated with high-grade tumors, lymph node metastasis, reduced E-cadherin expression, and disease recurrence (Blanco et al., 2002; Cheng et al., 2001; Moody et al., 2005). The expression of Snail has also been associated with the downregulation of E-cadherin in colorectal cancer (Pena et al., 2005). *In vitro* analysis of Snail

expression in mouse and human cancer cell lines has shown that the expression of Snail is inversely correlated with the expression of E-cadherin (Cano et al., 2000). Further analysis of human cancer cell lines has shown that the induction of *Snail* expression in a colon cancer cell line leads to a significant reduction in the level of *E-cadherin* mRNA expression, while reduced Snail expression in a pancreatic cancer cell line results in restored E-cadherin expression (Batlle et al., 2000).

The expression of Slug, a member of the Snail family of zinc finger transcription factors, has been associated with metastasis and disease recurrence in breast cancer, and has been reported to be an independent prognostic factor for colorectal cancer (Martin et al., 2005; Shioiri et al., 2006). In lung cancer, *Slug* was associated with disease relapse and shortened patient survival (Shih et al., 2005). Additionally, in esophageal squamous cell carcinoma Slug expression was inversely correlated with E-cadherin expression and associated with poor clinical outcome (Uchikado et al., 2005). *In vitro* analysis has shown that Slug is able to bind E-box elements in the *E-cadherin* promoter, and represses the expression of both endogenous E-cadherin as well as an *E-cadherin* reporter gene construct in a dose dependent manner in human breast cancer cell lines (Hajra et al., 2002). Additionally, the stable expression of Slug leads to transcriptional repression of *E-cadherin* in MDCK cells (Bolos et al., 2002). It was demonstrated that this transcriptional repression was mediated by the binding of Slug to E-boxes in the *E-cadherin* promoter, however the binding affinity of Slug was found to be lower than that of Snail. Interestingly, transient or

stable expression of Slug in the rat bladder carcinoma NBT-II cell line results in the disappearance of DP and DSG from sites of cell-cell contact, while the expression of E-cadherin is not significantly downregulated in these cells (Savagner et al., 1997). Taken together these results suggest that Slug can induce the loss of cell-cell adhesion in cancer by downregulating the expression of either E-cadherin or desmosomal proteins depending on the cellular context.

12. The PI3K/AKT Signaling Pathway and Cancer

As mentioned previously, the PI3K/AKT signaling pathway is crucial for the regulation of processes such as proliferation and survival in normal cells. These processes are also extremely useful for cancer cells, accordingly the aberrant activation of the PI3K/AKT signaling pathway is a frequent occurrence in human cancers. One of the most commonly altered genes in the PI3K/AKT signaling pathway is the *PTEN* tumor suppressor gene which was originally identified by mapping homozygous deletions of chromosome 10q23 in primary breast tumors (Li et al., 1997). Loss of heterozygosity (LOH) at chromosome 10q23 is a frequent occurrence in a variety of human cancers, such as breast cancer, melanoma, gastric cancer, and prostate cancer (Feilotter et al., 1999; Reifenberger et al., 2000; Byun et al., 2003; Cairns et al., 1997). In prostate cancer it has been reported that up to 62% to 65% of cases show LOH of chromosome 10q23-25 (Gray, 1995; Lacombe et al, 1996). Additionally, LOH was reportedly detected in 18% of primary prostate tumors, while in pelvic node

metastasis that percentage increased to 60%, supporting the idea that *PTEN* is associated with prostate cancer progression (Cairns et al., 1997).

Though inactivation of the *PTEN* tumor suppressor is perhaps the most notorious alteration of the PI3K/AKT signaling pathway, alterations of other members within the pathway have also been detected. The AKT family is comprised of three genes encoding three AKT isoforms (AKT1, AKT2 and AKT3), all of which are similar in structure and size, and regulated by similar mechanisms (Scheid and Woodgett, 2001). In breast cancer, colorectal cancer, ovarian cancer, and lung squamous cell carcinoma it has been reported that *AKT1* is aberrantly activated via a somatic mutation of its PH domain (E17K) which results in the localization of AKT1 to the plasma membrane (Carpten et al., 2007; Malanga et al., 2008; Boormans et al., 2010). Additionally, rare amplification of *AKT1* has been reported in gastric cancer and prostate cancer (Staal et al., 1987; Kirkegaard et al., 2010). Further, the overexpression of AKT1 has been reported in thyroid cancer, prostate cancer, breast cancer, and ovarian cancer (Ringel et al., 2001; Sun et al., 2001).

The significance of the PI3K/AKT signaling pathway in prostate cancer was recently highlighted by the work of Taylor et al. who utilized a combination of DNA copy number analysis, mRNA expression analysis, and resequencing analysis to perform the most comprehensive genomic profiling of prostate cancer to date (Taylor et al., 2010). The results of this profiling show that PI3K/AKT signaling is altered in 42% of primary prostate cancers and 100% of metastatic prostate cancers examined. Recurrent deletion of 10q23.31 targeting *PTEN* was

observed, confirming the previously reported loss of *PTEN* in prostate cancer. While mutations in *PIK3CA* were rarely detected, the aberrant upregulation of *PIK3CA* was detected via mRNA expression analysis. This upregulation, in combination with the observed downregulation of inhibitors of PI3K/AKT signaling such as *PTEN*, *INPP4B*, and *PHLPP*, results in the aberrant activation of PI3K/AKT signaling. Taken together these results suggest that the aberrant activation of the PI3K/AKT signaling pathway is associated with the progression of prostate cancer to a metastatic state.

The importance of the PI3K/AKT signaling pathway in prostate cancer has also been demonstrated by mouse models of prostate cancer harboring *Pten* mutations such as the heterozygous $Pten^{+/-}$ knock out mouse model which develops preneoplastic lesions with hyperplastic-dysplastic features in several tissues including the prostate (Di Cristofano, 1998; Di Cristofano 2001). Further, *Pten* compound mutant mouse models such as the *Nkx3.1*;*Pten* mouse model, show high grade PIN and invasive prostatic carcinoma lesions, while the $Cdkn1b^{-/-}$;$Pten^{+/-}$ mouse model also shows invasive prostate cancer (Kim et al., 2002; Abate-Shen et al., 2003; Di Cristofano et al., 2001). Interestingly, prostate neoplasia is dramatically inhibited in the compound $Pten^{+/-}$;$Akt1^{-/-}$ mutant mouse model which demonstrates the significance of AKT1 as a major effector of the PI3K/AKT signaling pathway in prostate cancer (Chen et al., 2006). Further, the transgenic MPAKT mutant mouse model of prostate cancer in which the expression of constitutively active Akt1 is driven by the prostate specific rat *probasin* promoter, was found to develop PIN (Majumder et al., 2003). This PIN

development in MPAKT mice is strikingly similar to that observed in the heterozygous *Pten*$^{+/-}$ knock out mouse model, further illustrating the significance of AKT1 mediated signaling in the development of prostate cancer (Majumder et al., 2003).

13. The PI3K/AKT Signaling Pathway in EMT and Cancer

The PI3K/AKT signaling pathway has been linked to EMT in cancer. *In vitro* analysis of the MCF-10A breast cancer cell line has shown that cells overexpressing IGF-IR in which *AKT1* has been downregulated via RNAi appear to undergo EMT and have enhanced cell migration (Irie et al., 2005). This phenotype is suppressed by the downregulation of *AKT2*, suggesting that EMT and cell migration are a result of AKT2 activity. Further, *in vitro* analysis of cell lines derived from mammary epithelial tumors induced by *ErbB2* in either *Akt*$^{+/+}$ or *Akt*$^{-/-}$ mice (i.e. *ErbB2;Akt*$^{+/+}$ or *ErbB2;Akt*$^{-/-}$ mice) has shown that *Akt*$^{+/+}$ cell lines display a lack of polarization and enhanced migration (Ju et al., 2007). These EMT-like features are absent in *Akt*$^{-/-}$ cell lines, suggesting that AKT1 is also able to promote an EMT-like phenotype in breast cancer cell lines. Additionally, AKT may have a role in the loss of E-cadherin expression as it has been shown that expression of constitutively active Akt in squamous cell carcinoma lines leads to a downregulation of *E-cadherin* mRNA expression (Grille et al., 2003). Interestingly, this same study showed that there was a mislocalization of desmoplakin, such that it displayed granular staining in the cytoplasm and failed to localize to the cell-cell border. This downregulation of *E-*

cadherin may be mediated via Snail as constitutively active Akt was shown to induce the expression of *Snail* mRNA. The activation of AKT signaling has also been shown to result in the stabilization of Snail through the inhibition of GSK3β, a kinase that inhibits Snail through phosphorylation at two consensus motifs which then leads to the ubiquitination and subsequent degradation of Snail (Zhou et al., 2004). Taken together this data suggests that the activation of AKT in cancer cells leads to an EMT-like phenotype which includes a loss of *E-cadherin* expression that may be mediated via transcriptional repression by Snail.

14. Work Described in this Thesis

My doctoral studies were focused on examining the role of cell-cell adhesion in the progression of prostate cancer as well as the mechanism by which this adhesion is regulated. While most studies of cell-cell adhesion in cancer have focused on adherens junctions alone, I sought to conduct a more comprehensive analysis of cell-cell adhesion in prostate cancer by broadening my focus to include both adherens junctions and desmosomes. Prior to this study, the expression profile of desmosomal cadherins in the prostate was unknown. I therefore began this study with an examination of the expression of desmosomal cadherins in prostate tissue as well as prostate cancer cell lines. In chapter II of this study I describe this analysis of the desmosomal cadherin expression profile in normal prostate tissue and prostate cancer cell lines, and discuss the how the results of this analysis led me to focus on the expression of DSG2 in the progression of prostate cancer.

The reduction or loss of E-cadherin expression has been reported in a variety of cancers — including prostate cancer — and previous studies have demonstrated that the formation of adherens junctions precedes that of desmosomes both in early development as well as in the *de novo* assembly of cell-cell anchoring junctions. I therefore hypothesized that the loss of E-cadherin based adherens junctions in prostate cancer results in the reciprocal loss of desmosomal adhesion. I describe the functional analysis used to examine this hypothesis and the surprising results of this analysis as well as the implications of these results with respect to anchoring junction assembly in chapter III. Additionally, in this chapter I describe the functional analysis used to examine the effects of the loss of E-cadherin expression on the formation of both primary and metastatic tumors. Further, I discuss a novel role for E-cadherin as a tumor promoter, in addition to its established role as a tumor suppressor, suggested by the results of this functional analysis.

While the reduction of E-cadherin expression has been reported in primary prostate cancer, the results of the analysis performed in chapter III illustrate a dual role for E-cadherin in the progression of prostate cancer, suggesting that the repression of E-cadherin expression observed in primary prostate cancer may need to be a transient event. This potential requirement for the transient repression of E-cadherin in the progression of prostate cancer coupled with the demonstrated significance of PI3K/AKT signaling in the progression of prostate cancer and the association of this signaling with EMT-like events in several other types of cancer, led me to hypothesize that PI3K/AKT signaling may lead to the

EMT-like transcriptional repression of *E-cadherin* via Snail in prostate cancer. I describe the functional analysis performed to examine this hypothesis and discuss the implications of this analysis regarding the regulation of both E-cadherin based adherens junctions and DSG2 based desmosomes in prostate cancer in chapter IV.

Though the reduction of E-cadherin expression has been reported in primary prostate cancer, no large-scale study has yet examined the association of E-cadherin expression and biochemical recurrence in prostate cancer; and, as mentioned previously, the expression of DSG2 in prostate cancer had been unexplored to date. Chapter V describes the analysis of E-cadherin and DSG2 expression in primary prostate cancer tissue performed for a large cohort of patients with prostate cancer who underwent radical prostatectomy. I discuss the demonstrated utility of these cadherins as markers of aggressive prostate cancer, and describe the analysis of pAKT and Snail expression performed for this cohort. The chapter concludes with a discussion of the results of this analysis regarding the regulation of E-cadherin based adherens junctions and DSG2 based desmosomes in prostate cancer.

The work presented in this thesis provides the first examination of the expression of desmosomal cadherins in both normal prostate tissue and prostate cancer, and suggests that the loss of E-cadherin and DSG2 expression in primary prostate cancer may be regulated by separate mechanisms. Further, this study provides evidence for a new role for E-cadherin in promoting the formation of primary and metastatic tumors, and demonstrates that the transient repression

of E-cadherin in prostate cancer can be mediated by the PI3K/AKT signaling pathway. Finally, the work presented provides the first demonstration of the utility of E-cadherin and DSG2 as markers of aggressive prostate cancer.

Chapter II

Expression of Desmosomal Cadherins in Normal Human Prostate and Human Prostate Cancer Cell Lines

Chapter II.1

Overview

While the presence of E-cadherin containing adherens junctions in the prostate is well established, and the presence of desmosomes in the prostate has been described, the expression profile of desmosomal cadherins in normal human prostate has not been well characterized, to date (Umbas et al., 1992; Fisher and Jeffrey, 1965). As mentioned previously, desmosomes are found in tissues that undergo a high degree of mechanical stress, and loss of desmosomal adhesion is associated with diseases affecting the skin, hair, and heart. The expression of desmosomal cadherins has been thoroughly characterized in the epidermis and hair follicle. The epidermis is a continuously self-renewing tissue that is made up of several cell layers. The basal layer is the epidermal cell layer closest to the dermis that directly contacts the basement membrane and contains the least differentiated keratinocytes; this layer is followed by the spinous layer, the granular layer, and the stratum corneum which is the most superficial of the epidermal cell layers and is comprised of the most differentiated dead keratinocytes (Kanitakas, 2002). As keratinocytes differentiate, the expression patterns of their keratins change. The less differentiated keratinocytes in the basal layer express keratins 5 and 14, while the more differentiated keratinocytes in the spinous layer express keratins 1 and 10 (Ishida-Yamamoto et al., 2002). Like keratins, the expression pattern of desmogleins and desmocollins changes as keratinocytes differentiate. The less

differentiated keratinocytes in the basal layer express DSG2, DSC2, DSG3, and DSC3 while the more differentiated keratinocytes of the spinous layer express DSG1 and DSC1 (Yin and Green, 2004). Analysis of interfollicular epidermis via immunofluorescence (Bazzi and Getz et al., 2006) has shown that DSG4 is found in the highly differentiated upper spinous and granular layers. While the expression of DSG4 in the epidermis overlaps with that of DSG1 and DSC1 for the most part, it also extends beyond DSG1 and DSC1 expression into the uppermost cells of the granular layer (Figure 1 and 2).

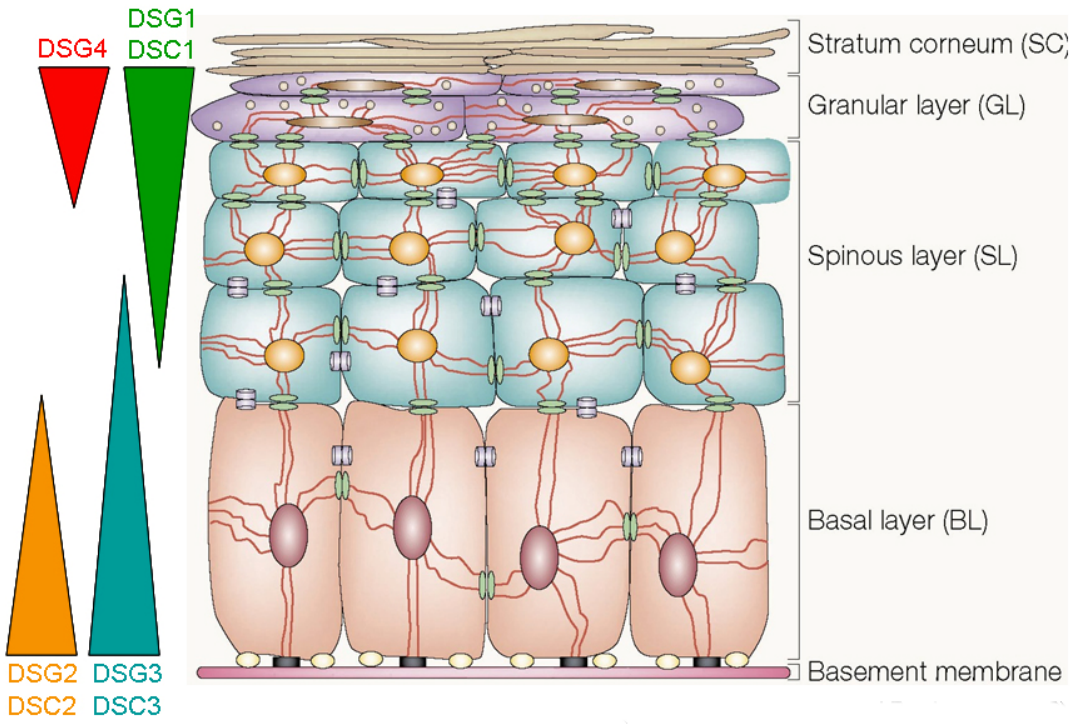

Figure1: Desmosomal cadherin expression in the human epidermis (Adapted from Fuchs and Raghavan, 2002)

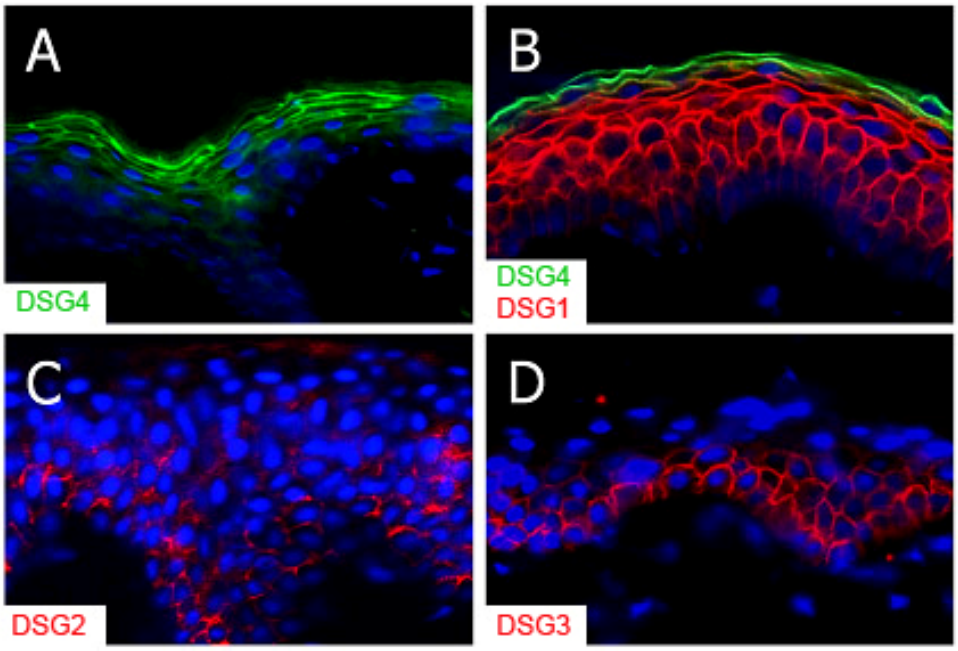

Figure 2: Desmoglein expression in the human epidermis (Bazzi and Getz et al., 2006)

The hair follicle (HF) is composed of concentric epithelial sheets that arise due to signaling from the dermal papilla to neighboring matrix cells which results in their proliferation and differentiation. As the matrix cells withdraw from the cell cycle they move away from the dermal papilla in concentric cylinders forming the three cell layers of the inner root sheath (IRS) — Henle's layer, Huxley's layer, and the IRS cuticle — and the three cell layers of the hair shaft — the hair cuticle, the cortex, and the medulla. The IRS is surrounded by the companion layer and outer root sheath (ORS), the latter of which is contiguous with the epidermis and is composed of the first matrix cells to lose contact with the dermal papilla during the original downward growth of the hair follicle (Fig. 4) (Fuchs et al., 2001). The expression of DSG1 is found in the IRS at the lower portion of the HF. DSG2 is expressed in precortical trichocytes and the lower hair cuticle as

well as ORS in the region above the precortex. DSG3 is expressed in the lower precortical trichocytes as well as the ORS in the upper follicle and the medulla. DSG4 is found in the cells of the precortex and extends to the cortex and cuticle of the hair shaft, as well as the inner root sheath cuticle. Interestingly, DSG4 is the only desmoglein represented in the hair shaft cortex (Fig 5) (Bazzi et al., 2006; Kurzen et al., 1998). Taken together with the observed expression of DSG4 in the epidermis, these findings indicate that DSG4 is uniquely expressed in the most highly differentiated and mechanically stressed cells of the epidermis and hair shaft.

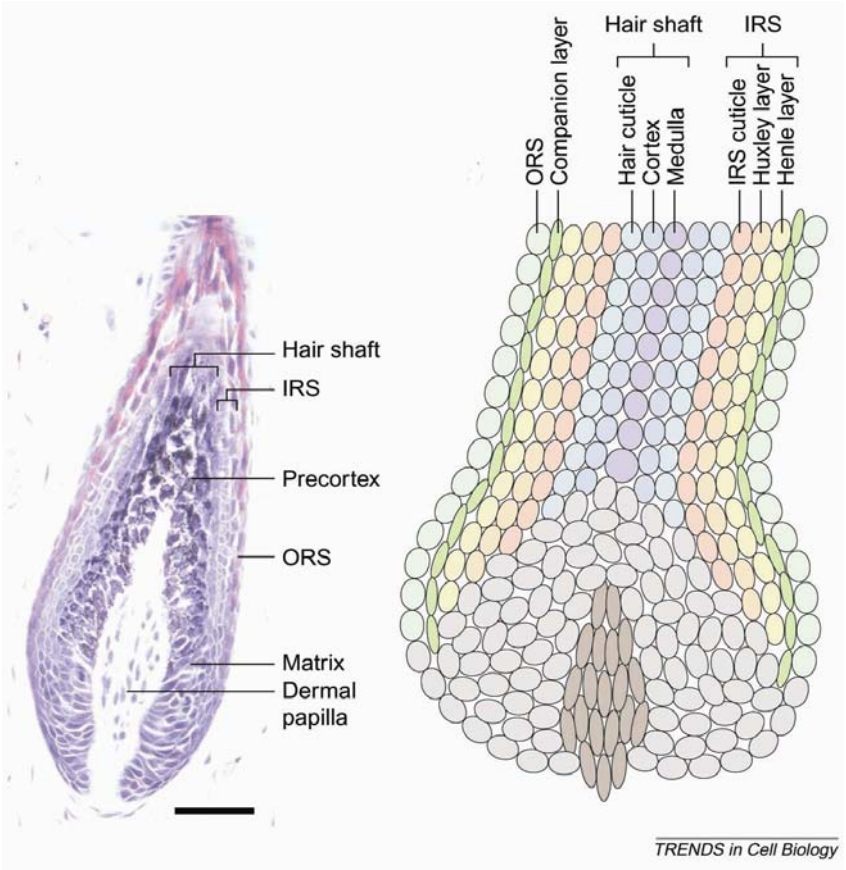

Figure 3: Anatomy of the hair follicle. (Adapted from Niemann and Watt, 2002.)

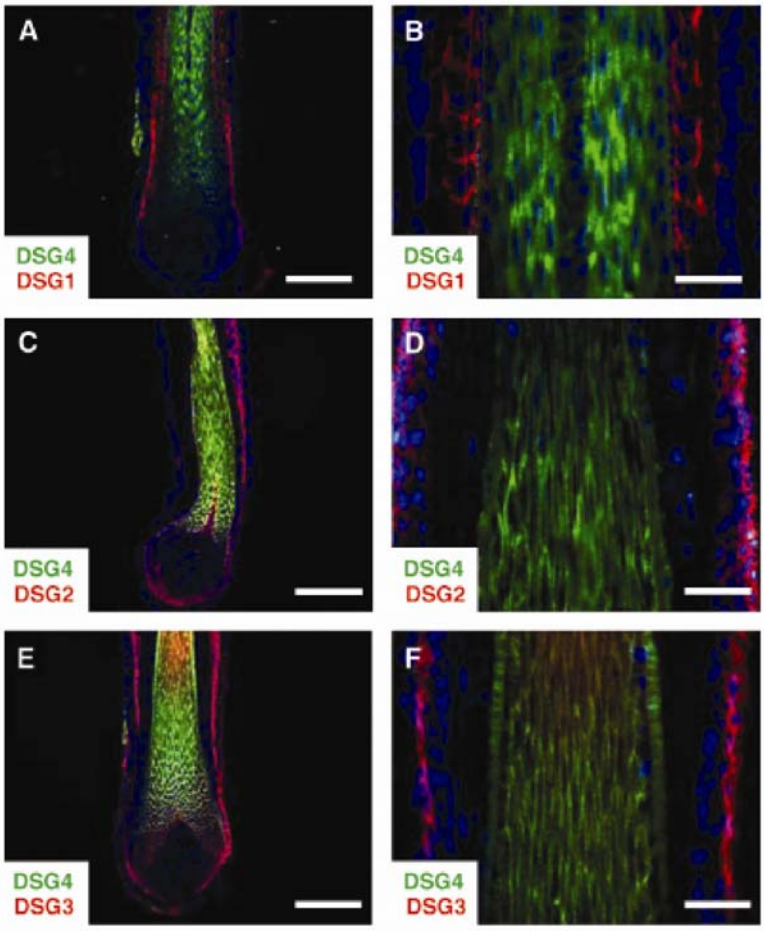

Figure 4: Expression of desmogleins in the hair follicle (Bazzi and Getz et al., 2006)

The expression of DSG2 is known to be ubiquitous in all desmosome forming tissues; however, the expression of the remaining desmosomal cadherins outside of the epidermis and hair follicle is poorly understood (Schafer et al., 1996). A study by Whittock and Bower in 2003 utilized RT-PCR to analyze the expression of *DSG4* in a panel of tissues and found that *DSG4* could be detected in several tissues including the prostate, suggesting that the desmosomal cadherin expression profile of the prostate may extend beyond the ubiquitous expression of DSG2. To examine this idea, in chapter II.2 I characterized the expression of desmosomal cadherins in normal human

prostate and determined the cell type in which prostate specific desmogleins are expressed. Interestingly, only DSG2, DSC2, and DSG4 were found to be expressed in normal human prostate at both the RNA and protein level.

Though aberrant expression of desmosomal cadherins has been reported in several types of cancer as described in Chapter I.10, the expression of desmosomal cadherins in prostate cancer has not been thoroughly analyzed to date. In chapter II.3 I sought to determine whether the expression of prostate specific desmogleins is altered metastatic prostate cancer cell lines. While DSG2 and DSG4 are expressed in normal human prostate, only DSG2 can be detected in the metastatic prostate cancer cell lines. I discuss the prostate specific desmosomal cadherin expression of DSG2, DSC2, and DSG4 in normal human prostate as well as the expression of DSG2 in metastatic prostate cancer cell lines in chapter II.4. The methods used to characterize the expression of desmosomal cadherins in normal human prostate and human metastatic prostate cancer cell lines is described in chapter II.5.

Chapter II.2

The Expression of Desmosomal Cadherins in Normal Human Prostate

The first goal of this study was to determine the desmosomal cadherin expression profile of normal human prostate tissue using RT-PCR and immunofluorescence analysis. RT-PCR analysis showed that most desmosomal cadherins, with the exception of *DSG1*, could be detected in normal human

prostate at the RNA level (Figure 5). However, immunofluorescence analysis revealed that only the expression of DSG2, DSC2, and DSG4 could be readily and consistently detected in the prostate at the protein level (Figure 6).

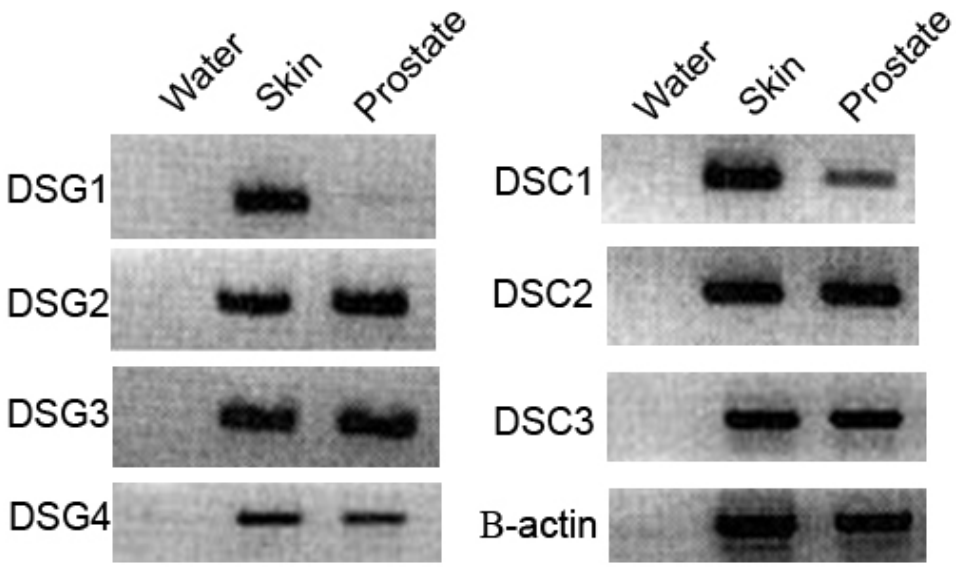

Figure 5: RT-PCR analysis of desmosomal cadherin expression in normal human prostate. Expression of mRNA can be detected for most desmosomal cadherins.

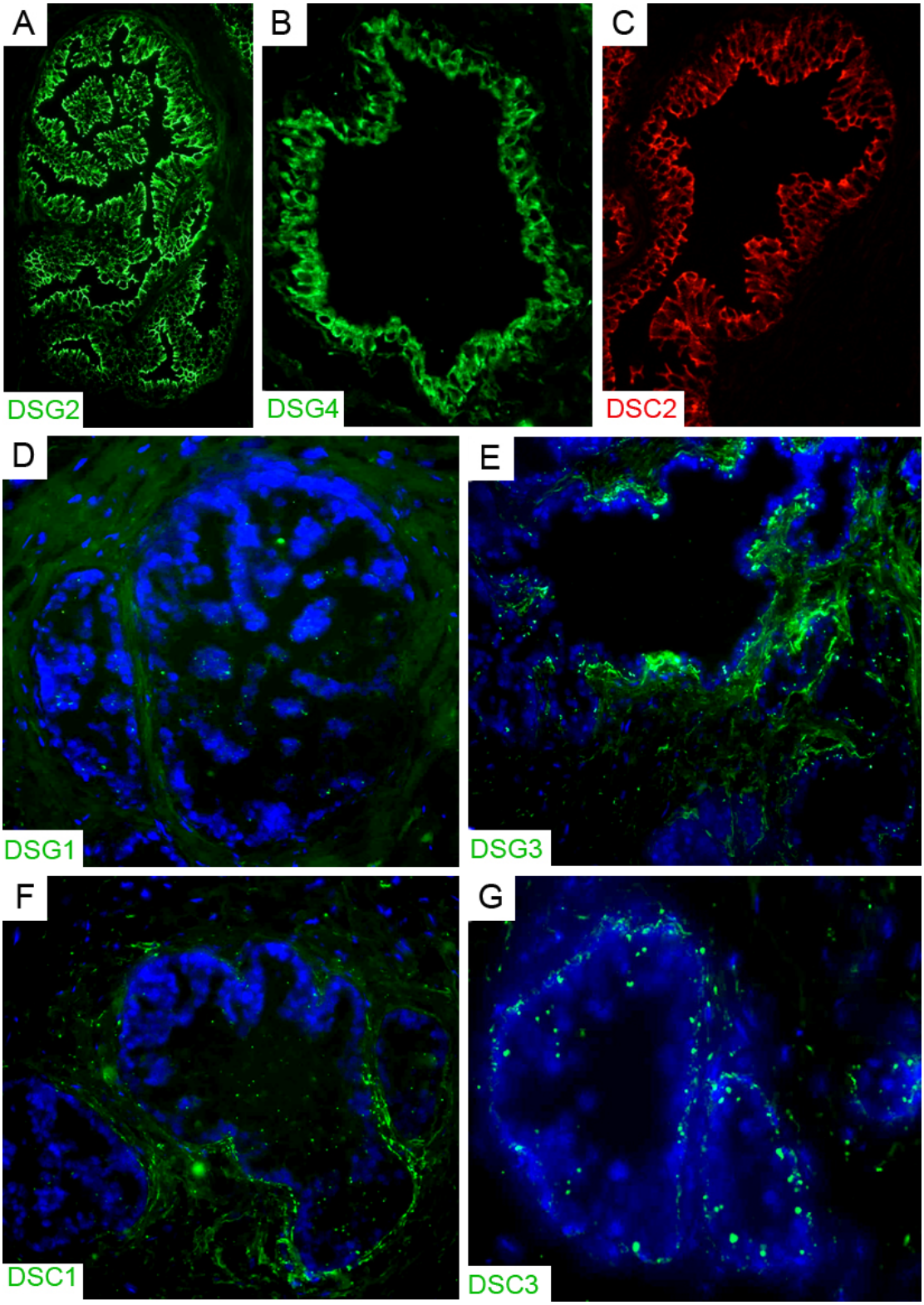

Figure 6: Immunofluorescence analysis of desmosomal cadherin expression in normal human prostate. DSG2 (A), DSG4 (B), and DSC2 (C) are detected at the cell border in normal human prostate. Cell border expression of DSG1 (D), DSG3 (E), DSC1 (F), and DSC3 (G) cannot be detected.

Having established the expression of desmosomal cadherins in normal human prostate, the next goal of this study was to determine the cell type specific expression of DSG2 and DSG4. Co-immunofluorescence analysis was performed to examine the localization of DSG2 and DSG4 with K14 — a keratin specifically expressed in the basal cells of the prostate — and prostate specific antigen (PSA) — a protein secreted by the luminal cells of the prostate. Co-immunofluorescence analysis of DSG2 and K14 shows that DSG2 is robustly expressed in the luminal cells of the prostate and that this expression rarely colocalizes with that of basal K14 expression (Figure 7A-C). The expression of DSG4 is very similar to that of DSG2, showing strong expression in the luminal cells, colocalization with luminal PSA expression, and rare colocalization with basal K14 expression (Figure 7D-I). While analysis of DSG2 and PSA expression could not be performed as the antibodies for these antigens were made in the same animal and are therefore incompatible, the expression of DSG2 was found to colocalize with that of DSG4 (Figure 7J-L). Taken together these results show that the expression of DSG2 and DSG4 is mainly restricted to the luminal cells of the human prostate.

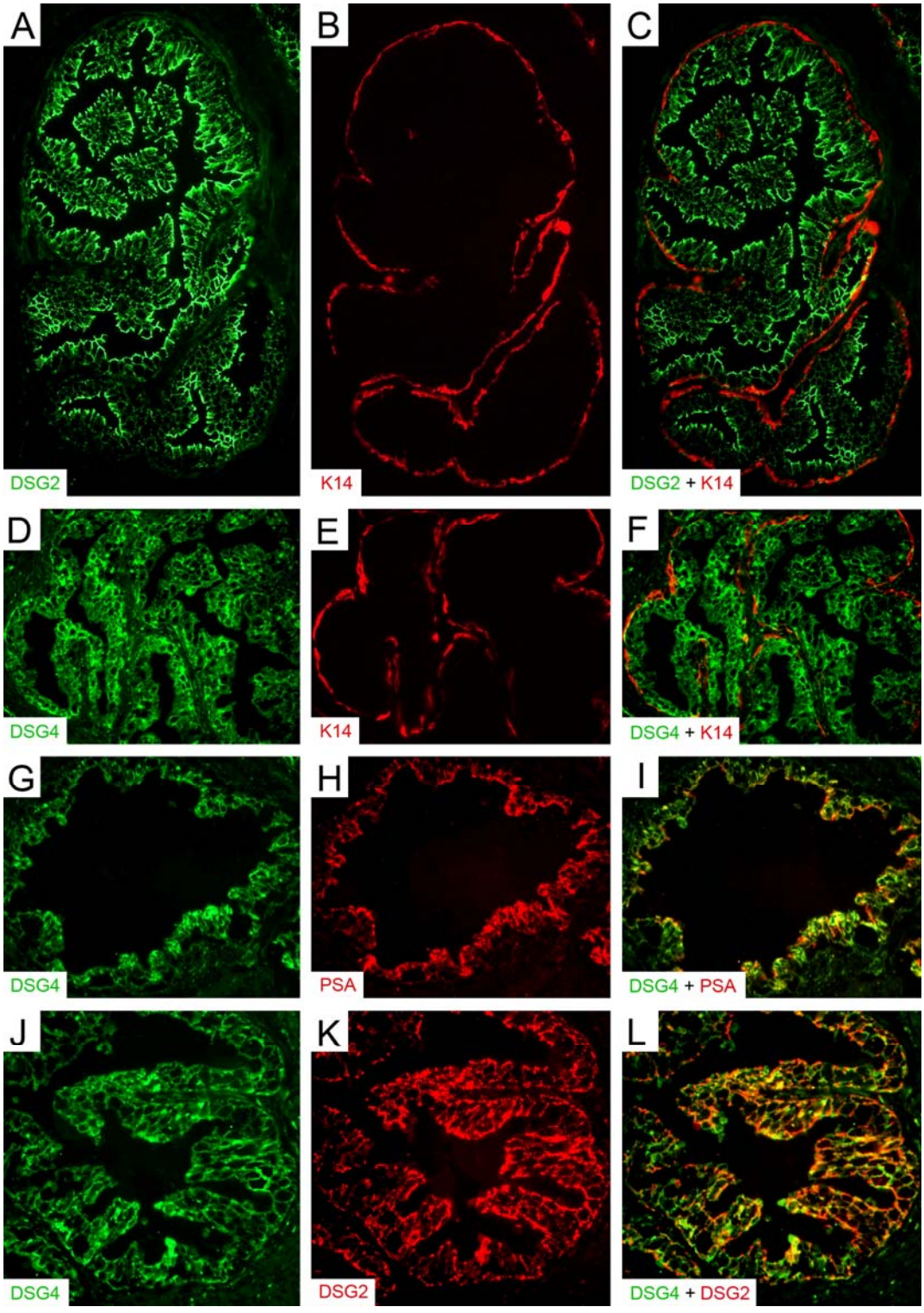

Figure 7: Co-immunofluorescence analysis of DSG2 and DSG4 and prostate cell type specific markers. DSG2 is expressed in the luminal cells and this expression rarely colocalizes with basal cell K14 expression (A-C). DSG4 is also expressed in the luminal cells and rarely colocalizes with basal cell K14 expression (D-F), however DSG4 expression does colocalize luminal cell PSA expression. The expression of DSG4 also colocalizes with that of DSG2 in the luminal cells (J-L).

Chapter II.3

The Expression of DSG2 and DSG4 in Human Prostate Cancer Cell Lines

The discovery that DSG2 and DSG4 show a high level of expression in normal human prostate led me to ask whether these proteins were expressed in human prostate cancer cell lines. To examine this question, qRT-PCR was performed on metastatic human prostate cancer cell lines (Figure 8). The cancer cell lines utilized for this portion of the study include the LNCaP cell line, which was derived from a prostate cancer that metastasized to the lymph node; the PC3 cell line, which was derived from a prostate cancer that metastasized to the bone; and the DU145 cell line, which was derived from a prostate cancer that metastasized to the brain (Horoszewicz et al., 1980; Kaighn et al., 1979; Stone et al., 1978). The BPH-1 cell line served as a positive control for this study. This cell line is an immortalized, non-tumorigenic prostatic epithelial cell line derived from a patient with benign prostatic hyperplasia, a condition which affects the stroma of the prostate (Hayward et al., 1995). The results of this qRT-PCR analysis show that that *DSG2* is expressed in all cell lines examined. Further, the expression of *DSG2* is greater in all the metastatic prostate cancer cell lines examined than it is in the non-tumorigenic BPH-1 control. Conversely, though expressed in the BPH-1 control, the expression of *DSG4* is undetectable in all metastatic prostate cancer cell lines examined.

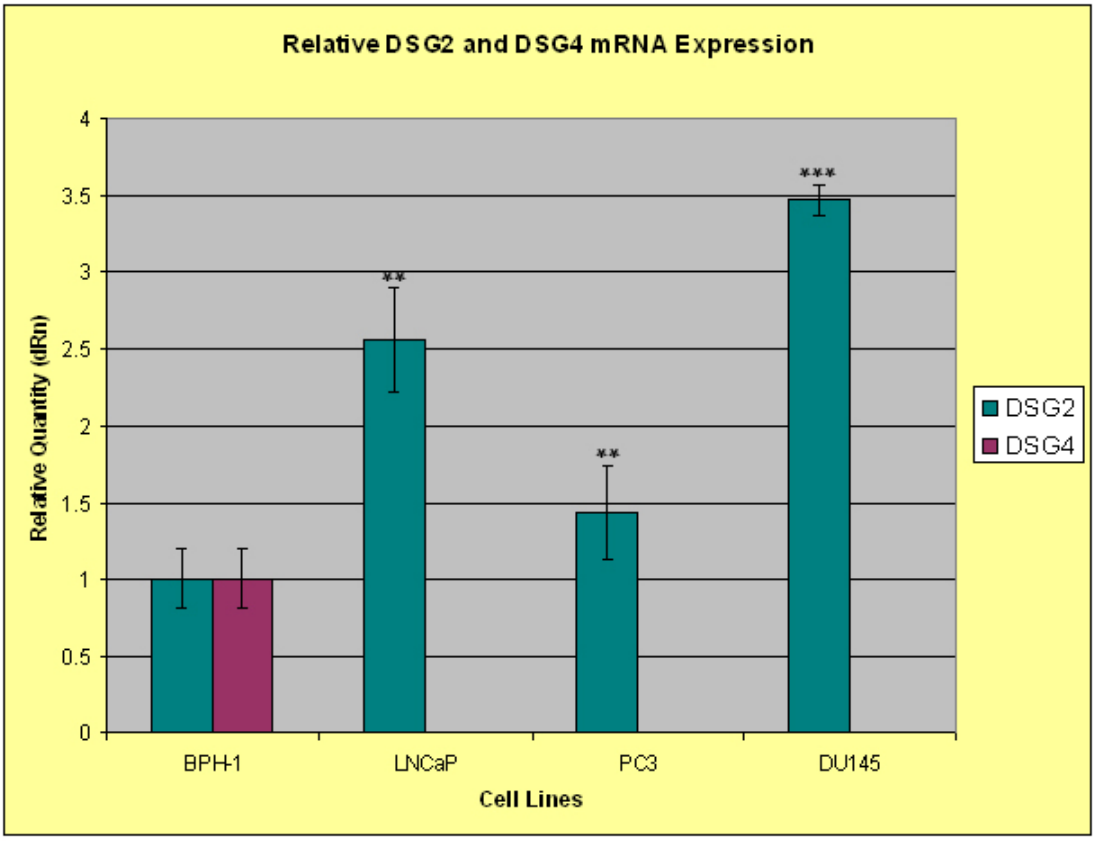

Figure 8: qRT-PCR of *DSG2* and *DSG4* in human metastatic prostate cancer cell lines. *DSG2* expression is detected in all cell lines examined, while *DSG4* expression is not detected in any of the prostate cancer cell lines. Scale bars represent standard deviation; (**) represents $P < 0.01$; (***) represents $P < 0.001$.

Next, immunofluorescence analysis was utilized to examine the expression of DSG2 in these metastatic human prostate cancer cell lines at the protein level (Figure 9). Cell border expression of DSG2 was detected in BPH-1, LNCaP, and DU145 cells. However, PC3 cells lack the expression of DSG2 at the cell border, while a small population of cells shows only a diffuse granular staining for DSG2 in the cytoplasm. These results are consistent with reported ultrastructural analysis of prostate cancer cell lines grown in spheroid cultures showing that LNCaP cells form extensive cell-cell contacts with detectable desmosomes while PC3 cells are capable of forming only loose cell aggregates

with few cell-cell contacts (Hedlund et al., 1999). The results of the qRT-PCR and immunofluorescence analysis show that the expression of *DSG4* is absent in prostate cancer cell lines, while the expression of *DSG2* is present. Further, in most of the prostate cancer cell lines examined, DSG2 localizes to the cell border suggesting that desmosomal formation is retained in most metastatic prostate cancer cell lines examined *in vitro*.

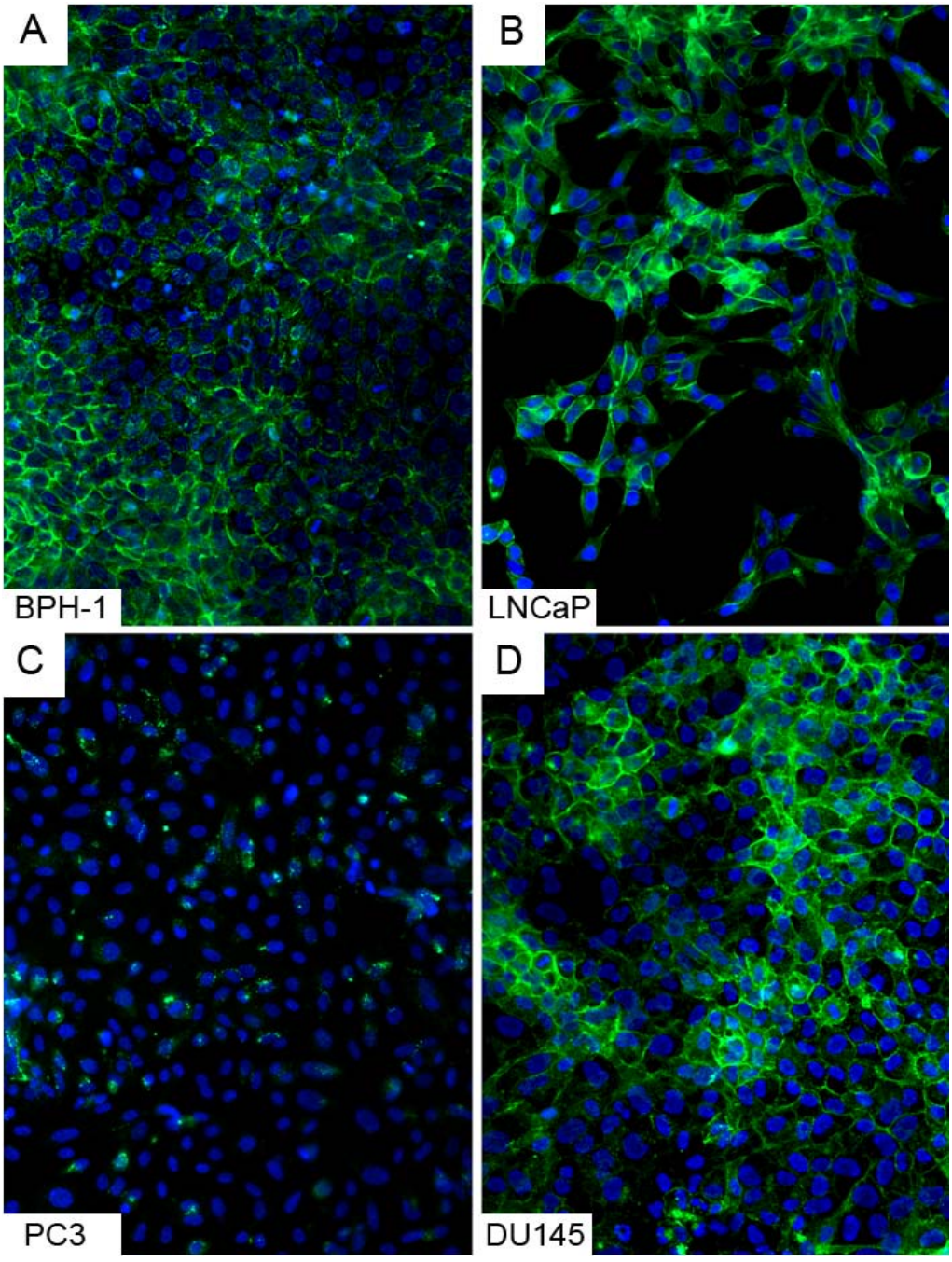

Figure 9: Immunofluorescence analysis of DSG2 in metastatic prostate cancer cell lines. DSG2 is expressed at the cell border of LNCaP (B) and DU145 (D) cells, however expression is not detected in PC3 cells (C).

Chapter II.4

Discussion

Prior to this study, the expression of desmosomal cadherins in normal human prostate had not been thoroughly examined. The results presented in this chapter show that while most desmosomal cadherins are expressed in the human prostate at the RNA level, only DSG2, DSC2, and DSG4 are consistently expressed at a high level in normal human prostate at the protein level. Though desmosomal cadherin mediated cell-cell adhesion has been shown to occur via heterophilic interactions between the extracellular domains of desmogleins and desmocollins, this idea of heterophilic interaction is somewhat controversial, as homophilic binding of desmosomal cadherins has also been reported (Chitaev et al., 1997; Syed et al., 2002). Biochemical analysis of the binding affinity of desmosomal cadherins shows that desmocollins are able to engage in homophilic and heterophilic interactions, while desmogleins preferentially engage in heterophilic interactions with desmocollins (Syed et al., 2002). The observation that desmogleins preferentially interact with desmocollins *in vitro* suggests that desmosomal cadherin based adhesion in the prostate may be mediated via heterophilic interactions of DSG2 and DSG4 with DSC2.

Further, the expression of DSG2 and DSG4 was found to be largely restricted to the luminal cells of the prostate. In both the epidermis and the hair shaft, DSG4 is found in cells that undergo the highest degree of mechanical stress within their respective tissues. While the prostate epithelium is not mechanically stressed to the degree of the epidermis or hair shaft, the exposure

of this epithelium to the movement of prostatic fluid does subject the luminal cells to a mechanical force. Given that this tissue is relatively dormant with respect to cell proliferation, luminal cells must be protected from this regular mechanical force to prevent them from being sloughed off. The expression of DSG4 in the most mechanically stressed layers of the epidermis and hair shaft suggests that this desmoglein may provide for stronger adhesion than the other desmoglein isoforms. The presence of DSG4 in the human prostate may then provide an additional level of adhesive strength in the desmosomes of luminal cells beyond that provided by DSG2 alone. Interestingly, the expression of DSG2 is present in metastatic prostate cancer cell lines *in vitro,* while the expression of *DSG4* is absent in all cancer cell lines examined. If the presence of DSG4 does in fact confer an additional degree of adhesive strength, this finding may reflect a need for cell-cell adhesion in metastatic cells that is strong enough to maintain the integrity of a metastatic tumor, yet not so strong as to prevent invasive behaviors.

In summary, the results presented in this chapter provide the first characterization of desmosomal cadherin expression in normal human prostate and metastatic prostate cancer cell lines. Given that *DSG4* is undetectable in metastatic prostate cancer cell lines coupled with limitations of the antibodies generated against DSG4 to usage on only frozen tissue samples, DSG4 will not be examined beyond this chapter. However, the role of DSG2 in aggressive prostate cancer will be further explored in chapters III, IV and V.

Chapter II.5

Materials and Methods

Cell Culture and RNA Isolation

The BPH-1 cell line (a generous gift from Dr. Ralph Buttyan) was cultured in RPMI with 10% fetal bovine serum (FBS) (Invitrogen, Carlsbad, CA, USA). The DU145 human prostate cancer cell line (ATCC, Manassas, VA, USA) was cultured in MEM with 10% fetal bovine serum (Invitrogen, Carlsbad, CA, USA). The PC3 human prostate cancer cell line (ATCC, Manassas, VA, USA) was cultured in F12K with 10% FBS (Invitrogen, Carlsbad, CA, USA). The LNCaP human prostate cancer cell line (ATCC, Manassas, VA, USA) was cultured in RPMI with 10% FBS (Invitrogen, Carlsbad, CA, USA).

To isolate RNA, cells grown four days past confluency were washed in 1X PBS, trypsinized, and pelleted via centrifugation. The cell pellets were resuspended in 1X PBS and then pelleted via centrifugation to wash. This wash step was repeated twice to remove all traces of media prior to harvesting RNA. RNA was then harvested using the RNeasy Mini Kit and QIAshredder following the manufacturer's protocol entitled "Purification of Total RNA from Animal Cells Using Spin Technology" (Qiagen, Valencia, CA, USA).

Antibodies

Anti-DSG3 (clone 5H10) and DSG1 (clone 27B2) mouse monoclonal antibodies have been previously described and were given to us as a generous

gift from Dr. James Wahl; both were used at a dilution of 1:10 for immunofluorescence analysis (Wahl, 2002). Anti-DSG2 mouse monoclonal antibody (clone 10G11) was purchased from ARP, Inc™ (Belmont, MA, USA) and used at a dilution of 1:50 for immunofluorescence analysis. Anti-DSG4 guinea pig polyclonal antibody, anti-DSC1 mouse monoclonal antibody, and anti-DSC3 mouse monoclonal antibody were generated by Dr. Lutz Langbein and given to us as a generous gift; the anti-DSG4 antibody was used at dilution of 1:2000 while both the anti-DSC1 and anti-DSC3 antibodies were used at a dilution of 1:10 for immunofluorescence analysis. Anti-DSC2 mouse monoclonal antibody (clone 7G6) was purchased from Santa Cruz Biotechnology, Inc (Santa Cruz, CA, USA) and used at a dilution of 1:200 for immunofluorescence analysis. Anti-K14 rabbit polyclonal antibody was purchased from Covance (Princeton, NJ, USA) and used at a dilution of 1:1000 for immunofluorescence analysis. Anti-PSA mouse monoclonal antibody was purchased from Dako (Carpinteria, CA, USA) and used at a dilution of 1:20 for immunofluorescence analysis. Alexa Fluor® 594 or Alexa Fluor® 488 secondary antibodies were purchased from Invitrogen (Carlsbad, CA, USA) and were used at a dilution of 1:600 for immunofluorescence analysis.

RT-PCR

Total RNA for human skin and prostate was purchased commercially (Agilent Technologies Inc., Santa Clara, CA, USA). First strand cDNA was made using Oligo dT and the SuperScript® II First-Strand Synthesis System

(Invitrogen, Carlsbad, CA, USA) following the manufacturer's instructions. PCR was performed using Platinum PCR Supermix (Invitrogen, Carlsbad, CA, USA) and primers for the transcript of interest (listed in Table 1). The following PCR protocol was used: step 1: 94ºC for 3 min; step 2: 94 ºC for 30 sec, 56 ºC for 45 sec, 72ºC for 2min; step 3: 72 ºC for 10 min; repeat step 2 for 34 cycles. PCR products were electrophoresed on a 1% agarose/1X TBE gel containing ethidium bromide and visualized using Kodak Electrophoresis Documentation and Analysis System 120 Camera (Kodak, Rochester, NY, USA).

Table 1: RT-PCR Primers and qRT-PCR Primers

RT-PCR Primers		
Transcript	Forward Primer	Reverse Primer
DSG1	5'-CACTCAGATTGTGCTGCAAAC-3'	5'-GTCCTGCAAATGTAGCCATTG-3'
DSG2	5'TCTTGAGGCCCTATGCAGTT-3'	5'-GCTGCACTCAACTCTTCAAC-3'
DSG3	5'-GAGATGACTATGCAACAAGCT-3'	5'-TTCTCTACATCTAGTCCTTGG-3'
DSG4	5'-ATGGATTGGCTCTTCTTCAGA-3'	5'-ACTCTAAGCTCAAGAGGCCT-3'
DSC1	5'-GCGATGCTTGTCAGAAAGTTT-3'	5'-GTTTTCTCTTGCTGACAGTAC-3'
DSC2	5'-CCTGAAAGAGTGCTTTACAGC-3'	5'GCATCGAACAAGGAATTGGAG-3'
DSC3	5'-TTGGAAGAGTGCTTCAGGTCT-3'	5'-ATTCTCTTGCATAGAGCAAGG-3'
β-actin	5'-GATGATGATATCGCCGCGCT -3'	5'-CCTGGATAGCAACGTACATG-3'
qRT-PCR Primers		
DSG2	5'-ATCAATGCAACAGATGCAGATGA-3'	5'-TGTCAAAGTGTAGCTGCTGTGT-3'
DSG4	5'-CTGAATTCACGGGGTGAAGATT-3'	5'-CATCTGCATCTGTGGCACATAA-3'
β-actin	5'-AAACTGGAACGGTGAAGGTG-3'	5'-GTGGCTTTTAGGATGGCAAG-3'

qRT-PCR

RNA was harvested from cell lines of interest as described. First strand cDNA was made using Oligo dT and the SuperScript® III First-Strand Synthesis System (Invitrogen, Carlsbad, CA, USA) following the manufacturer's instructions. qRT-PCR was performed on a Stratagene Mx3005P machine and analyzed using Stratagene MxPro QPCR software (Stratagene, Santa Clara, CA, USA). All reactions were performed using QuantiTect™ SYBR® Green PCR Master Mix (Qiagen, Valencia, CA, USA), 200nM primers (shown in Table 1), and 10ng cDNA in a 20 µL reaction volume. The following PCR reaction was used: step 1: 95 ºC for 10 min; step 2: 95 ºC for 15 sec, 60 ºC for 1 min; repeat step 2 for 40 cycles. All samples were run in quadruplicate, and samples were normalized against an endogenous internal control, β-actin.

Immunofluorescence—Frozen Tissues and Cell Lines

Frozen normal human prostate tissue slides were obtained from the Columbia Tumor Bank Service in accordance with the Institutional Review Board of Columbia University Protocol #AAAB2447. Cell lines were grown on glass coverslips (Fisher, Pittsburgh, PA, USA) in 6-well tissue culture plates (BD Falcon, Bedford, MA, USA). Slides/coverslips were fixed in cold 100% methanol for 15 min at -20˚C. Slides/coverslips were then fixed in cold 100% acetone for 2 min at -20˚C. Slides/coverslips were washed in 1X phosphate buffered saline (PBS) with agitation, permeabilized with 1% Triton-X100 in 1X PBS at room

temperature for 5 min, and washed again in 1X PBS with agitation. Slides/coverslips were incubated in 0.1% Triton X-100/ 1% bovine serum albumin (BSA)/ 1X PBS block at room temperature for 1 hour. Block was then aspirated, primary antibody was added, and slides/coverslips were incubated overnight at 4ºC. The following day slides/coverslips were washed in 1XPBS with agitation, then a 1:600 dilution of secondary antibody, either Alexa Fluor® 594 or Alexa Fluor® 488 (Invitrogen, Carlsbad, CA, USA), was added and slides/coverslips were incubated at room temperature for 45 min. Slides/coverslips were then washed in 1XPBS with agitation, immersed briefly in water and mounted using VECTASHIELD® mounting medium with DAPI (Vector Laboratories, Burlingame, CA, USA).

Chapter III

Functional Analysis of Cell-Cell Adhesion in Prostate Cancer

Chapter III.1

Overview

The loss of E-cadherin is a common occurrence in a variety of cancers including prostate cancer. In contrast, while aberrant desmosomal cadherin expression has been reported in several cancer types, the status of desmosomal cadherin expression in prostate cancer has not been explored to date.

As described in chapter I, the formation of adherens junctions has been shown to precede that of desmosomes in both early development and in the *de novo* formation of anchoring junctions. Additionally, *in vitro* analysis has shown that desmosomes are able to form only in the presence of a classic cadherin (Lewis et al., 1997). The reported downregulation of E-cadherin expression in prostate cancer and the reduced desmosomal cadherin expression reported in several cancer types, coupled with the classic model of *de novo* anchoring junction assembly led me to hypothesize that the loss of E-cadherin based adherens junctions in prostate cancer results in the loss of desmosomal adhesion. In chapter II, I established that the expression of DSG2 is present in both normal human prostate and human metastatic prostate cancer cell lines. In this chapter I sought to examine desmosomal adhesion in a prostate cancer environment lacking adherens junctions by focusing on the expression of DSG2 in the absence of E-cadherin expression.

In chapter III.2, I knocked down the expression of *E-cadherin* mRNA via the expression of an shRNAmir targeting *E-cadherin* in the DU145 prostate cancer cell line — a cell line that is positive for markers of both adherens junctions and desmosomes under normal conditions. I then characterized the expression of E-cadherin and DSG2 in the resulting EcadKD cell lines. Surprisingly, the expression of DSG2 remained relatively unperturbed even when *E-cadherin* expression was reduced to an almost undetectable level.

I next sought to examine the effects of disrupted adherens junction formation on tumorigenesis. In chapter III.3, I performed an *in vivo* tumorigenesis assay in NOD/SCID mice by injecting my cell lines of interest subcutaneously, allowing for tumor formation, and subsequently analyzing the resulting tumors for the expression of E-cadherin and DSG2. Interestingly, I found that the loss of E-cadherin based adherens junctions results in a dramatic reduction in the size of tumors formed despite the retention of desmosomal adhesion.

My final goal for this portion of the study was to examine the effects of this *E-cadherin* knockdown on extravasation and metastatic tumor colony formation. In chapter III.4, I performed an *in vivo* metastasis assay by injecting my cell lines of interest into the lateral tail vein of NOD/SCID mice, allowing for tumor formation, and subsequently analyzing the lungs of the injected animals for the formation of metastatic tumor colonies. Again, the loss of E-cadherin based adherens junctions had a dramatic effect on both the amount and overall size of tumors formed in the lungs of injected animals despite the retention of desmosomal adhesion. In chapter III.5, I describe the relationship between E-

cadherin based adherens junctions and desmosomal adhesion *in vitro* as well as the role of E-cadherin based adherens junctions and desmosomal adhesion in prostate tumorigenesis, extravasation, and metastatic tumor colony formation *in vivo*. The methods utilized for this portion of the study are described in chapter III.6.

Chapter III.2

In Vitro Analysis of Desmosomes and the Loss of Adherens Junctions in Prostate Cancer

The first goal of this study was to test the hypothesis that the loss of E-cadherin based adherens junctions in prostate cancer results in the loss of desmosomal adhesion. To accomplish this goal, I wanted to perform an *in vitro* examination of desmosomal adhesion in a prostate cancer environment lacking adherens junctions. The DU145 human metastatic prostate cancer cell line was utilized as the *in vitro* prostate cancer model system for this study. I chose to focus on this cell line, as cell border expression of both desmosomal (as described in chapter II.3) and adherens junction proteins are detected in the DU145 cell line under normal conditions (Mitchell et al., 2000).

To disrupt the formation of E-cadherin based adherens junctions in the DU145 cell line I utilized an shRNAmir targeting *E-cadherin*. DU145 cells were infected with an shRNAmir-*E-cadherin* retroviral construct and grown under selective conditions. Mutant DU145 cell lines stably expressing the shRNAmir-*E-*

cadherin construct (hereafter referred to as EcadKD cell lines) were selected and mRNA knockdown efficiency was analyzed via qRT-PCR (Figure 1). Most mutant cell lines showed a significant reduction in *E-cadherin* expression, with EcadKD9 showing a 99.6% reduction in *E-cadherin* expression. Cell lines with >80% knockdown of *E-cadherin* expression were chosen for further analysis. The expression of E-cadherin was examined at the protein level via immunofluorescence analysis in EcadKD2, EcadKD3, EcadKD5, and EcadKD9 (Figure 2). Consistent with the qRT-PCR results, the cell border expression of E-cadherin was noticeably reduced in all EcadKD cell lines as compared to the DU145 parental cell line. Importantly, the most striking reduction of E-cadherin expression was found in EcadKD9 where the cell border expression of E-cadherin was undetectable via immunofluorescence analysis and was shown to be dramatically reduced via Western analysis (Figure 2E, 2F).

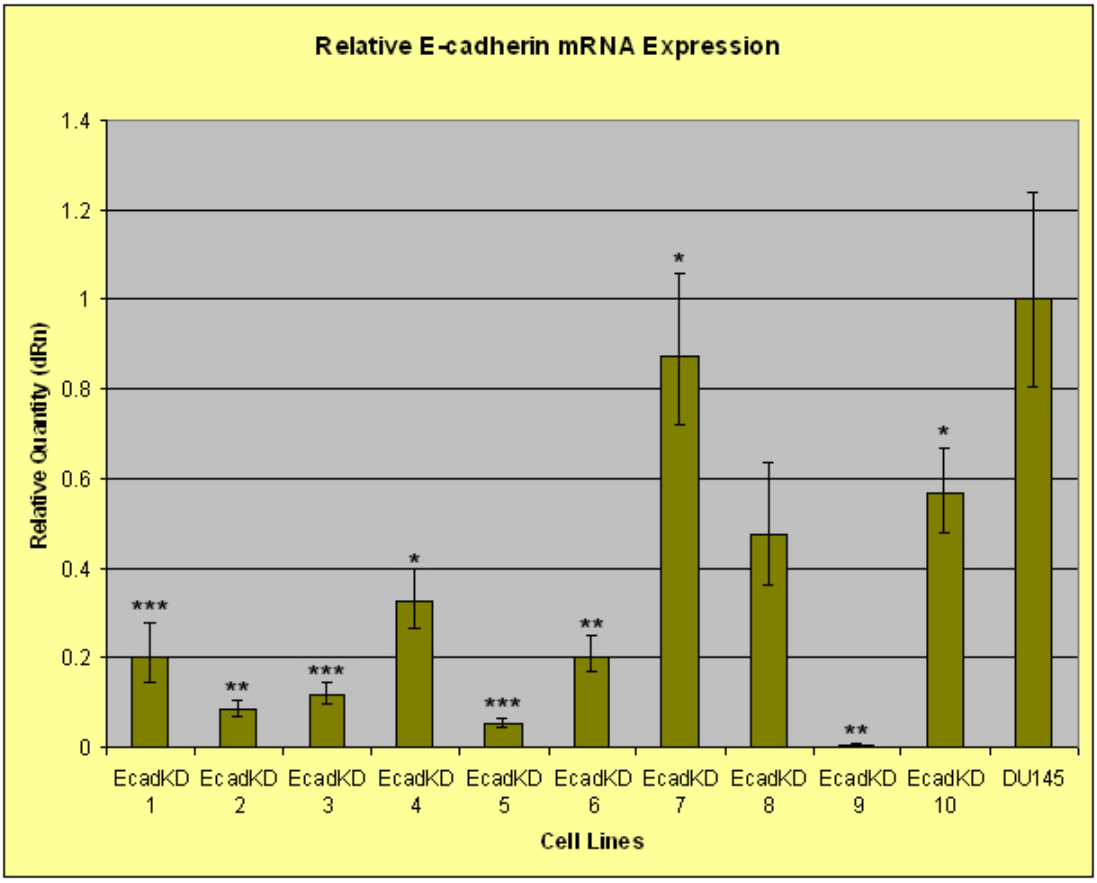

Figure1: qRT-PCR analysis of *E-cadherin* mRNA expression in DU145 cell lines stably expressing an shRNAmir-*E-cadherin* construct. EcadKD9 shows the most dramatic reduction of *E-cadherin* expression (99.6%). Scale bars represent standard deviation; (*) represents $P < 0.05$; (**) represents $P < 0.01$; (***) represents $P < 0.001$.

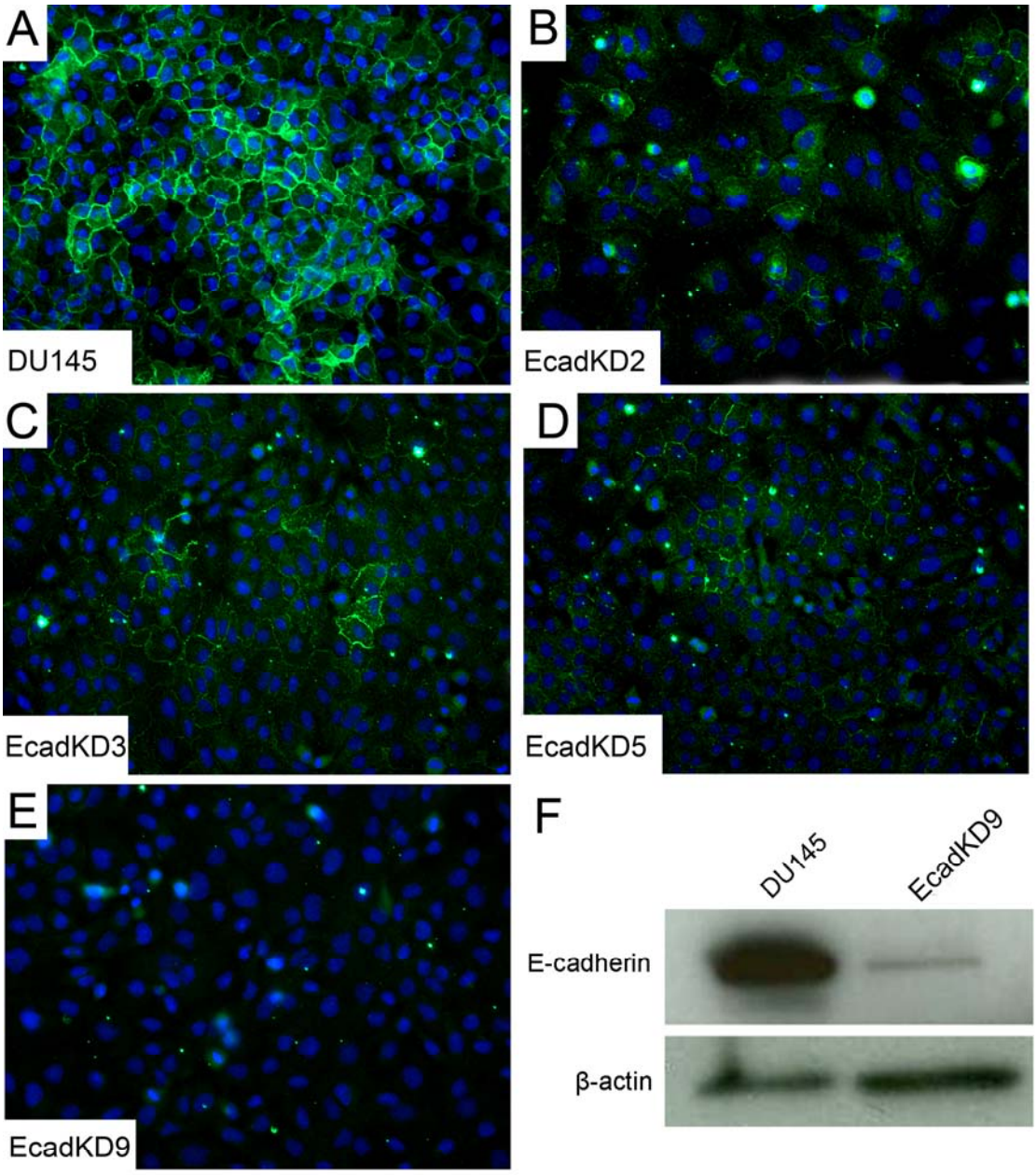

Figure 2: Immunofluorescence analysis of E-cadherin expression in EcadKD cell lines. All mutant cell lines examined show reduced expression of E-cadherin at the cell border as compared to the DU145 parental cell line (A-E). Notably, E-cadherin expression is undetectable at the cell border of EcadKD9 (E). Western analysis confirms the significantly reduced level of E-cadherin protein expression in EcadKD9 (F).

Having examined the expression of E-cadherin in the EcadKD cell lines, I next examined the expression of *DSG2* via qRT-PCR in the EcadKD cell lines showing a >80% knockdown of *E-cadherin* expression (Figure 3). Interestingly, despite the dramatic reduction in *E-cadherin* expression, the level of *DSG2* expression in the EcadKD cell lines was relatively unaffected. Most notably, the level of *DSG2* expression was only slightly lower (5.3%) in EcadKD9 than in the parental DU145 cell line. The expression of DSG2 at the protein level was then examined via immunofluorescence analysis in the EcadKD cell lines of interest (Figure 4). Consistent with the qRT-PCR findings, cell border expression of DSG2 was detected in all EcadKD cell lines examined. Importantly, the level of DSG2 in EcadKD9 was only slightly less than that of the parental DU145 cell line (Figure 4E, 4F).

In summary, the results of mRNA and protein expression analysis show that the expression of E-cadherin has been reduced to virtually undetectable levels in the EcadKD9 cell line. Unexpectedly, the expression of DSG2 is relatively unaffected by the reduction or loss of E-cadherin expression. This finding suggests that the formation of desmosomes in prostate cancer is not dependent upon the prior formation of adherens junctions. The effects of the loss of E-cadherin based adhesion in the presence of retained desmosomal adhesion on prostate tumorigenesis, extravasation, and metastatic tumor colony formation will be examined in chapters III.3 and III.4.

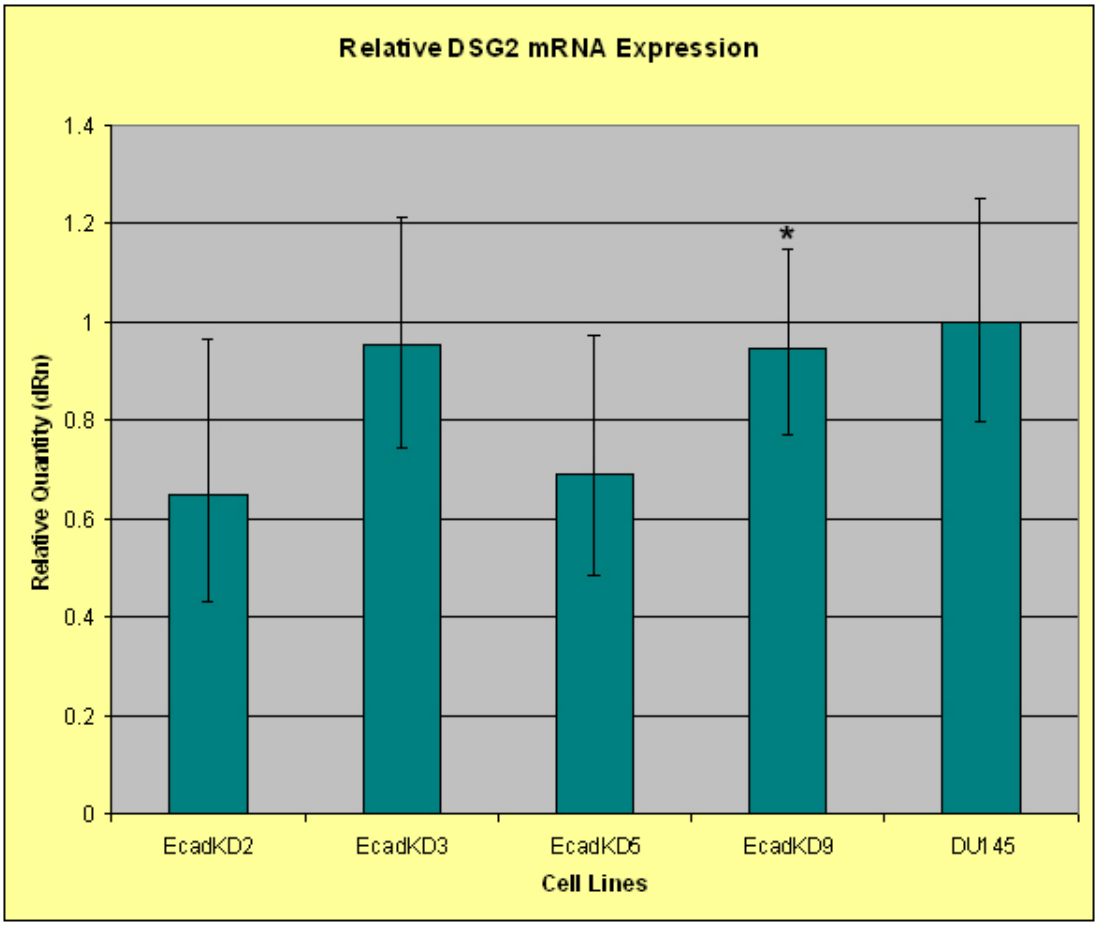

Figure 3: qRT-PCR analysis of *DSG2* mRNA expression in DU145 cell lines stably expressing an shRNAmir-*E-cadherin* construct. The level of *DSG2* expression is relatively unaffected in the EcadKD cell lines. Scale bars represent standard deviation; (*) represents $P < 0.05$.

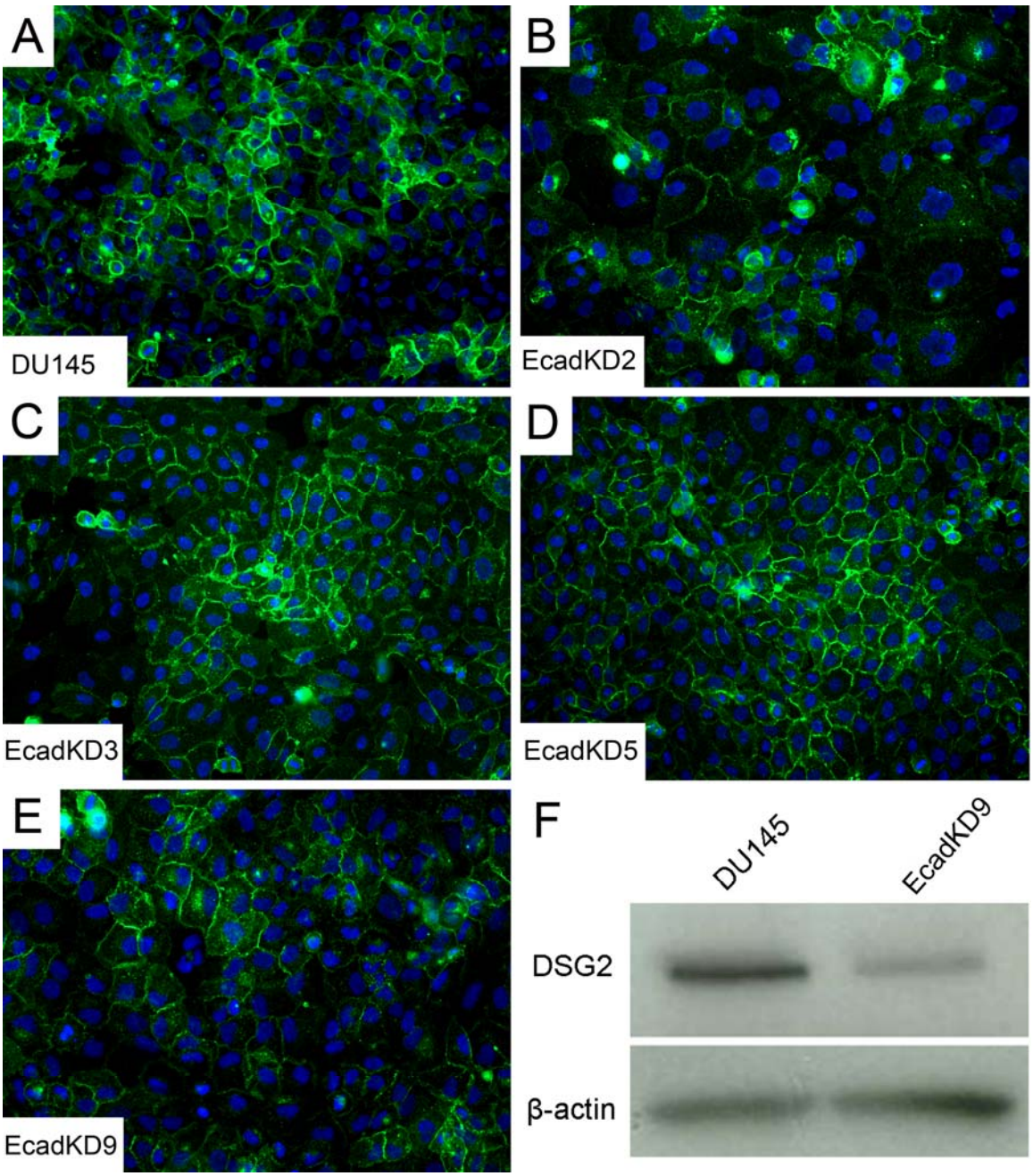

Figure 4: Immunofluorescence analysis of DSG2 expression in EcadKD cell lines. All mutant cell lines examined show expression of DSG2 at the cell border (A-E). Western analysis confirms DSG2 protein expression in EcadKD9 cells at a level slightly lower than that of the DU145 parental cell line (F).

Chapter III.3

In Vivo Tumorigenesis Analysis of Cell-Cell Adhesion in Prostate Cancer

Having found that the loss of E-cadherin based adherens junctions did not have an effect on the formation of DSG2 based desmosomes in the DU145 cell line *in vitro*, I next asked whether this loss of adherens junctions had an effect on the ability of the DU145 cell line to form tumors *in vivo*. Given that desmosomes are linked to the intermediate filament cytoskeleton and therefore provide a degree of strength greater than that of actin cytoskeleton linked adherens junctions, it is possible that desmosomal adhesion alone is sufficient to support the growing mass of cells that form a tumor. However, it is also possible that tumorigenesis may require a level of adhesion greater than that of desmosomal adhesion. To answer this question, I performed an *in vivo* tumorigenesis assay in which cells from the parental DU145 cell line and EcadKD9 were injected subcutaneously into the backs of age matched male immunodeficient NOD/SCID mice. Tumors were then allowed to grow for eight weeks at which point the mice were sacrificed and the tumors were collected for analysis. Two separate trials of the *in vivo* tumorigenesis assay were performed, and the combined results from these assays are discussed.

Interestingly, there was a striking difference between the size of the tumors formed by the parental DU145 cell line and those formed by EcadKD9 (Figure 5). The tumors formed by the DU145 parental cell line (Figure 5A, 5B,

5D) were large (1.33 cm^3 ± 0.71) while the tumors formed by EcadKD9 (Figure 5A, 5C, 5D) were significantly smaller by comparison (0.04 cm^3 ± 0.02; $P < 0.001$).

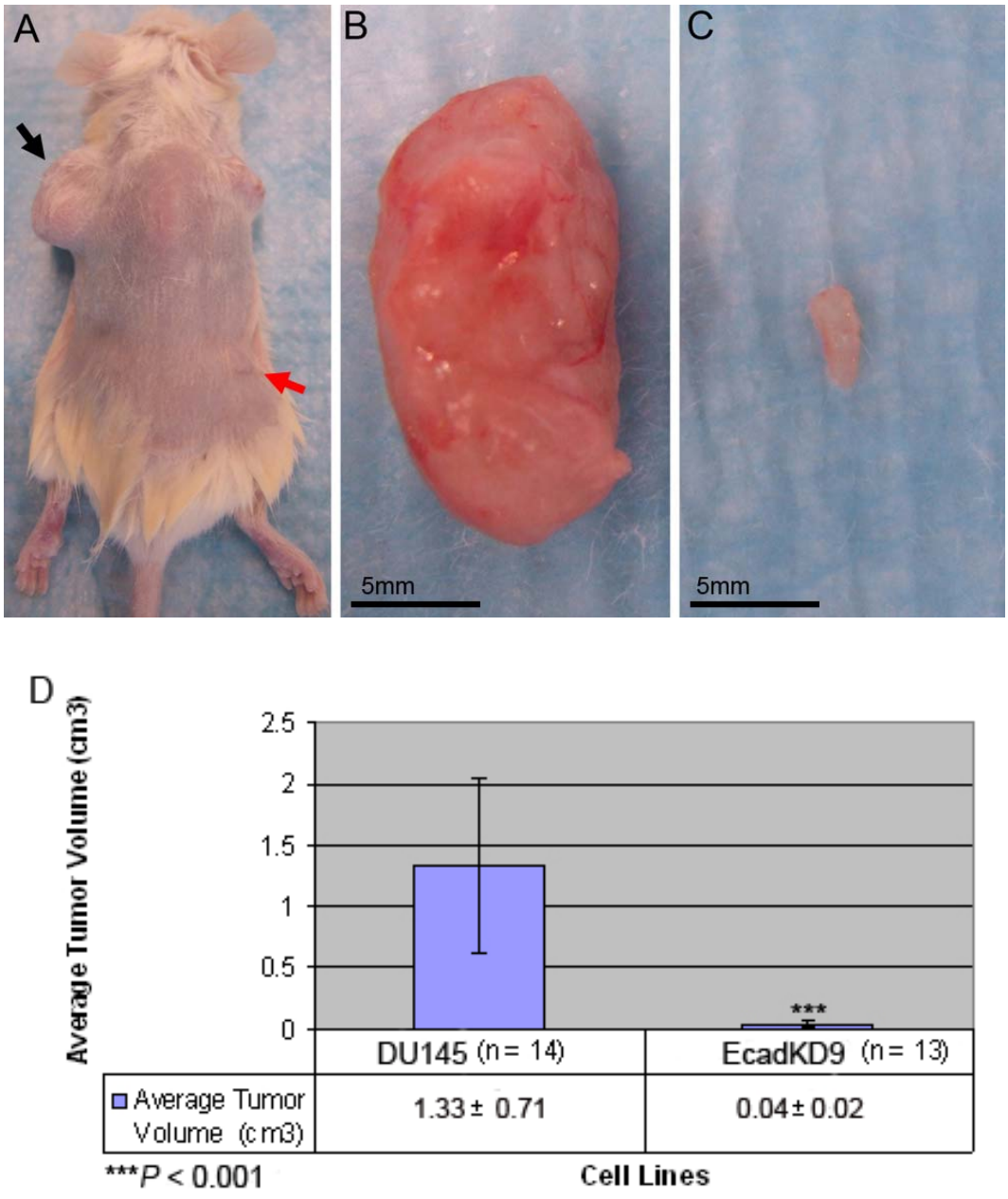

Figure 5: *In vivo* tumorigenesis assay. Cells from the DU145 parental cell line (A, black arrow) and EcadKD9 (A, red arrow) were injected subcutaneously in NOD/SCID mice. The DU145 parental cell line produced large tumors (B and D) while EcadKD9 produced tumors that were significantly smaller (C and D). Scale bars represent standard deviation.

Frozen OCT embedded sections of the tumors were then analyzed for the expression of E-cadherin and DSG2 via immunofluorescence to ensure that the cadherin expression profile observed *in vitro* was maintained in the tumors formed *in vivo* (Figure 6). Indeed the DU145 parental cell line formed tumors with robust expression of both E-cadherin and DSG2 at the cell-cell border (Figure 6A and 6C), while tumors formed by the EcadKD9 cell line showed robust expression of only DSG2 at the cell-cell border (Figure 6B and 6D). Faint expression of E-cadherin was sometimes detectable in the EcadKD9 tumors, though this expression was highly irregular as it was only detected in small areas of the tumor and the classic chicken-wire pattern of expression was not observed. Taken together these results strongly suggest that the loss of E-cadherin based adherens junctions dramatically impairs prostate tumorigenesis. These results also suggest that the presence of DSG2 based desmosomal adhesion alone is not sufficient to support prostate tumor formation.

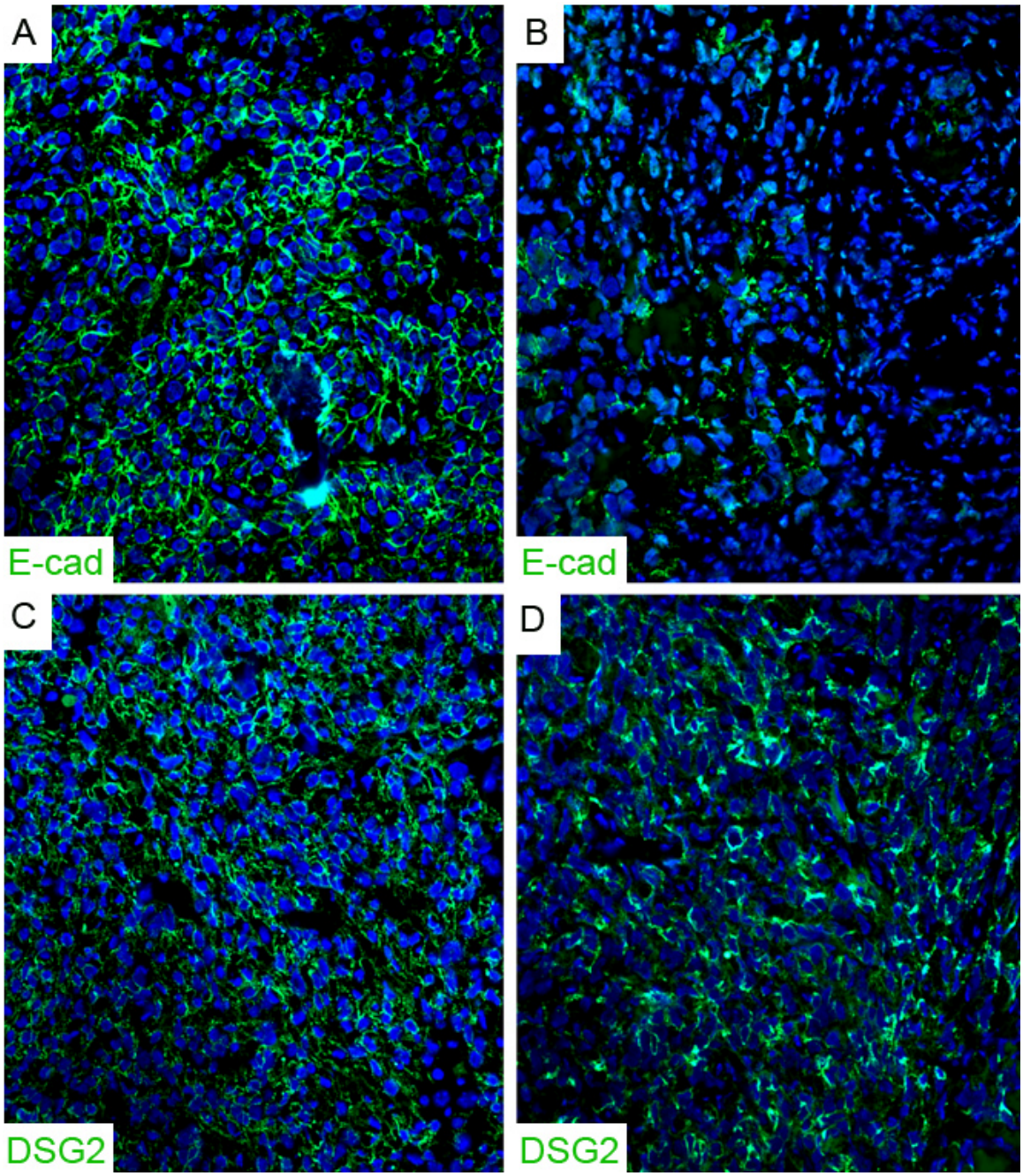

Figure 6: Immunofluorescence analysis of tumors formed by the DU145 parental cell line (A, C) and EcadKD9 (B, D). E-cadherin showed a high level of expression in the tumors formed by the DU145 parental cell line (A), however only small areas of faint, irregular expression could be detected in EcadKD9 tumors (B). Strong expression of DSG2 could be detected in both the DU145 (C) and EcadKD9 (D) tumors.

Chapter III.4

In Vivo Analysis of Cell-Cell Adhesion in Extravasation and Metastatic Tumor Colony Formation

Having examined the effects of the loss of E-cadherin based adherens junctions on tumorigenesis, I next sought to determine the effects of this loss on metastatic tumor colony formation *in vivo*. Given that the loss of E-cadherin results in a significant impairment of the formation of primary tumors, I hypothesized that this loss of E-cadherin would similarly lead to an impairment of the formation of metastatic tumor colonies. While cells lacking the expression of E-cadherin may be able to undergo extravasation at a rate similar to that of E-cadherin expressing cells, I predicted that ultimately the inability to re-establish E-cadherin based adherens junctions would result in either a lack of metastatic tumor colony formation, or a significant reduction in the size of the tumor colonies formed.

To examine this hypothesis I performed an *in vivo* extravasation and metastasis assay. In this assay, cells from the parental DU145 cell line and EcadKD9 were injected into the lateral tail vein of age matched male immunodeficient NOD/SCID mice. The assay was allowed to continue for eight weeks at which point the mice were sacrificed and their lungs were collected, fixed in formalin, and embedded in paraffin. The formalin fixed paraffin embedded (FFPE) lungs were then cut into 5μm sections — each section separated by 100μm — and stained with hematoxylin and eosin (H&E).

Metastatic tumor colonies were counted in six H&E sections per animal. To account for extravasation, intravascular metastatic tumor colonies were not counted (Figure 7A); only metastatic tumor colonies found in the lung parenchyma were counted (Figure 7B, 7D). Two separate trials of the *in vivo* extravasation and metastasis assay were performed, and the combined results from these assays are discussed.

Interestingly, the amount of animals that developed metastatic tumor colonies was significantly less for those injected with the EcadKD9 cell line (40%) as compared to those injected with the parental DU145 cell line (92%) (Figure 7F). While the number of tumors formed in animals that were positive for the formation of metastatic tumor colonies did not differ significantly between animals injected with the EcadKD9 cell line or the DU145 parental cell line, there was a striking difference in the size of the tumors formed (Figure 7B-7F). Animals injected with the EcadKD9 cell line developed many small metastatic tumor colonies (Figure 7D, 7E, 7F) — some comprised of no more than ten cells — while those injected with the DU145 parental cell line developed much larger metastatic tumor colonies (Figure 7B, 7C, 7F). To provide perspective on the size differential between the tumors formed in animals injected with the EcadKD9 cell line versus those injected with the parental DU145 cell line, one representative slide from each positive case was scored for tumors with a diameter measuring ≥1mm. The cut-off value of 1mm was chosen because, from a histopathological point of view, this value served as a robust measurement for differentiating the two populations of tumor size. This analysis showed that the diameter of 44% of

the tumors scored from animals injected with the parental DU145 cell line measured ≥1mm, while no tumor scored in animals injected with the EcadKD9 cell line had a diameter that measured ≥1mm (Figure 7F).

These results support the hypothesis that the loss of E-cadherin based adherens junctions results in the impaired formation of metastatic tumor colonies. Taken together with the results from the tumorigenesis assay, these results suggest that both primary and metastatic tumor colony formation is dependent upon the presence of E-cadherin based adherens junctions and that the presence of desmosomal adhesion alone is not sufficient to support extensive tumor growth.

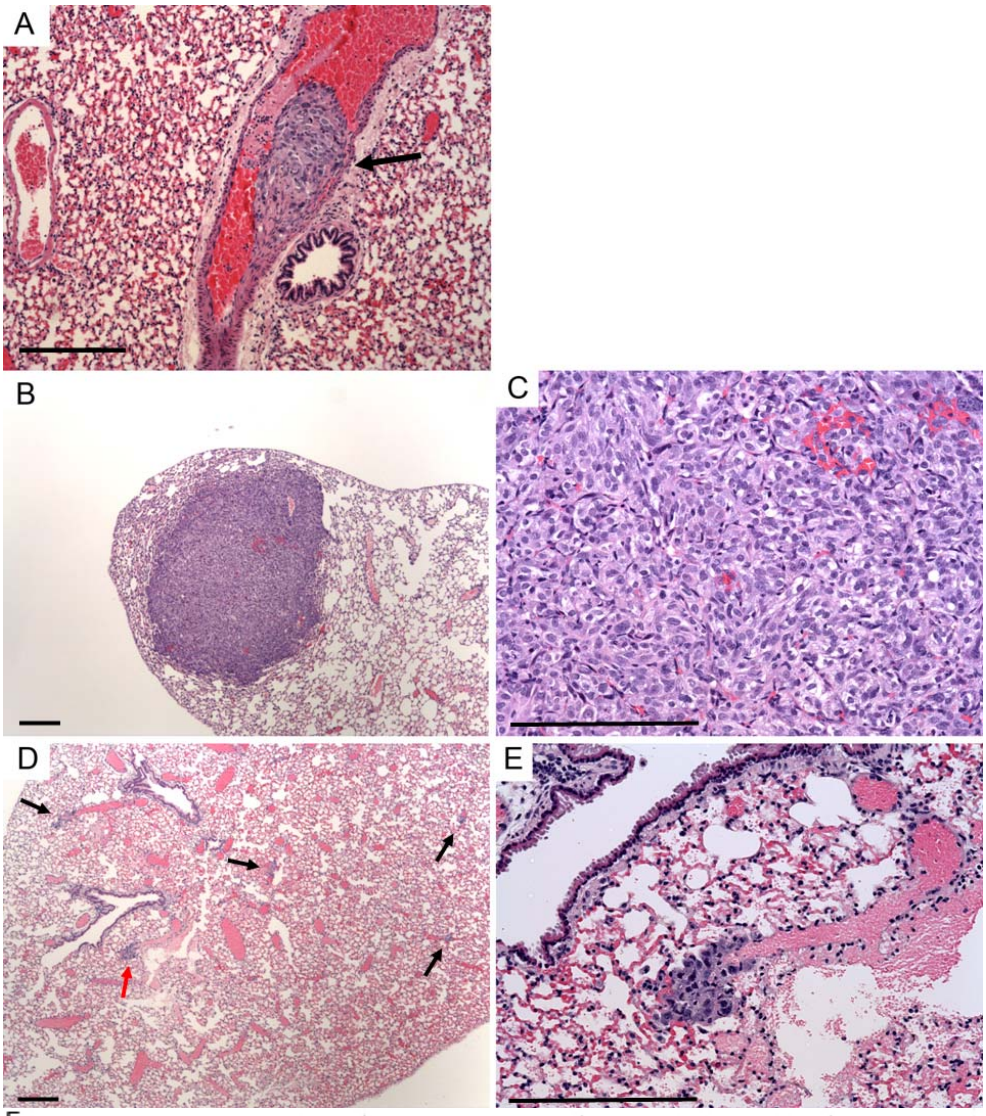

F

	DU145 (n = 13)	EcadKD9 (n = 15)	P-value
Cases Positive for Metastatic Tumor Colonies	12/13 (92%)	6/15 (40%)	0.03
Average Number of Tumors Formed in Positive Cases	9.3 ± 8.9	6.7 ± 16.36	0.84
Percentage of Tumors ≥1mm in Representative Cases	24/54 (44%)	0/39 (0%)	N/A

Figure 7: *In vivo* extravasation and metastatic tumor colony formation assay. Tumors which remained in the vasculature, and therefore did not undergo extravasation, were not counted in this assay (A). Tumors formed in the lung parenchyma of animals injected with the parental DU145 cell line (B, C, F) were large as compared to those formed in the lung parenchyma of animals injected with the EcadKD9 cell line (D, E, F; in figure D arrows point to tumors with the red arrow indicating the tumor shown in figure E). Significantly fewer animals injected with the EcadKD9 cell line developed metastatic tumor colonies as compared to those injected with the parental DU145 cell line, and these tumors were significantly smaller than those formed by the DU145 parental cell line (F).

Chapter III.5

Discussion

The conventional understanding of the relationship between adherens junctions and desmosomes holds that the assembly of desmosomes is preceded by and dependent upon the assembly of adherens junctions. In prostate cancer, the loss or reduction of E-cadherin expression is a common occurrence, while the expression of desmosomal cadherins has not been examined. Based on the conventional understanding of cell-cell anchoring junction assembly, I hypothesized that the loss of E-cadherin based adherens junctions in prostate cancer would result in the loss of desmosome formation. Surprisingly, my *in vitro* loss-of-function analysis in chapter III.2 revealed that the loss of *E-cadherin* expression in prostate cancer cells did not alter the expression of DSG2, therefore suggesting that the loss of adherens junctions in prostate cancer cells does not result in the reciprocal loss of desmosomes.

The idea that the formation of desmosomes is dependent upon the formation of adherens junctions is not without controversy; several studies have shown that the formation of desmosomes is unperturbed in tissues lacking the expression of *E-cadherin*. Conditional deletion of *E-cadherin* in the mouse epidermis and epidermal appendages results in hyperplasia and impaired terminal differentiation of the epidermis, as well as loss of integrity in the IRS and hair cuticle of the hair follicle (Tinkle et al., 2004). Interestingly, despite the absence of *E-cadherin* and a reduction in adherens junction protein expression, desmosomal cadherins were expressed and were even found to be upregulated

in the spinous layer of the mutant epidermis. Additionally, the formation of desmosomes in the hair follicles of mutant mice was detected at levels comparable to that of the hair follicles of their wild-type counterparts. This observed retention of desmosomal cadherin expression and desmosome formation in the epidermis and hair follicle was also observed in mice lacking the expression of both *E-cadherin* and *P-cadherin* in the epidermis and epidermal appendages (Tinkle et al., 2008). Further, the expression of desmosomal proteins and retained desmosome formation has been reported in E4.5 embryos lacking the expression of *E-cadherin* (Ohsugi et al., 1997). Taken together with the results of my loss-of-function analysis, these results suggest that while adherens junction assembly precedes that of desmosomes in early development as well as *de novo* anchoring junction formation, the formation of desmosomes does not strictly require the presence of adherens junctions.

With the knowledge that desmosomes are able to successfully form in the absence of anchoring junctions comes the question of whether the resulting adhesion is sufficient to support tissue integrity. The findings of Tinkle et al. demonstrate that the loss of E-cadherin based adhesion in the presence of desmosomal adhesion has differential consequences with respect to tissue integrity depending upon the tissue in which the loss occurred (Tinkle et al., 2004). Extending these findings to tumorigenesis, the likelihood that the loss of adherens junctions would interfere with tumor formation is equal to the likelihood that tumorigenesis would be unaffected by this loss.

In chapter III.3, I sought to determine the effects of the loss of E-cadherin based adherens junctions in the presence of DSG2 based desmosomes on prostate tumorigenesis. I found that the loss of E-cadherin based adherens junctions results in a dramatic reduction in the size of tumors formed despite the retention of desmosomal adhesion. These results led to the hypothesis that metastatic tumor colony formation would also be impaired by the loss of E-cadherin based adherens junctions. In chapter III.4, I sought to examine this hypothesis utilizing an *in vivo* extravasation and metastatic tumor colony formation assay. The finding that animals injected with prostate cancer cells lacking the capacity to form E-cadherin based adherens junctions are able to form metastatic tumor colonies suggests that extravasation is not impaired by the loss of E-cadherin. However, the significant difference between the amount of animals that develop metastatic tumor colonies when injected with cells that have lost E-cadherin based adherens junctions as compared to those injected with cells that retain these junctions suggests that the loss of E-cadherin inhibits metastasis at the level of metastatic tumor colony formation. This idea is further supported by the finding that the metastatic tumor burden of animals injected with cells that have lost E-cadherin based adherens junctions is significantly lower than that of animals injected with cells that retain these junctions.

As the functional analysis performed in chapter III.3 and III.4 focused on a single EcadKD cell line with an undetectable level of E-cadherin expression, future directions will focus on repeating this *in vivo* analysis using EcadKD cell lines with reduced E-cadherin expression such as EcadKD2 and EcadKD3.

Given that heterogeneous E-cadherin expression is still detectable in these mutant cell lines at a low level, if the loss of E-cadherin does in fact impair prostate tumorigenesis, then an intermediate phenotype would be expected such that the resulting primary and metastatic tumors would be smaller in size than those formed by the parental cell line yet larger than those formed by the EcadKD9 cell line. Additionally, to verify that the observed impaired tumorigenesis is specific to the loss of E-cadherin expression, a rescue experiment will be performed in which the *in vivo* assays are repeated using EcadKD cell lines in which the expression of E-cadherin has been re-introduced. Moreover, to verify that the observed inhibition of primary and metastatic tumor formation is due to the loss of E-cadherin based adherens junctions and not the reciprocal loss of DSG2 based desmosomes, further immunofluorescence analysis of desmosomal proteins including plakoglobin and desmoplakin will be performed, and electron microscopy will be utilized to verify the formation of desmosomes in primary and metastatic tumors.

The findings described in this chapter shed a new light on the role of cell-cell anchoring junctions in prostate tumorigenesis and metastatic prostate tumor colony formation as they suggest that adherens junctions are required for the formation of both primary and metastatic prostate tumors, while desmosomal adhesion alone is not sufficient to support extensive tumor formation. Interestingly, while E-cadherin is regarded as a tumor suppressor, the results of these *in vivo* analyses suggest a novel role for E-cadherin in promoting prostate

tumorigenesis as well as metastasis in the context of metastatic prostate tumor colony formation.

The role of E-cadherin as a tumor suppressor is supported by the frequently observed loss of E-cadherin in a variety of different cancers as well as the results of *in vivo* and *in vitro* analyses highlighting the role of E-cadherin as an inhibitor of invasive cancer (described in chapter I.9). The potential tumor promoting role of E-cadherin highlighted by this study provides a more extensive understanding of the dynamics of cell-cell adhesion in the progression of cancer. The putative role of E-cadherin as both a tumor suppressor and tumor promoter suggests that the loss of E-cadherin expression in cancer may need to be a transient event. This raises the question of how E-cadherin based adherens junctions are regulated in the progression of cancer. In chapter IV, I will explore this question by examining the role of the PI3K/AKT pathway in the regulation of cell-cell anchoring junctions in prostate cancer.

Chapter III.6

Materials and Methods

Mice

Both the *in vivo* tumorigenesis and *in vivo* extravasation and metastatic tumor colony formation assays were performed on 5-6 week old male NOD.CB17-Prkdc^{Scid} mice purchased from Jackson Laboratories (The Jackson Laboratories, Bar Harbor, ME, USA). Animal use and care followed institutional guidelines established by the Columbia University, Institutional Animal Care and Use Committee.

Antibodies

The anti-E-cadherin mouse monoclonal antibody was purchased from Invitrogen (Carlsbad, CA, USA) and used at a dilution of 1:400 for immunofluorescence analysis of fresh fixed cells and OCT-embedded frozen tissue sections; a dilution of 1:1000 was used for Western Blot analysis. The anti-DSG2 (DG3.10) mouse monoclonal antibody was purchased from Fitzgerald (Acton, MA, USA) and used at a dilution of 1:50 for immunofluorescence analysis of fresh fixed cells and OCT-embedded frozen tissue sections; a dilution of 1:500 was used for Western blot analysis. The β-actin rabbit monoclonal antibody was purchased from Sigma-Aldrich (St. Louis, MI, USA) and used at a dilution of 1:2000 for Western blot analysis.

Generation of Stable E-cadherin Knockdown Cell Lines

A pSMP retroviral shRNAmir construct targeting *E-cadherin* was purchased from Open Biosystems (Thermo Fisher Scientific, Huntsville, AL, USA). One day prior to transfection, Phoenix2™-Ampho cells (Allele Biotechnology, San Diego, CA, USA) were plated in 10cm plates at a density of 1 X 10^6 in MEM media containing 10% FBS. On the day of transfection, 12µg of plasmid DNA and 63µg of Arrest-In™ transfection reagent (Open Biosystems/Thermo Fisher Scientific, Huntsville, AL, USA) were added to cells in serum-free culture medium according to the manufacturer's protocol. Two days after transfection, media from the target DU145 cell line was aspirated and the cells were infected once via a direct transfer of filtered media containing 10µg/mL Polybrene (Millipore, Billircia, MA, USA) from the transfected Phoenix2™-Ampho cells. This infection procedure was repeated twice the following day. The day after the final infection, cells were collected via trypsinization and split into 96-well plates. The culture media (MEM with 10% FBS) was changed two days after plating, and fresh media containing 2 µg/mL puromycin (Invitrogen, Carlsbad, CA, USA) was added for selection. Surviving cell lines were maintained under selective conditions and used for further analysis.

RNA and Protein Isolation

RNA isolation was conducted as described in chapter II.5. To isolate protein, cells were washed twice in 1XPBS. 200µL RIPA buffer (50mM Tris-HCl, pH 7.4, 150 mM NaCl, 1% NP-40, 0.5% Sodium deoxycholate, 0.1% SDS)

containing a protease inhibitor cocktail (Complete, EDTA-free, Roche Diagnostics, Indianapolis, IN, USA) was added to cells on ice. Cells were then scraped using a rubber policeman and collected in an eppendorf tube. Cells were kept on ice for 1 hour, and vortexed for 10sec every 5 minutes. Cells were then centrifuged at 14,000rpm for 10 min at 4ºC, and the protein lysate was transferred to a new eppendorf tube. Protein concentration was determined using the Bio-Rad Protein Assay (Bio-Rad, Hercules, CA, USA).

qRT-PCR

qRT-PCR was conducted as described in chapter II.5. Primers used for qRT-PCR analysis are shown in Table 1.

Table 1: RT-PCR Primers and qRT-PCR Primers

qRT-PCR Primers		
Transcript	Forward Primer	Reverse Primer
E-cadherin*	5-'CAGCACGTACACAGCCCTAA-3'	5'-ACCTGAGGCTTTGGATTCCT-3'
DSG2	5'-ATCAATGCAACAGATGCAGATGA-3'	5'-TGTCAAAGTGTAGCTGCTGTGT-3'
β-actin	5'-AAACTGGAACGGTGAAGGTG-3'	5'-GTGGCTTTTAGGATGGCAAG-3'

*E-cadherin primers designed as reported by Chen et al., 2010.

Immunofluorescence Analysis

Immunofluorescence analysis was conducted as described in chapter II.5.

Western Blot Analysis

Western Blot analysis was performed by adding 4X SDS Sample Buffer (Novagen, San Diego, CA, USA) to 35µg of protein lysate isolated from the cell lines of interest. Samples were boiled for 5 min and separated by 4%-20% Tris-HCl SDS-PAGE. Gel transfer to a nitrocellulose membrane was conducted using the iBlot® gel transfer system (Invitrogen, Carlsbad, CA, USA) following the manufacturer's protocol. Membranes were blocked in 5% nonfat milk/1X TBST for one hour with constant agitation. Membranes were incubated overnight at 4ºC in 5% nonfat milk/1X TBST containing the primary antibody of interest with constant agitation. Membranes were washed three times for 5 min in 1X TBST with constant agitation. Membranes were incubated in 5% nonfat milk/1X TBST containing a 1:2000 dilution of either anti-mouse or anti-rabbit HRP conjugated secondary antibody (GE Healthcare, Little Chalfont Buckinghamshire, UK) with constant agitation. Samples were treated with ECL Plus Western Blotting Detection reagent (GE Healthcare, Little Chalfont Buckinghamshire, UK) for 1 min and visualized on Amersham Hyperfilm™ ECL (GE Healthcare, Little Chalfont Buckinghamshire, UK).

In vivo Tumorigenesis Assay

Cell lines of interest were trypsinized, pelleted, and counted. Following counting, 100µL of $1X10^6$ cells in MEM with 10% FBS were combined with 100µL of Matrigel™ (BD Biosciences, Franklin Lakes, NJ, USA) on ice. Age-matched male immunodeficient NOD/SCID mice were subcutaneously injected with 200µL

of the 1:1 cell-Matrigel suspension. Tumors were allowed to form for 8 weeks at which point the animals were sacrificed. Tumors were collected and tumor volume was assessed via caliper measurement. Tumors were then dissected, embedded in O.C.T. Compound (Sakura Finetek, Torrance, CA, USA), snap frozen, and 5μm sections were made for immunofluorescence analysis. Two separate trials of the assay were performed.

In vivo Extravasation and Metastatic Tumor Colony Formation

Cell lines of interest were trypsinized, pelleted, washed in 1X PBS, and counted. Following counting, 100μL of $1X10^6$ cells in 1X PBS were injected into the lateral tail vein of age matched male immunodeficient NOD/SCID mice with the kind assistance of Magda Stumpfova, a graduate student in the laboratory of Dr. David Owens. Two separate trials of the assay were performed. Animals were sacrificed eight weeks after the injection and their lungs were collected, formalin fixed, and paraffin embedded. Six 5μm tissue sections were cut from each FFPE block and the sections were stained with H&E. Each 5μm section was separated by 100μm to minimize overlap in tumor counting. Tumors in each H&E section were counted with kind assistance from Mireia Castillo-Martin, a pathologist in the laboratory. Tumors found exclusively in one tissue section were counted, while tumors found in multiple sections were only counted as present in the tissue section in which they first appeared.

Statistical analysis

Experimental data is expressed as mean ± standard deviation; statistical analysis was performed using a Student's t-test. Fisher's exact test was used for the analysis of categorical data. Values were considered statistically significant at $P \leq 0.05$.

Chapter IV

Functional Analysis of the Regulation of Cell-Cell Adhesion by PI3K/AKT Mediated Signaling in Prostate Cancer

Chapter IV.1

Overview

As demonstrated in chapter III, the permanent loss of E-cadherin expression in prostate cancer results in impaired tumorigenesis and metastatic tumor colony formation. While the role of E-cadherin in cancer has been well established as that of a tumor suppressor, the findings of this study suggest an additional role for E-cadherin as a tumor promoter in specific stages of prostate cancer progression. The duality of this role intimates the need for a transient means of E-cadherin repression in prostate cancer. One such mechanism by which *E-cadherin* may be transiently repressed in cancer is via EMT, as hallmarks of EMT include reversibility and the downregulation of *E-cadherin*. As described in chapter I.11, the expression of Snail has been associated with the downregulation of E-cadherin in breast and colorectal cancer while the transcriptional repression of *E-cadherin* via Snail has been demonstrated in a variety of cancer cell lines *in vitro* (Blanco et al., 2002; Cheng et al., 2001; Pena et al., 2005; Cano et al., 2000; Batlle et al., 2000). This Snail mediated EMT-like transcriptional repression of *E-cadherin* in cancer may be regulated by the PI3K/AKT signaling pathway. As described in chapter I.13, *in vitro* analysis of breast cancer cell lines has demonstrated that AKT is able to promote an EMT-like phenotype, while analysis of squamous cell carcinoma cell lines has shown that overexpression of activated AKT results in the downregulation of *E-cadherin* (Irie et al., 2005; Ju et al., 2007; Grille et al., 2003). Further, the downregulation

of *E-cadherin* in the presence of activated AKT was concomitant with the upregulation of *Snail*, and AKT activity has also been shown to stabilize Snail via the repression of the Snail inhibitor GSK3β (Grille et al., 2003; Zhou et al., 2004). The PI3K/AKT signaling pathway is known to be central to the progression of prostate cancer. As described in chapter I.12, *in vivo* analysis of mouse models of prostate cancer — such as the heterozygous *Pten*$^{+/-}$ knock out mouse model, the *Nkx3.1*;*Pten* compound mutant mouse model, and the transgenic MPAKT mutant mouse model — demonstrate that the aberrant activation of the PI3K/AKT pathway results in the formation of PIN and invasive prostatic carcinoma lesions (Di Cristofano, 1998; Di Cristofano 2001; Kim et al., 2002; Abate-Shen et al., 2003; Majumder et al., 2003). The potential requirement for transient repression of E-cadherin in the progression of prostate cancer coupled with the demonstrated significance of PI3K/AKT signaling in the progression of prostate cancer and the association of this signaling with EMT-like events in several other types of cancer, led me to hypothesize that PI3K/AKT signaling may lead to the EMT-like transcriptional repression of *E-cadherin* via Snail in prostate cancer.

To investigate this hypothesis I sought to examine the effects of activated PI3K/AKT signaling on *E-cadherin* expression in a prostate cancer environment. I again chose to utilize the DU145 human metastatic prostate cancer cell line as the representative prostate cancer environment for this portion of the study, as this cell line reportedly contains an intact PI3K/AKT signaling pathway insofar as it is positive for wild-type PTEN expression and negative for pAKT expression

under normal cell culture conditions (Grunwald et al., 2002). In chapter IV.2 I stably expressed a construct containing constitutively active AKT in the DU145 cell line, and examined the effects of AKT activity on the expression of E-cadherin and DSG2. I found that activated AKT expression results in a significant reduction in the expression of *E-cadherin*, while the expression of *DSG2* was relatively unaffected *in vitro*. In chapter IV.3 I examined the effects of activated AKT expression on the expression of Snail and found that there was a dramatic increase in the nuclear accumulation of Snail, indicative of increased Snail activity.

I next sought to examine the effects of activated AKT and E-cadherin inhibition on tumorigenesis. In chapter IV.4 I performed an *in vivo* tumorigenesis assay in NOD/SCID mice by injecting my cell lines of interest subcutaneously, allowing for tumor formation, and subsequently analyzing the resulting tumors for the expression of E-cadherin, DSG2, pAKT and Snail. Interestingly, the tumors formed by the activated AKT expressing cells were significantly smaller than those formed by the parental DU145 cell line; however they were unexpectedly positive for the expression of E-cadherin as well as DSG2. Further analysis revealed that there appears to be an inverse correlation between the expression of E-cadherin and that of pAKT, such that areas of the tumor with high levels of AKT expression generally showed low or no expression of E-cadherin. This inverse correlation could also be observed for the expression of Snail versus the expression of E-cadherin.

Lastly, I sought to examine the effects of activated AKT on extravasation and metastatic tumor colony formation. In chapter IV.5, I performed an *in vivo* metastasis assay by injecting my cell lines of interest into the lateral tail vein of NOD/SCID mice, allowing for tumor formation, and subsequently analyzing the lungs of the injected animals for the formation of metastatic tumor colonies. Interestingly, there was a significant decrease in the amount of animals that formed metastatic tumor colonies as well as the amount tumors formed in positive cases for animals injected with activated AKT expressing cells. In chapter IV.6, I describe the relationship between activated AKT mediated signaling, Snail, and E-cadherin *in vitro* as well as the effects of activated AKT on Snail and E-cadherin in tumorigenesis, extravasation, and metastatic tumor colony formation *in vivo*. The relationship between activated AKT mediated signaling, Snail, and DSG2 is also discussed. The methods utilized for this portion of the study are described in chapter IV.7.

Chapter IV.2

In Vitro Analysis of Anchoring Junctions and Activated AKT Signaling

The first goal of this study was to test the hypothesis that PI3K/AKT signaling may lead to an EMT-like transcriptional repression of *E-cadherin* via the transcription factor Snail in prostate cancer. To accomplish this goal I wanted to activate the PI3K/AKT signaling pathway in a prostate cancer environment and examine the effects of this activation on the expression of Snail and E-cadherin.

To activate the PI3K/AKT signaling pathway I chose to overexpress a construct containing a myristoylated form of AKT that is HA-tagged (hereafter referred to as MAH). The myristoylation of AKT targets AKT to the cell membrane resulting in its constitutive activation (Kohn et al., 1996). Therefore the overexpression of MAH in the DU145 cell line results in the constitutive activation of the PI3K/AKT signaling pathway as a result of the constitutive activation of AKT.

DU145 cells were infected with an MAH retroviral construct and grown under selective conditions. The resulting stable mutant DU145 cell lines (hereafter referred to as MAH cell lines) were then screened for the expression of MAH via its HA-tag using immunofluorescence analysis. MAH cell line 6 (hereafter referred to as MAH6) displayed a relatively high and homogeneous level of MAH expression (Figure 1A); while MAH cell line 7 (hereafter referred to as MAH7) also displayed a relatively high level of MAH expression, however this expression was very heterogeneous by comparison (Figure 1B).

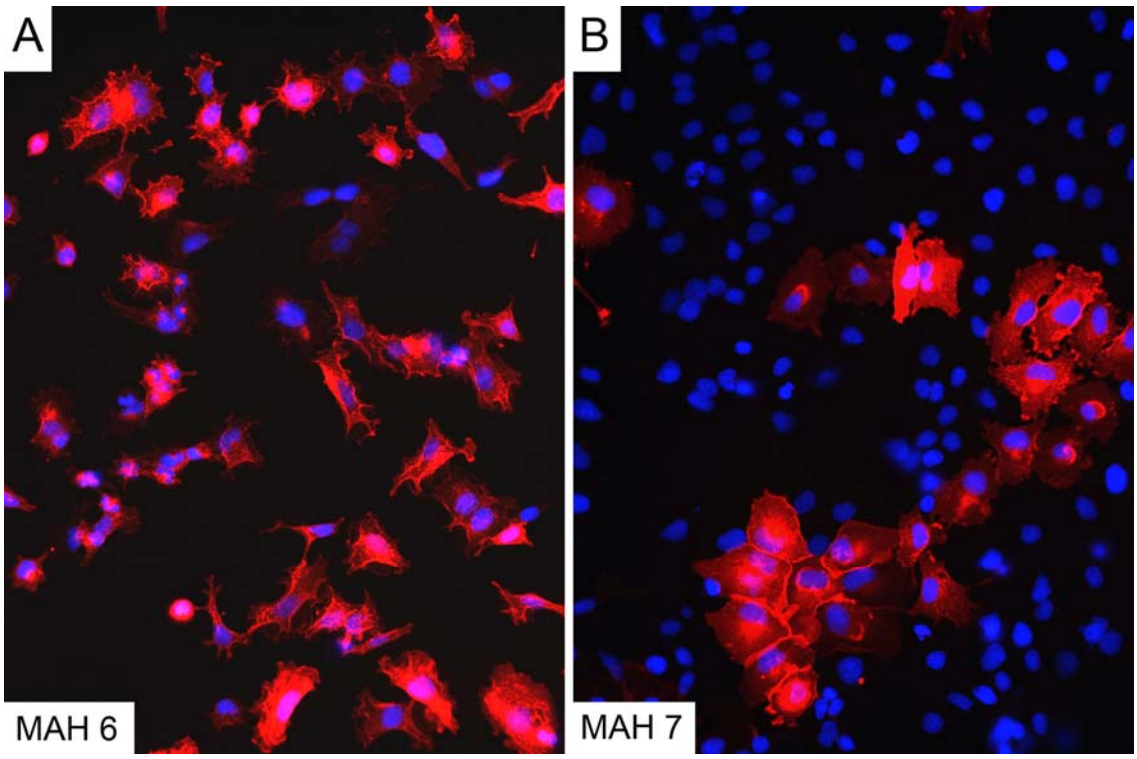

Figure 1: Immunofluorescence analysis to screen for the expression of Myr-AKT-HA in DU145 cell lines stably transfected with the MAH construct. MAH6 (A) shows a high and homogeneous level of MAH expression, while MAH7 (B) shows a heterogeneous mix of cells showing either high levels of MAH expression or no MAH expression.

I next examined the effects of AKT activity on *E-cadherin* expression in the MAH cell lines via qRT-PCR (Figure 2). Interestingly, the expression of *E-cadherin* was reduced in both of the MAH cell lines analyzed, however only MAH6 showed a significant reduction (93%) in the expression of *E-cadherin*. I then examined the expression of E-cadherin at the protein level in the MAH cell lines using immunofluorescence analysis. Consistent with the qRT-PCR results, the expression of E-cadherin was dramatically reduced and effectively undetectable at the cell border in MAH6 (Figure 3B, 3C, 3D). However E-cadherin expression could be detected at the cell border in MAH7, though this expression was either low or undetectable in cells with a high level of MAH

expression (Figure 3E, 3F). These results show that the expression of *E-cadherin* is most dramatically reduced in the presence of a homogeneously high level of activated AKT expression, which supports the hypothesis that AKT mediated signaling results in the transcriptional repression of *E-cadherin* in prostate cancer.

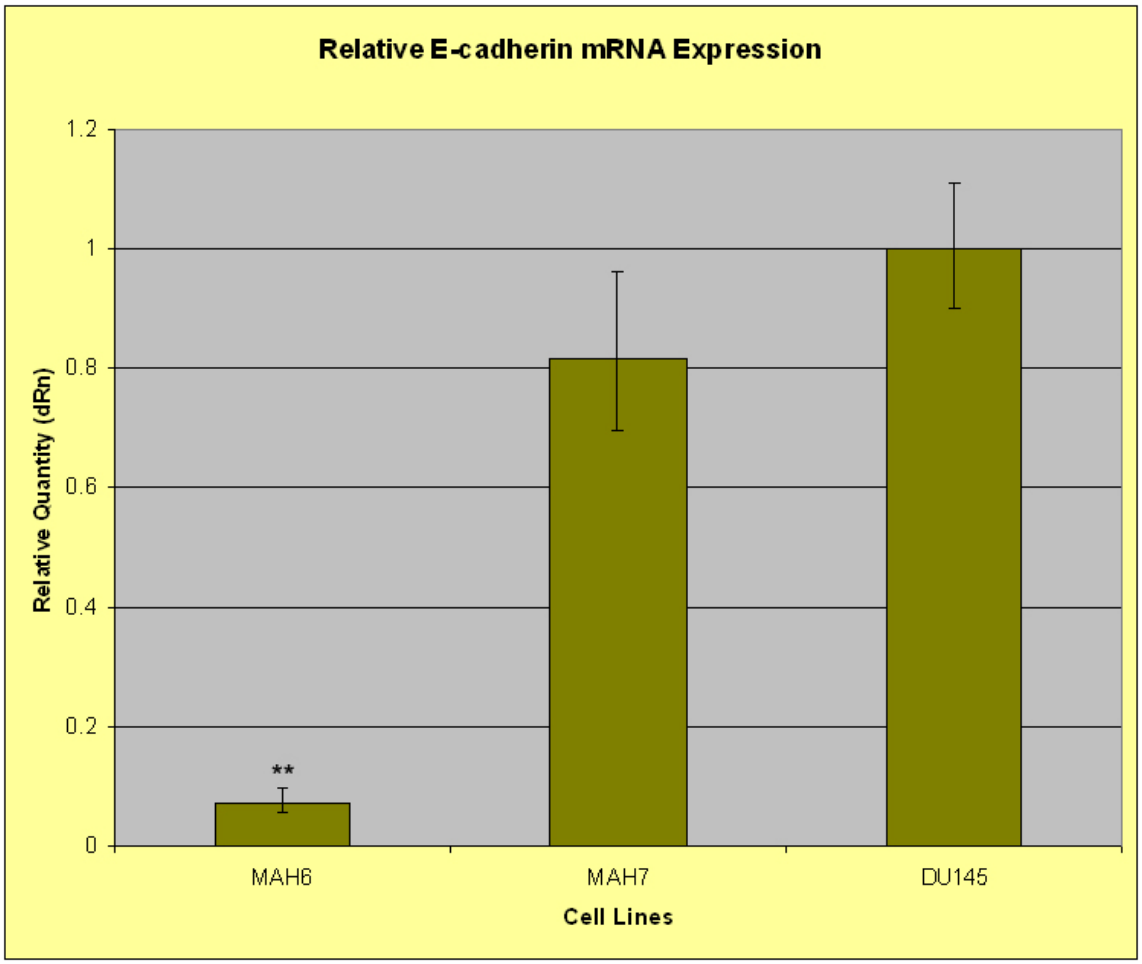

Figure 2: qRT-PCR analysis of *E-cadherin* mRNA expression in the MAH cell lines. MAH6 shows a significant reduction (93%) of *E-cadherin* expression, while MAH7 shows a modest reduction (18%) of *E-cadherin* expression. Scale bars represent standard deviation; (**) represents $P < 0.01$.

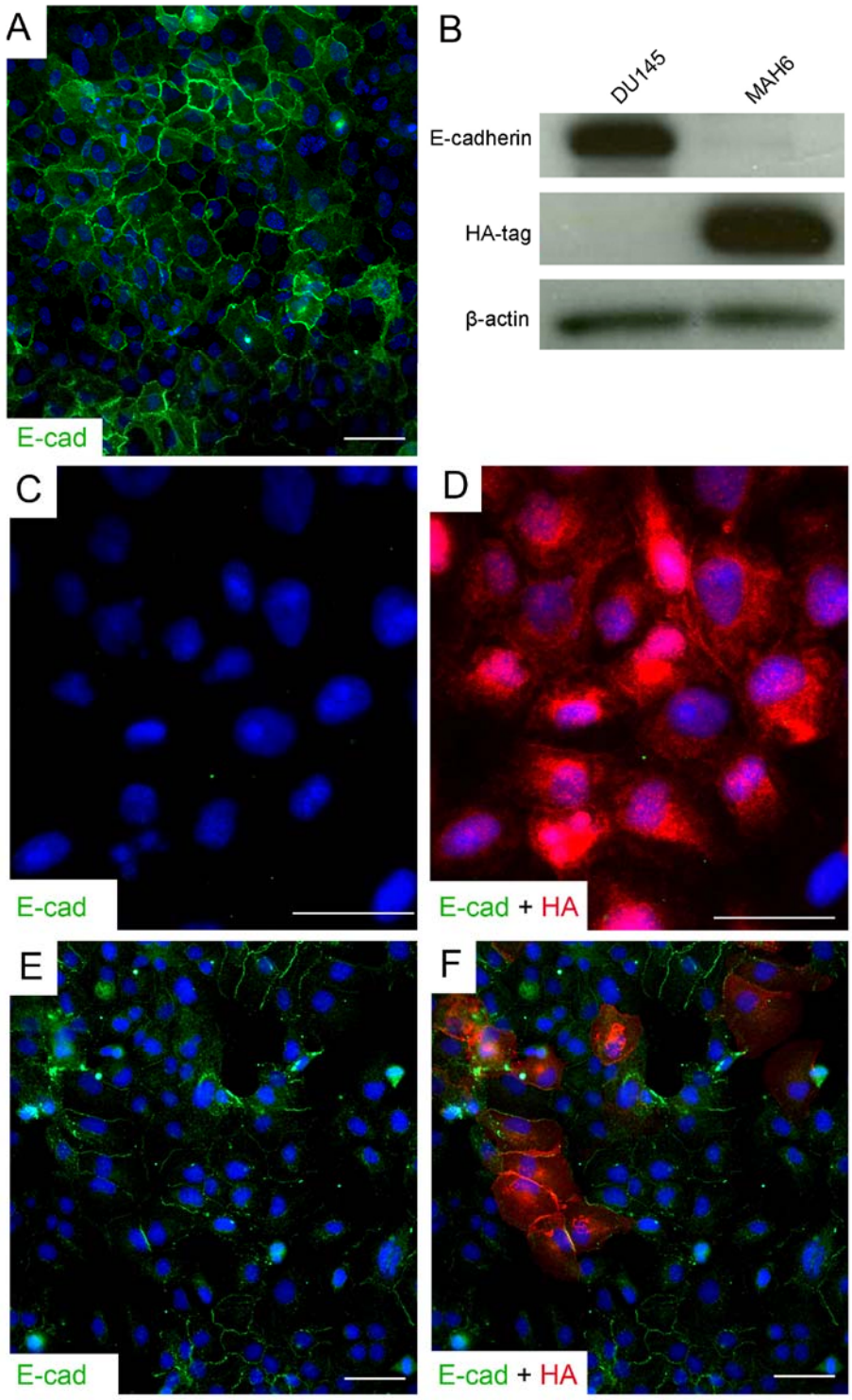

Figure 3: Immunofluorescence and Western blot analysis of E-cadherin expression in MAH cell lines. The expression of E-cadherin is dramatically reduced in MAH6 and is effectively undetectable at the cell border (B, C, D). The expression of E-cadherin is detectable at the cell border of MAH7, however this expression is low or absent in cells expressing a high level of MAH.

As mentioned in chapter I.13 a study conducted by Grille et al. found that overexpression of activated AKT in a squamous cell carcinoma cell line results in reduced *E-cadherin* mRNA expression (Grille et al., 2003). This study also showed that there was a mislocalization of desmoplakin in the presence of activated AKT expression, such that desmoplakin displayed granular staining in the cytoplasm and failed to localize to the cell-cell border. This mislocalization of desmoplakin is indicative of a failure of desmosome formation, thereby suggesting that activated AKT mediated signaling may influence the formation of desmosomes. To examine the possibility that activated AKT may result in the transcriptional repression of *DSG2*, I examined the expression of *DSG2* via qRT-PCR in the MAH cell lines. Interestingly, I found that the expression of *DSG2* varied in the mutant cell lines examined. There was a small but significant increase (1.6X) in the expression of *DSG2* in MAH6, while there was a significant decrease (56%) in the expression of *DSG2* in MAH7 (Figure 4). These results may reflect that the level of *DSG2* in the MAH cell lines is arbitrary, suggesting that the expression of *DSG2* is not affected by activated AKT expression. Alternatively, these results may suggest that the expression of *DSG2* is affected by activated AKT expression; however this effect is negated in cases where *E-cadherin* expression is significantly reduced.

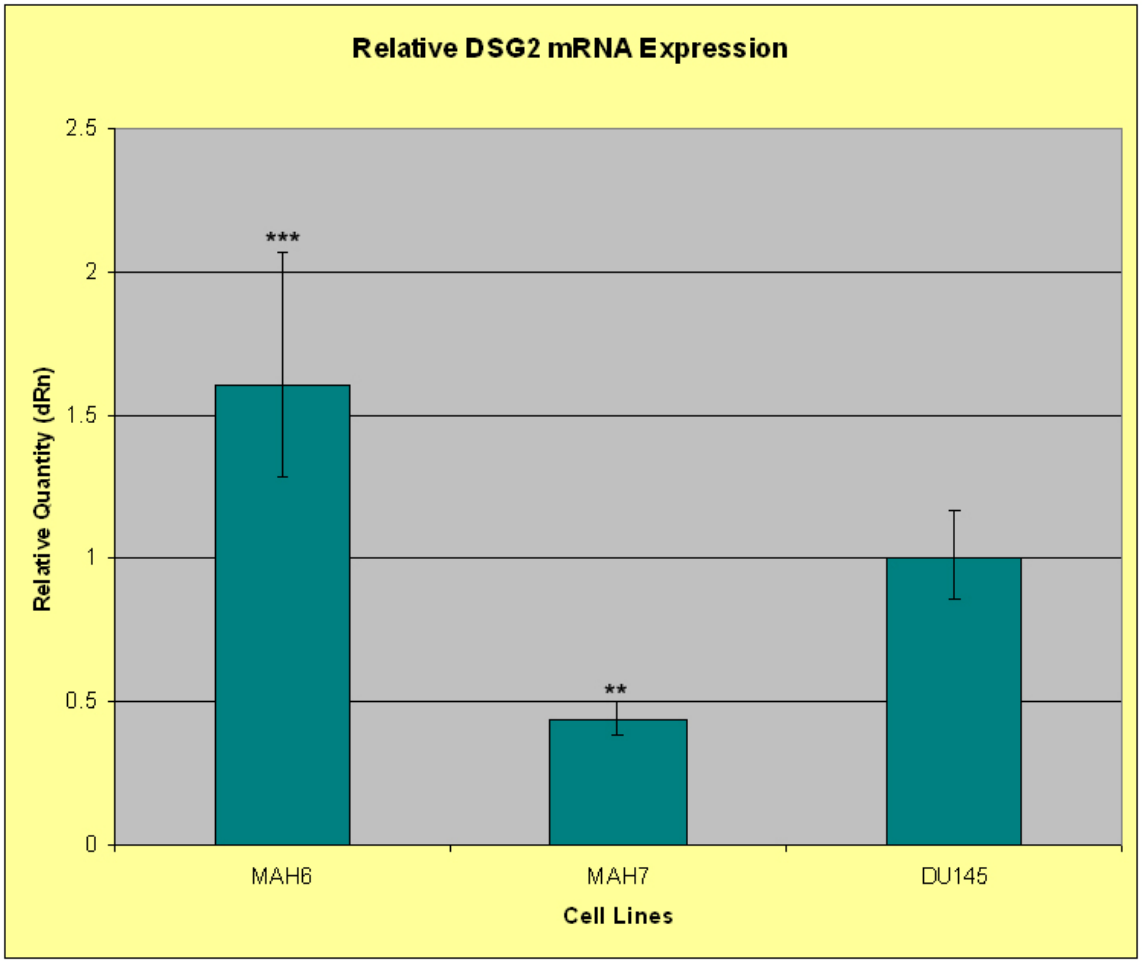

Figure 4: qRT-PCR analysis of *DSG2* mRNA expression in the MAH cell lines. There is a small but significant increase (1.6X) of *DSG2* expression in MAH6, while a significant decrease (56%) of *DSG2* expression is detected in MAH7. Scale bars represent standard deviation; (**) represents $P < 0.01$; (***) represents $P < 0.001$.

I then analyzed the expression of DSG2 at the protein level in the MAH cell lines using immunofluorescence analysis. The expression of DSG2 could be detected at the cell border of both MAH6 and MAH7 cells (Figure 5C-5F). Consistent with the qRT-PCR results, Western blot analysis shows that there is a higher level of DSG2 expression in MAH6 cells than in the DU145 parental cell

line. Interestingly, despite this higher level of DSG2 protein expression, cell border localization of DSG2 is detected in fewer cells of the MAH6 cell line as compared to the DU145 parental cell line. In general, DSG2 cell border expression could be detected in cells expressing a high level of activated AKT, however activated AKT expressing cells in which DSG2 expression is either low or absent were detected on occasion. This pattern of DSG2 expression may signify that the effect of activated AKT mediated signaling on DSG2 expression is context dependent.

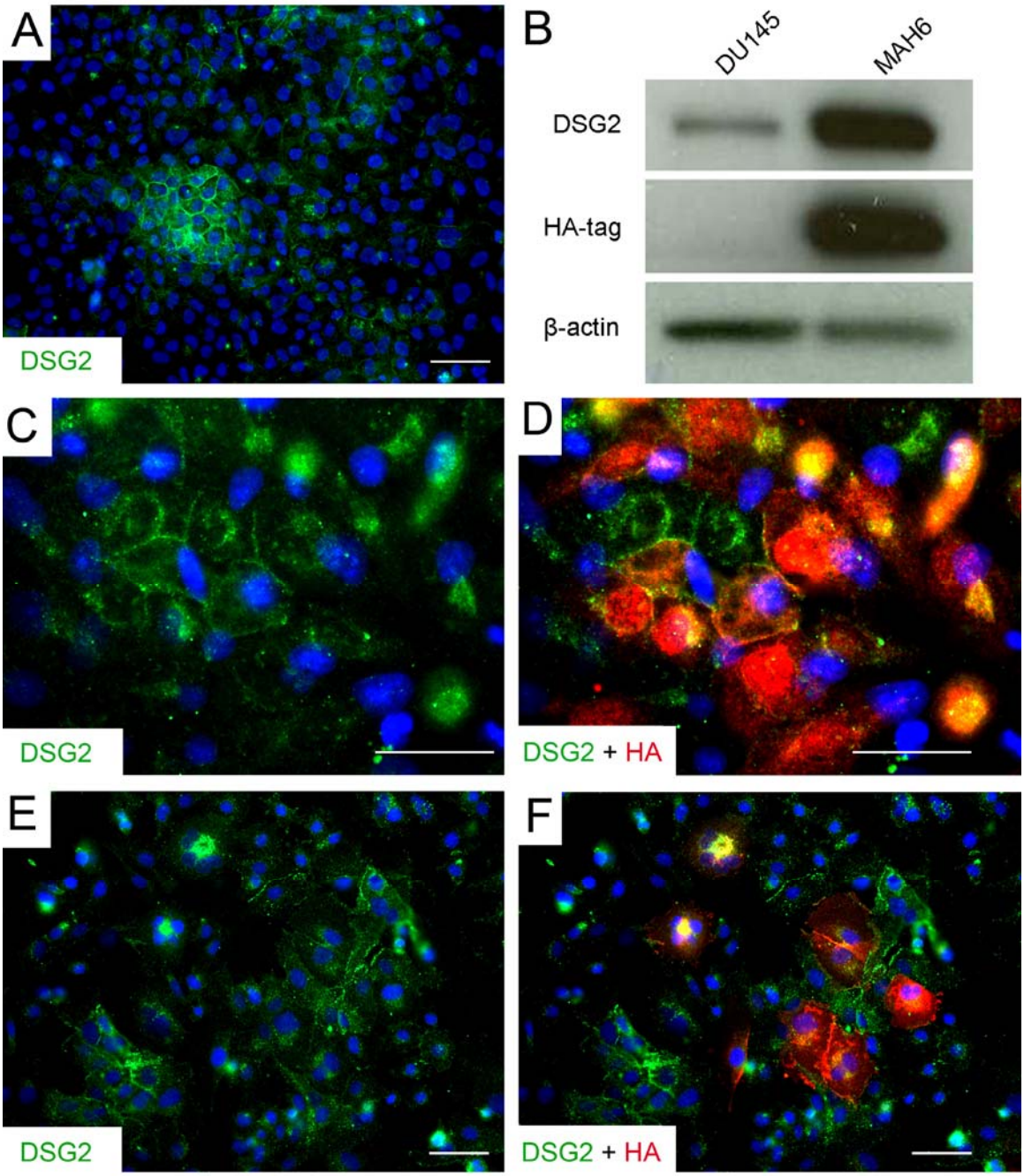

Figure 5: Immunofluorescence and Western blot analysis of DSG2 expression in the MAH cell lines. The level of DSG2 protein expression in MAH6 cells is greater than that of the parental DU145 cell line (B). DSG2 expression can be detected at the cell border of MAH6 (C, D) and MAH7 cells (E, F).

Chapter IV.3

In Vitro Analysis of EMT and Adherens Junctions

Having found that the expression of activated AKT results in decreased *E-cadherin* expression at the mRNA level, I next sought to examine the possibility that this transcriptional repression of *E-cadherin* may be mediated by Snail. As the expression of *E-cadherin* was most significantly reduced in MAH6, I chose to move forward with the analysis of this particular cell line for the remainder of the study. I first analyzed the expression of *Snail* in MAH6 cells utilizing qRT-PCR, and found that there was a small but significant increase (1.8X) in the expression of *Snail* in this cell line (Figure 6). I then utilized immunofluorescence analysis to examine the expression of Snail at the protein level. Interestingly, there was a dramatic increase in the nuclear localization of Snail in the MAH6 cell line as compared to the parental DU145 cell line (Figure 7). While nuclear localization of Snail can be detected in the parental DU145 cell line, this expression is very low and is difficult to detect above background fluorescence (Figure 7A, 7B). However, the expression of Snail in MAH6 cells is robust and readily detectable in the nucleus (Figure 7C, 7D).

As described in chapter I.11, the expression of the EMT-associated transcription factor Slug has also been associated with reduced E-cadherin expression in esophageal squamous cell carcinoma (Uchikado et al., 2005). Additionally, Slug has been shown to bind E-box elements in the *E-cadherin* promoter, and has been found to repress *E-cadherin* in human breast cancer cell

lines as well as in the MDCK cell line (Hajra et al., 2002; Bolos et al., 2002). PI3K/AKT signaling has been associated the stabilization of Slug via the indirect activation of β-catenin (Saegusa et al., 2009). The expression of the EMT-associated transcription factor Twist has also been shown to be associated with the loss of E-cadherin in invasive lobular carcinoma, and the expression of exogenous Twist has been shown to inhibit *E-cadherin* expression *in vitro* (Yang et al., 2004). Twist has been shown to be a direct target of AKT phosphorylation, and this phosphorylation has been found to have a positive effect on Twist activity (Vichalkovski et al., 2010). Given that Slug and Twist are known transcriptional repressors of *E-cadherin*, and that their activity has been associated with PI3K/AKT signaling, I wanted to examine the expression of Slug and Twist in MAH6 cells to determine if there was an increase in the nuclear accumulation of these transcription factors in addition to Snail. I therefore examined the expression of Slug and Twist in MAH6 cells via immunofluorescence and found that no increase in nuclear accumulation could be detected for either Slug (Figure 8) or Twist (Figure 9) in MAH6 cells as compared to the DU145 parental cell line. Interestingly, while the nuclear expression of both Slug and Twist could be detected in the parental DU145 cell line (Figure 8A, 8B, 9A, 9B), this expression appears to be lost in MAH6 cells where only a low level of diffuse cytoplasmic Twist expression can be detected (Figure 8C, 8D, 9C, 9D). Taken together these results suggest that activated AKT expression results in the nuclear accumulation of Snail and the transcriptional downregulation of *E-cadherin*. This transcriptional downregulation

of *E-cadherin* may be a result of Snail activity, but is not a result of the activity of Slug or Twist.

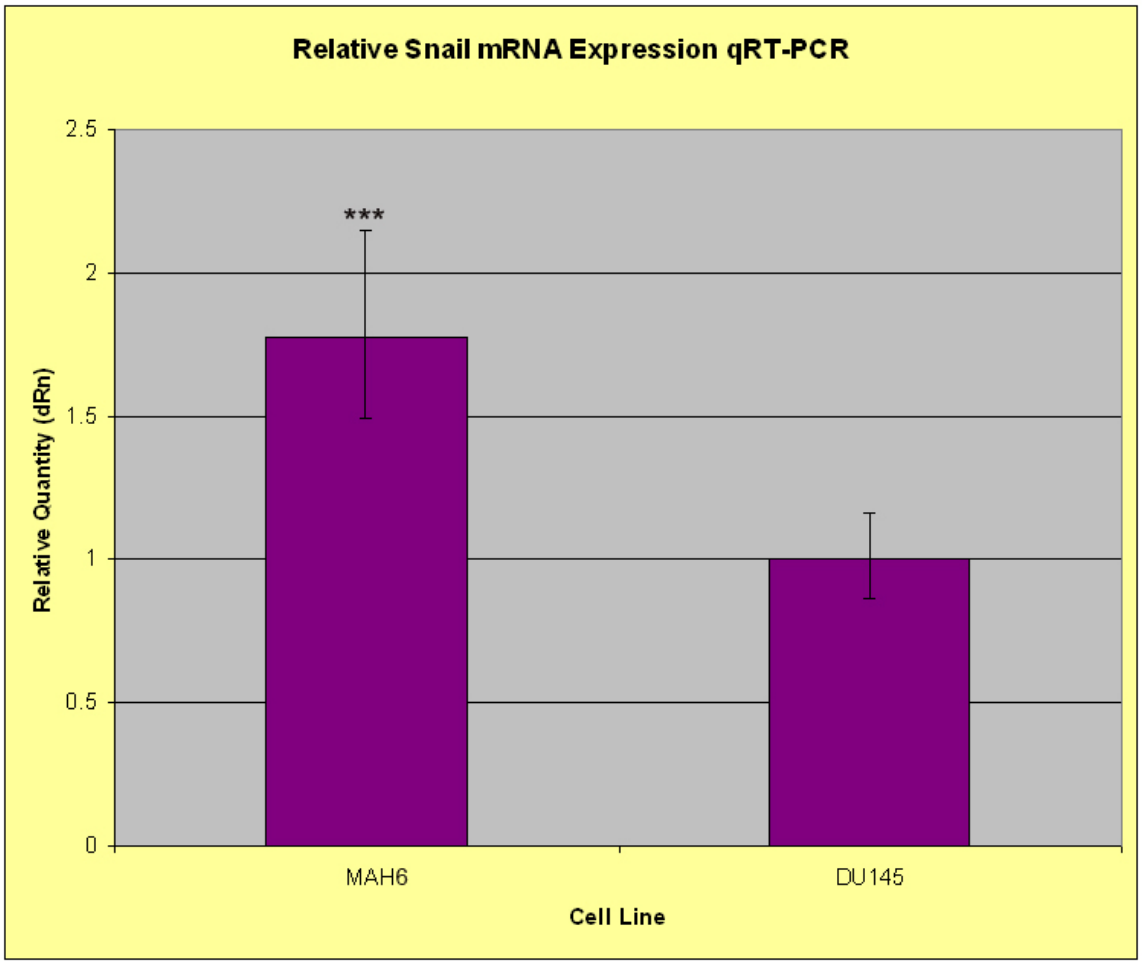

Figure 6: qRT-PCR analysis of *Snail* mRNA expression in MAH6 cells. There is a slight but significant increase in the expression of *Snail* in MAH6 cells. Scale bars represent standard deviation; (***) represents $P < 0.001$.

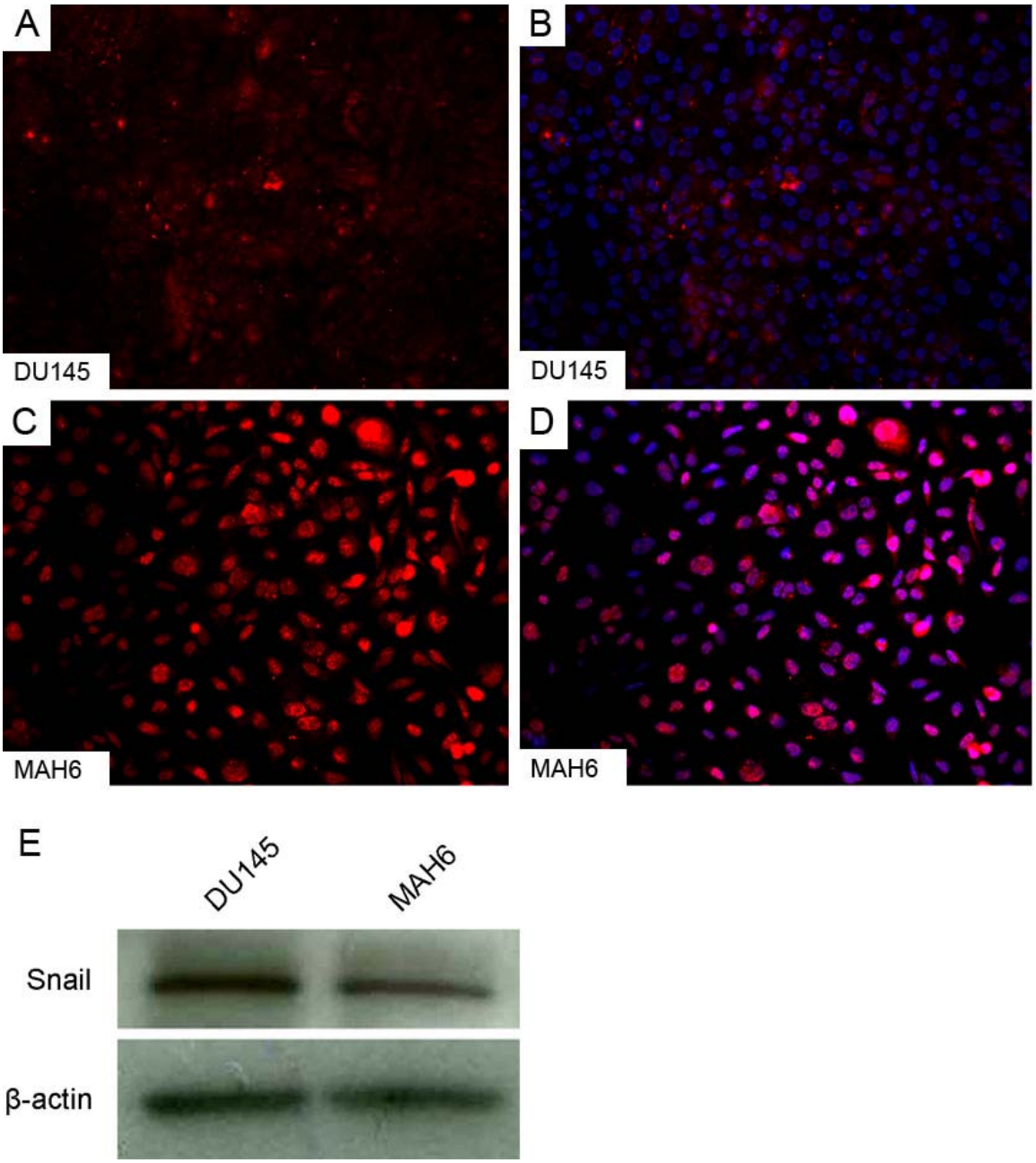

Figure 7: Immunofluorescence analysis of Snail expression in MAH6 cells. There is a high level of nuclear Snail expression in MAH6 cells (C, D) as compared to the DU145 parental cell line (A, B). This nuclear localization is indicative of Snail activity. The level of Snail expression is relatively equal in MAH6 cells and the DU145 parental cell line (E). (Snail is labeled in red, and nuclei are labeled with DAPI in blue.)

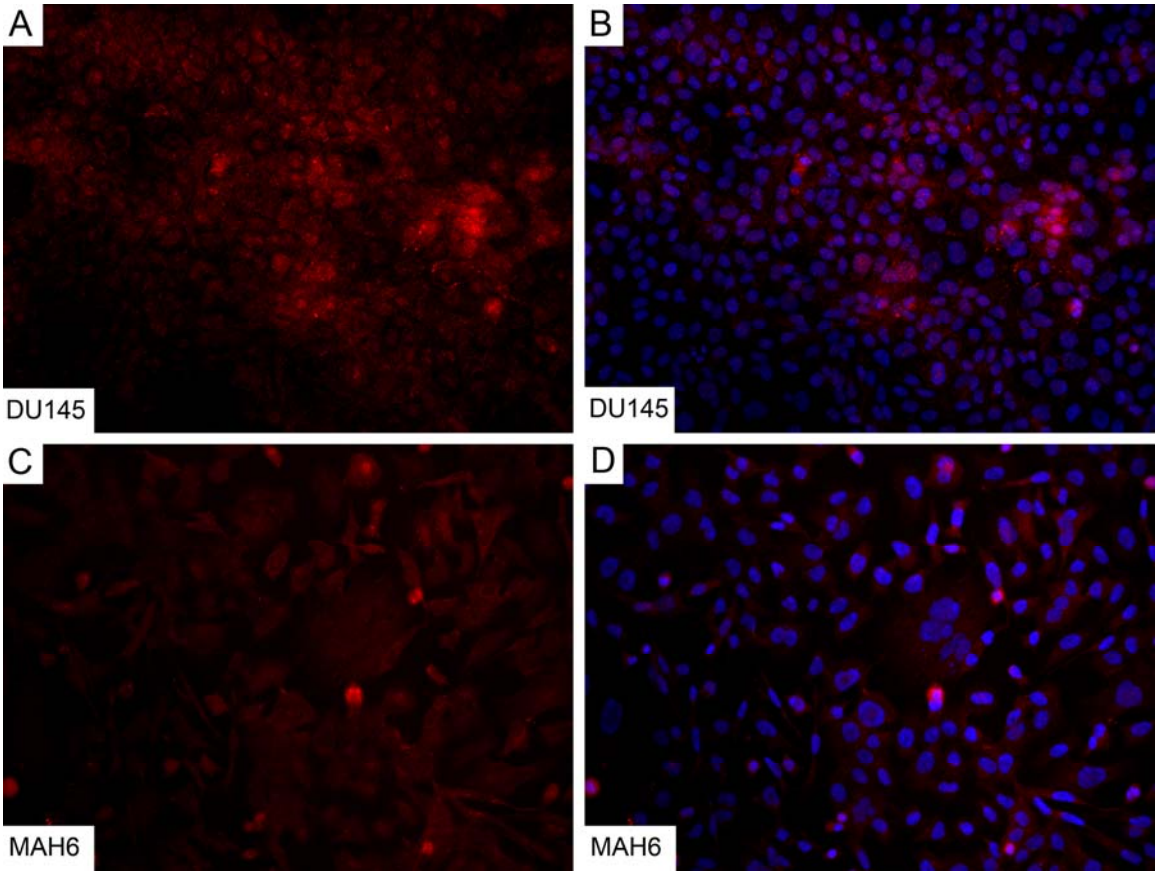

Figure 8: Immunofluorescence analysis of Slug expression in MAH6 cells. Expression of Slug can be detected in the nuclei of the DU145 parental cell line (A, B), however only a low level of diffuse cytoplasmic Slug expression can be detected in MAH6 cells (C, D) which is indicative of Slug inactivity. (Slug is labeled in red, and nuclei are labeled with DAPI in blue.)

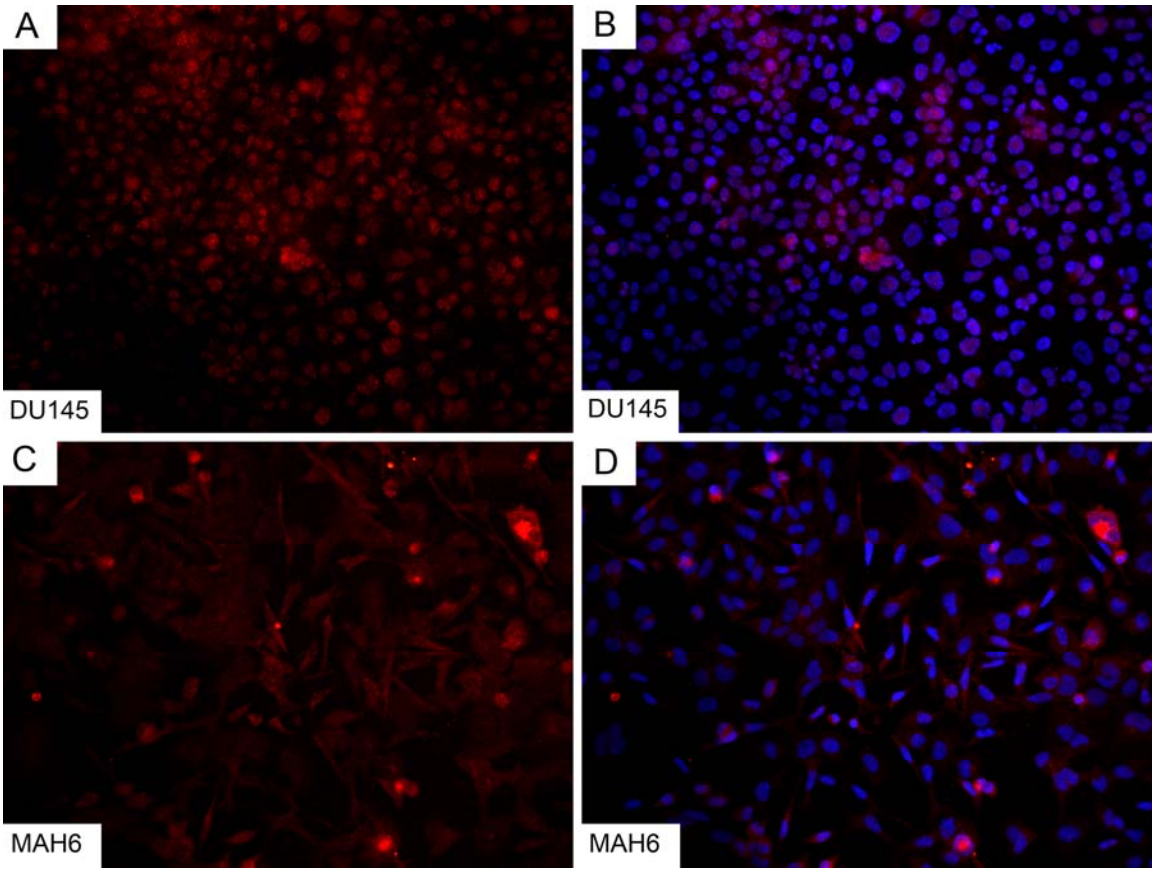

Figure 9: Immunofluorescence analysis of Twist expression in MAH6 cells. Expression of Twist can be detected in the nuclei of the DU145 parental cell line (A, B), however only a low level of diffuse cytoplasmic Twist expression can be detected in MAH6 cells (C, D) which is indicative of Twist inactivity. (Twist is labeled in red, and nuclei are labeled with DAPI in blue.)

Chapter IV.4

In Vivo Tumorigenesis Analysis of Cell-Cell Adhesion in Prostate Cancer

Having found that the expression of activated AKT results in the transcriptional repression of *E-cadherin* as a possible consequence of Snail activity, I next sought to examine the effects of activated AKT mediated signaling on tumorigenesis *in vivo*. Given that in chapter III.3 I found that the loss of E-cadherin expression results in impaired tumorigenesis, I hypothesized that a high level of activated AKT expression would similarly result in impaired tumorigenesis

due to the observed transcriptional repression of *E-cadherin*. To test this hypothesis I performed an *in vivo* tumorigenesis assay in which MAH6 cells and cells from the parental DU145 cell line were injected subcutaneously into the backs of age-matched male immunodeficient NOD/SCID mice. Tumors were then allowed to grow for eight weeks at which point the mice were sacrificed and the tumors were collected for analysis. Two separate trials of the *in vivo* tumorigenesis assay were performed, and the combined results from these assays are discussed.

Interestingly, much like the tumors formed by E-cadherin knockdown cells, there was a notable difference in the size of the tumors formed by MAH6 cells as compared to those formed by the parental DU145 cell line. The tumors formed by the DU145 parental cell line (Figure 10A, black arrow; 10B, left); were large (1.33 cm^3 ± 0.71) while the tumors formed by MAH6 cells (Figure 10A, red arrow; 10B, right) were significantly smaller by comparison (0.36 cm^3 ± 0.27; P = 0.0001). However, it should be noted that these MAH6 tumors, though small, were significantly larger (P = 0.001) than those formed by the EcadKD9 cell line (0.04 cm^3 ± 0.02).

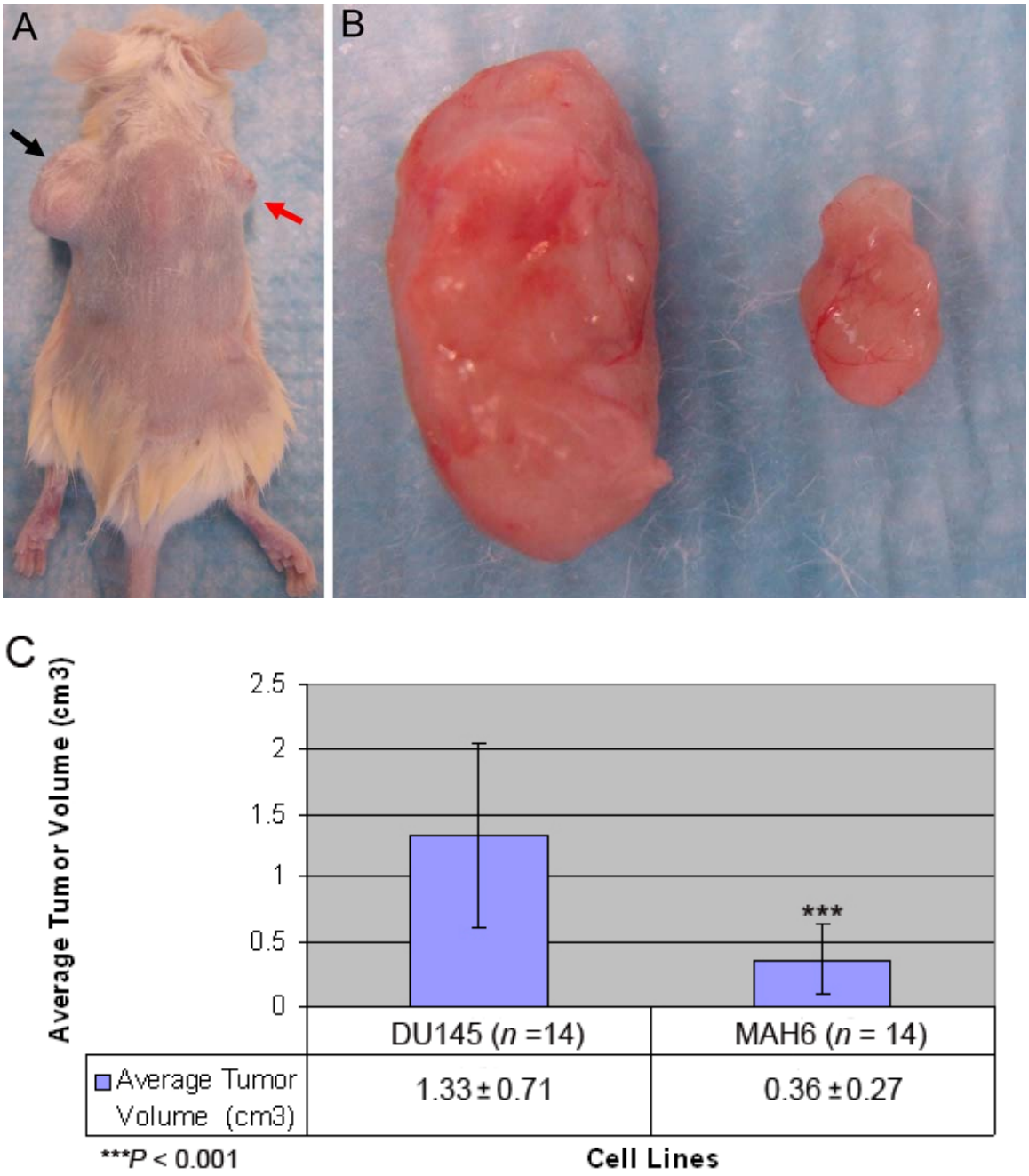

Figure 10: *In vivo* tumorigenesis assay. Cells from the DU145 parental cell line (A, black arrow) and MAH6 cells (A, red arrow) were injected subcutaneously in NOD/SCID mice. The DU145 parental cell line produced large tumors (B, tumor shown on the left; C) while MAH6 cells produced tumors that were significantly smaller (B, tumor shown on the right, C). Scale bars represent standard deviation.

Frozen OCT embedded sections of the tumors were then analyzed for the expression of E-cadherin and DSG2 via immunofluorescence to ensure that the cadherin expression profile observed *in vitro* was maintained in the tumors formed *in vivo*. As expected, the expression of DSG2 could be detected at the cell border of tumors formed by both MAH6 cells and the parental DU145 cell line (Figure 11C, 11D). Surprisingly, E-cadherin expression was also detected at the cell border of tumors formed by both the DU145 parental cell line and the MAH6 cells (Figure 11A, 11B).

To determine whether this unexpected E-cadherin expression was a result of the loss of MAH expression in the MAH6 tumors I performed co-immunofluorescence analysis for the expression of the HA-tagged myristoylated AKT and E-cadherin in MAH6 tumors. The results of this analysis show that MAH expression was retained in the MAH6 tumors, therefore the unexpected expression of E-cadherin was not due to the expansion of drug resistant cells lacking the expression of the MAH construct (Figure 12). Co-labeling analysis further revealed that the expression of E-cadherin appears to be inversely proportional to the expression of MAH, such that cells with a high level of MAH expression display a low level of E-cadherin expression while cells with a low level of MAH expression display a high level of E-cadherin expression (Figure 12A-C). Interestingly, further co-immunofluorescence analysis showed that this pattern of expression could also be detected for MAH and DSG2, though to a lesser extent (Figure 12D-F). While DSG2 expression could be detected in cells

with a high level of MAH expression, DSG2 expression was often more robust in cells with low or no MAH expression.

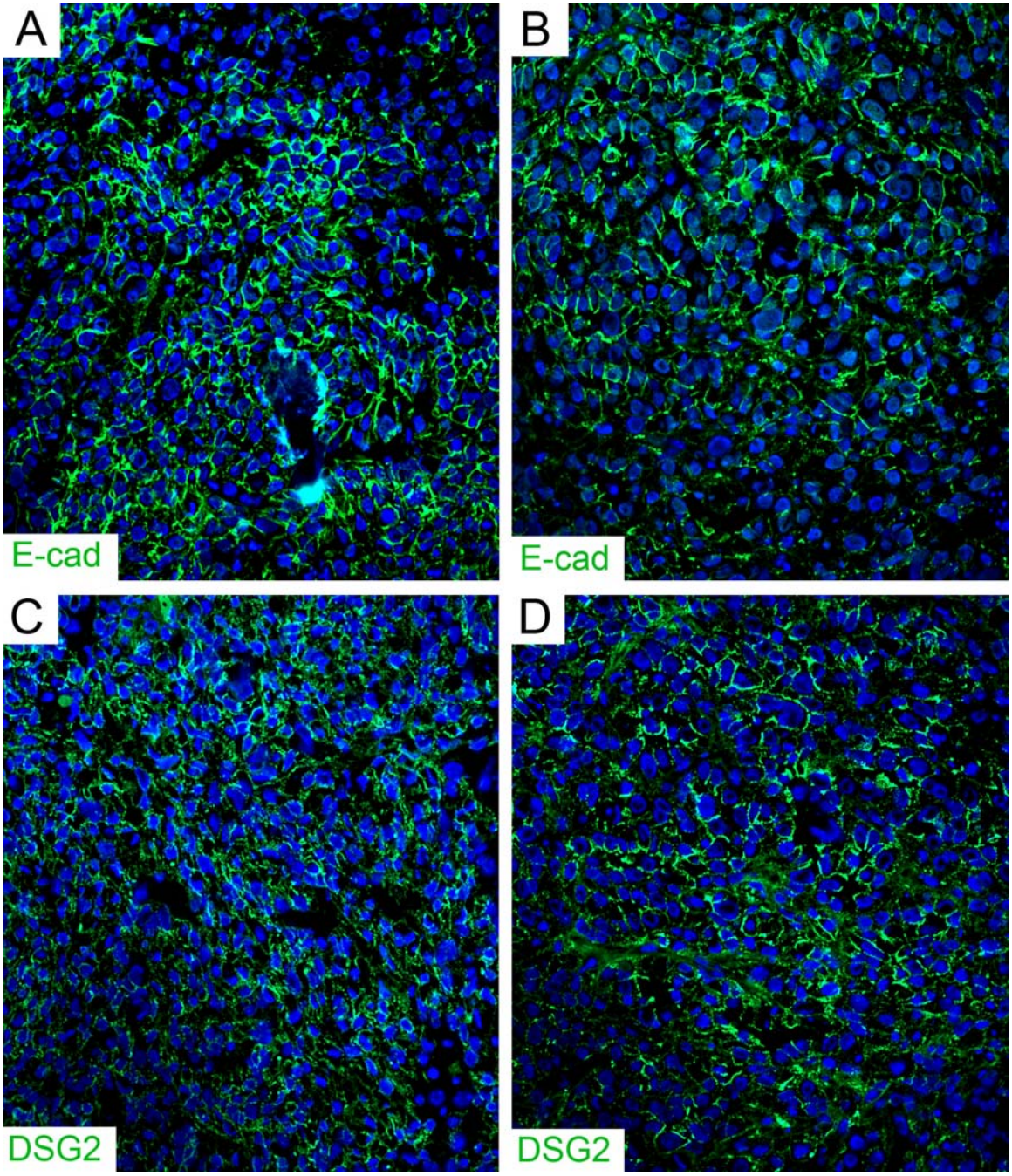

Figure 11: Immunofluorescence analysis of tumors formed by the DU145 parental cell line (A, C) and MAH6 cells (B, D). E-cadherin showed a high level of expression in the tumors formed by both the DU145 parental cell line (A) and MAH6 cells (B). Strong expression of DSG2 could also be detected in both the DU145 (C) and MAH6 (D) tumors.

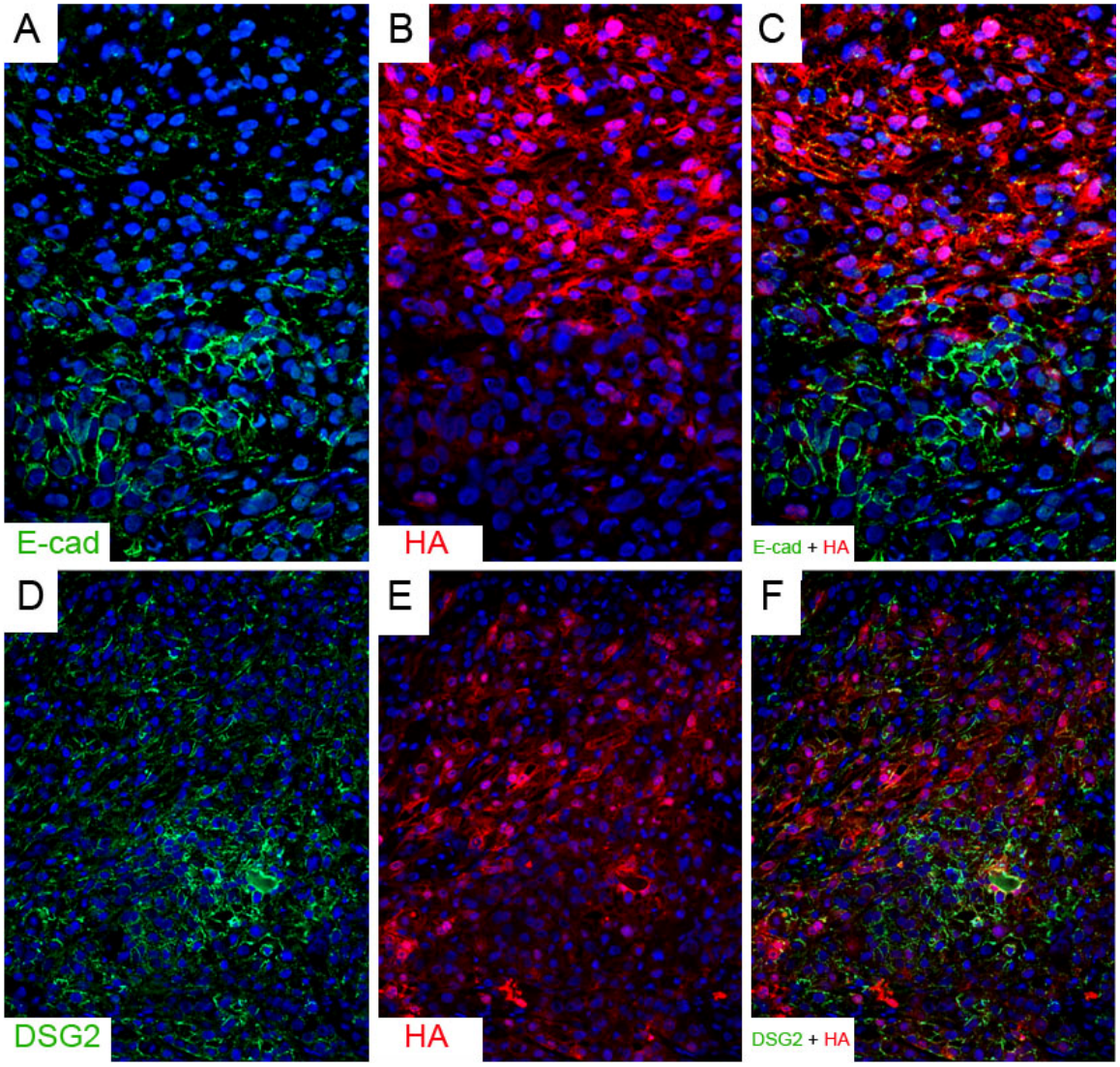

Figure 12: Co-immunofluorescence analysis of E-cadherin and MAH, and DSG2 and MAH in tumors formed by MAH6 cells. E-cadherin and DSG2 are shown in green. An anti-HA-tag antibody was used to detect the expression of MAH, shown in red. Nuclei are labeled with DAPI, shown in blue. The expression of E-cadherin appears to be inversely proportional to that of MAH (A-C). The expression of DSG2 also appears to be inversely proportional to MAH (D-F), though to a lesser extent than that of E-cadherin.

I next sought to determine whether the same inverse proportionality could be detected for Snail expression and E-cadherin expression. To accomplish this goal I examined the expression of Snail and E-cadherin via co-immunofluorescence analysis in tumors formed by MAH6 cells and the DU145 parental cell line. Interestingly, nuclear Snail expression could be detected in tumors formed by MAH6 cells, however this expression was generally not as robust as that observed *in vitro* (Figure 13F-H). Despite this fact, areas of MAH6 tumors that showed the highest levels of nuclear Snail expression often showed low or no expression of E-cadherin, while E-cadherin expression was often most robust in areas with low or no nuclear Snail expression. Interestingly, this pattern of expression was also detected in tumors formed by the parental DU145 cell line (Figure 13C-E). While the nuclear expression of Snail in the parental DU145 cell line was very low *in vitro*, areas of relatively high nuclear Snail expression could be detected *in vivo*. As in the tumors formed by MAH6 cells, the expression of Snail often appears to be inversely proportional to that of E-cadherin in the tumors formed by the DU145 parental cells. Given that the expression of activated AKT is not detected in the parental DU145 cell line *in vitro*, I asked whether the unexpectedly high level of nuclear Snail expression in the tumors formed by the DU145 parental cell line *in vivo* could be explained by unanticipated activated AKT expression in these tumors. Immunofluorescence analysis revealed that high levels of cytoplasmic pAKT (i.e. activated AKT) expression could be detected in certain areas of the tumors formed by the DU145 parental cell line (Figure 13A). While co-immunofluorescence analysis of

pAKT expression and Snail expression could not be performed due to antibody incompatibility, the correlation between pAKT expression and Snail expression in tumors formed by both the parental DU145 cell line and MAH6 cells illustrates the possibility that nuclear Snail expression is a result of AKT mediated signaling.

Taken together the results of this *in vivo* tumorigenesis assay show that the tumors formed by MAH6 cells are significantly smaller than those formed by the DU145 parental cell line. Unexpectedly, the expression of E-cadherin can be detected in tumors formed by both MAH6 cells and the DU145 parental cell line. This observation coupled with the comparatively small size of MAH6 tumors suggests that tumorigenesis favors the expression of E-cadherin, thereby raising the possibility that the reduced size of MAH6 tumors may be a reflection of the selection and expansion of a rare population of MAH6 cells with retained E-cadherin expression. Further, this E-cadherin expression appears to be inversely proportional to both activated AKT expression and Snail expression. This result supports the hypothesis that PI3K/AKT signaling may lead to an EMT-like transcriptional repression of *E-cadherin* via the transcription factor Snail in prostate cancer while suggesting that the extent of this transcriptional repression may be dependent upon the level of PI3K/AKT signaling and/or Snail activity. Additionally, DSG2 expression is retained in both MAH6 tumors and tumors formed by the DU145 parental cell line. This DSG2 expression appears to be inversely proportional to activated AKT expression, however to a lesser degree than that observed for E-cadherin. This result suggests that PI3K/AKT signaling

may influence DSG2 expression, though to a lesser degree than that of E-cadherin expression.

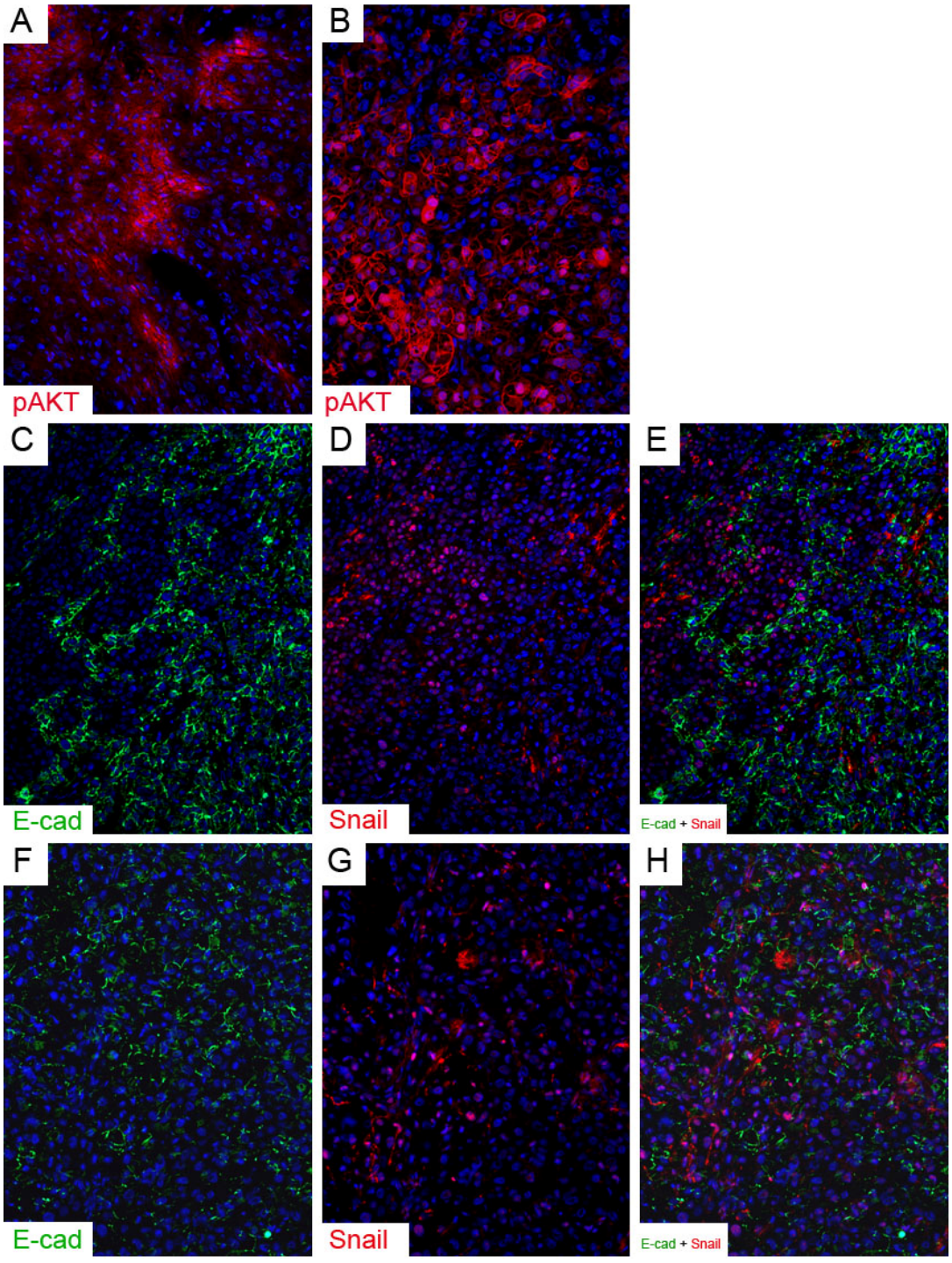

Figure 13: Immunofluorescence analysis of pAKT in tumors formed by MAH6 cells and the DU145 parental cell line (A-B). pAKT expression can be detected in tumors formed by both the DU145 parental cell line (A) and MAH6 cells (B). Co-immunofluorescence analysis of E-cadherin and Snail in tumors formed by the DU145 parental cell line and MAH6 cells (C-H). The expression of E-cadherin appears to be inversely proportional to that of Snail in tumors formed by both the DU145 parental cell line (C-E) and MAH6 cells (F-H). E-cadherin is shown in green. pAKT is shown in red. Snail is also shown in red. Nuclei are labeled with DAPI, shown in blue.

Chapter IV.5

In Vivo Analysis of Cell-Cell Adhesion in Extravasation and Metastatic Tumor Colony Formation

Having examined the effects of activated AKT mediated signaling on tumorigenesis, I next sought to determine the effects of this AKT mediated signaling on metastatic tumor colony formation *in vivo*. The results of the *in vivo* tumorigenesis assay in chapter IV.4 revealed that MAH6 tumors were unexpectedly positive for the expression of E-cadherin, yet the tumors formed in animals injected with MAH6 cells were significantly smaller that those formed in animals injected with the parental DU145 cell line. Given the observed inverse proportionality of activated AKT expression and E-cadherin expression *in vivo*, coupled with the observation that most MAH6 cells have a very high level of activated AKT expression *in vitro*, this size discrepancy may be explained by the selection and expansion of a rare population of MAH6 cells that have retained E-cadherin expression as a result of a low level of activated AKT expression. I therefore hypothesized that metastatic tumor colony formation would be impaired in animals injected with MAH6 cells as compared to those injected with the DU145 parental cell line, as only a rare population of MAH6 cells expressing a low level of activated AKT would be expected to retain the E-cadherin expression required to provide them with the capacity to form metastatic tumor colonies.

To examine this hypothesis I performed an *in vivo* extravasation and metastasis assay. In this assay, MAH6 cells and cells from the parental DU145 cell line were injected into the lateral tail vein of age-matched male immunodeficient NOD/SCID mice. The assay was allowed to continue for eight weeks at which point the mice were sacrificed and their lungs were collected, fixed in formalin, and embedded in paraffin. The formalin fixed paraffin embedded (FFPE) lungs were then cut into 5μm sections — each section separated by 100μm — and stained with hematoxylin and eosin (H&E). Metastatic tumor colonies were counted in six H&E sections per animal. To account for extravasation, intravascular metastatic tumor colonies were not counted; only metastatic tumor colonies found in the lung parenchyma were counted (Figure 14A, 14C). Two separate trials of the *in vivo* extravasation and metastasis assay were performed, and the combined results from these assays are discussed.

Interestingly, significantly fewer animals injected with MAH6 cells developed metastatic tumor colonies (24%) as compared to those injected with the parental DU145 cell line (92%) (Figure 14E). Additionally, significantly fewer tumors formed in the animals that were injected with MAH6 cells and were positive for the formation of metastatic tumor colonies (0.7 ± 2.4) as compared to animals injected with the DU145 parental cell line (9.3 ± 8.9) (Figure 14E). Moreover, the tumors that were able to form in animals injected with MAH6 cells were generally smaller than those injected with the parental DU145 cell line (Figure 14C-E). The diameter of only 16% of the representative tumors scored

from animals injected with MAH6 cells measured ≥1mm, while 44% of the tumors scored in animals injected with the parental DU145 cell line had a diameter that measured ≥1mm. These results support the idea that only a rare population of MAH6 cells retains the capacity to form metastatic tumor colonies, as the time required for the selection and expansion of this population would be expected to delay tumor formation. This delay in tumor formation would be expected to result in the formation of fewer tumors overall that are smaller in size than those formed by cells that did not have to undergo this same delay.

It must be noted that, though small, the metastatic tumor colonies formed in animals injected with MAH6 cells were consistently larger than those formed in animals injected with EcadKD9 cells, based on observation. The finding in chapter III that EcadKD9 cells have lost E-cadherin expression both *in vitro* and *in vivo* suggests that EcadKD9 cells are relatively homogeneous with respect to the loss of E-cadherin expression. Therefore the selection and expansion of a rare E-cadherin negative cell population resulting in the formation of the observed E-cadherin negative tumors in chapter III.3 would not be expected to have occurred for these cells. As a result, the time allowed for metastatic tumor colony formation by EcadKD9 cells would be effectively longer than that for the putative rare population of E-cadherin positive MAH6 cells. With this in mind, the observation that tumors formed in animals injected with MAH6 cells are actually larger than those formed in animals injected with EcadKD9 cells, despite the possibility that these MAH6 tumors had less time to form, supports the idea that the metastatic tumor colonies formed by MAH6 cells retain the expression of E-

cadherin as E-cadherin positive tumors have been found to be consistently larger than E-cadherin negative tumors in chapter III of this study. Additionally, the finding that the MAH6 tumors formed in the *in vivo* tumorigenesis assay described in chapter IV.4 were consistently positive for E-cadherin expression supports the idea that the metastatic tumor colonies formed by MAH6 cells retain the expression of E-cadherin.

In summary, the results of this *in vivo* extravasation and metastatic tumor colony formation assay support the prediction that metastatic tumor colony formation would be impaired in animals injected with MAH6 cells as compared to those injected with the DU145 parental cell line. Further, the observed impairment of metastatic tumor colony formation by MAH6 cells may be attributable to the selection and expansion of a rare population of E-cadherin positive cells.

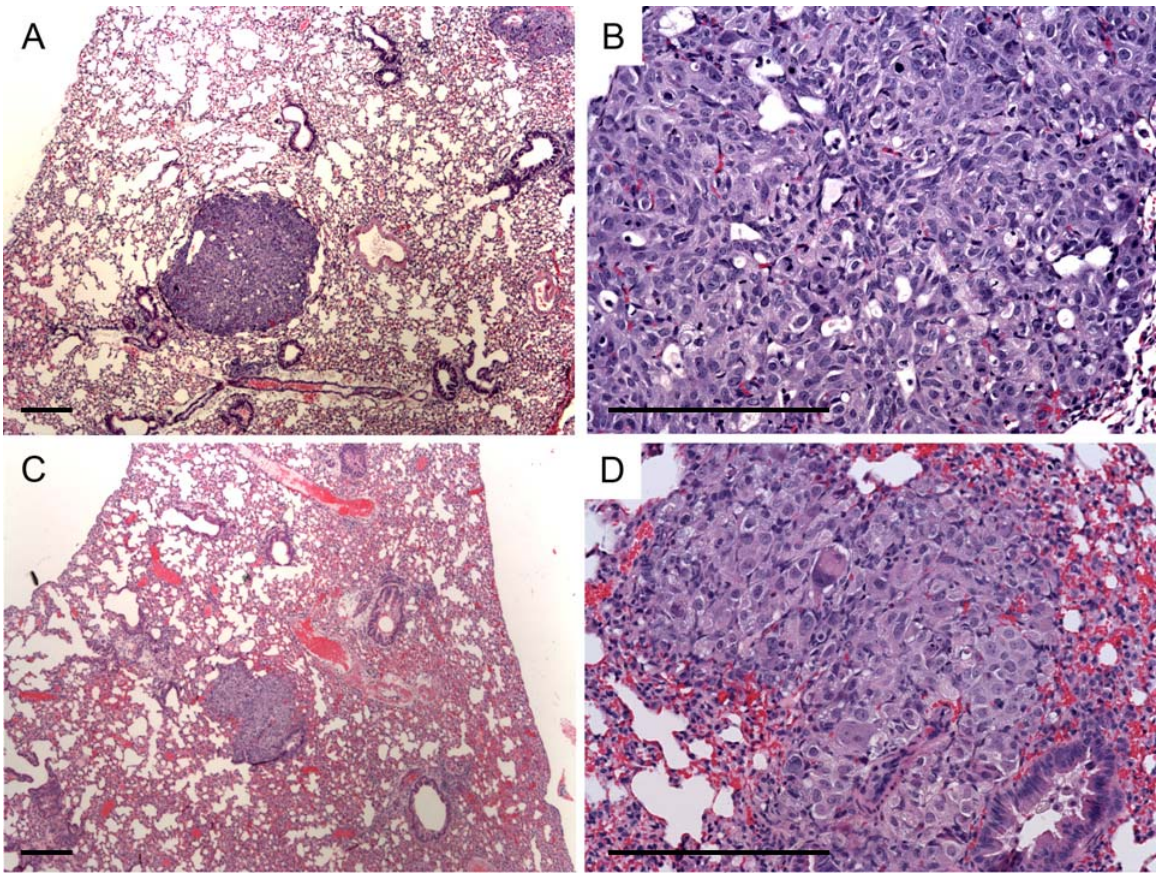

E

	DU145 (n = 13)	MAH6 (n = 17)	P-value
Cases Positive for Metastatic Tumor Colonies	12/13 (92%)	4/17 (24%)	<0.0001
Average Number of Tumors Formed in Positive Cases	9.3 ± 8.9	0.7 ± 2.4	0.013
Percentage of Tumors ≥1mm in Representative Cases	24/54 (44%)	1/6 (16%)	0.386

Figure 14: *In vivo* extravasation and metastatic tumor colony formation assay. Tumors formed in the lung parenchyma of animals injected with the parental DU145 cell line (A, B, E) were large as compared to those formed in the lung parenchyma of animals injected with MAH6 cells (C, D, E). Significantly fewer animals injected with EcadKD9 cells developed metastatic tumor colonies as compared to those injected with the parental DU145 cell line (E).

Chapter IV.6

Discussion

The role of E-cadherin as a tumor suppressor is well established. As described in chapter I.9, the loss of E-cadherin expression has been associated with many types of cancer, and the role of E-cadherin in the inhibition of tumor cell invasion has been extensively examined both *in vitro* and *in vivo*. However, there are exceptions to this rule, as the rare up-regulation or overexpression of E-cadherin has been documented in ovarian cancer and inflammatory breast cancer (Sundfeldt et al., 1997; Kleer et al., 2001). These exceptions suggest that while E-cadherin has clearly been shown to play a role in the inhibition of cancer cell invasion, the function of E-cadherin may also be advantageous at certain stages of cancer progression. As demonstrated in chapter III, the loss of E-cadherin impairs the formation of primary and metastatic prostate tumors *in vivo*, suggesting that the presence of E-cadherin based adherens junctions may be required for extensive tumor formation.

Given the possibility that E-cadherin may play both a positive and negative role in the progression of prostate cancer, flexibility in the regulation of E-cadherin expression could be distinctly advantageous in the progression of prostate cancer. While the permanent loss of E-cadherin via such mechanisms as LOH coupled with inactivating mutations has been documented in gastric cancer and lobular breast carcinoma, the loss of E-cadherin expression in cancer is most often associated with impermanent mechanisms such as transcriptional

silencing, transcriptional repression, or post-transcriptional modifications (Becker et al., 1994; Berx 1995; Yoshiura et al., 1995; Kanazawa et al., 2002; Johnson et al., 2007). In this chapter I wished to examine the transcriptional regulation of *E-cadherin* as a possible form of transient E-cadherin repression, focusing on the as yet unexplored relationship between the PI3K/AKT signaling pathway and the EMT-like repression of *E-cadherin* in prostate cancer. As described in the overview of this chapter, the demonstrated significance of PI3K/AKT signaling in the progression of prostate cancer and the association of this signaling with EMT-like events in several other types of cancer, led me to hypothesize that PI3K/AKT signaling may lead to the EMT-like transcriptional repression of *E-cadherin* via Snail in prostate cancer.

In chapter IV.2 I found that a homogenously high level of activated AKT expression was associated with the transcriptional repression of *E-cadherin*. Further, in chapter IV.3 it was demonstrated that this homogenously high level of activated AKT expression was also associated with the nuclear accumulation of Snail, indicative of Snail activity. It was also shown that this activated AKT expression was not associated with the nuclear accumulation of the EMT related transcription factors Slug and Twist. These *in vitro* findings strongly support the hypothesis that PI3K/AKT signaling leads to the transcriptional repression of *E-cadherin* specifically via the activation of the EMT-related transcription factor Snail.

To verify that the observed transcriptional repression of *E-cadherin* is a result of activated AKT expression, future directions will include an *in vitro*

analysis of *E-cadherin* expression in MAH6 cells treated with an inhibitor of AKT activity. Similarly, treatment of MAH6 cells with an AKT inhibitor will also be used to verify that the observed nuclear accumulation of Snail expression is a result of AKT activity. Treatment of MAH6 cells with an AKT inhibitor would be expected to result in the re-expression of *E-cadherin* and a loss of nuclear Snail accumulation. Additionally, to examine whether there is a direct interaction between Snail and *E-cadherin*, a chromatin immunoprecipitation (ChIP) assay will be performed to determine if Snail binds directly to the *E-cadherin* promoter in MAH6 cells at a level that is significantly greater than that observed in the DU145 parental cell line.

In chapter IV.4, *in vivo* tumorigenesis analysis of activated AKT expression in prostate cancer cells showed that tumors formed by MAH6 cells were significantly smaller than those formed by the DU145 parental cell line. Unexpectedly, both tumor types were found to express E-cadherin. This unexpected E-cadherin expression may be explained by the finding that, unlike MAH6 cells *in vitro*, MAH6 cell *in vivo* were found to express a comparatively low level of activated AKT. Further, this activated AKT expression was found to be inversely proportional to that of E-cadherin in MAH6 cells. This inverse proportionality of activated AKT and E-cadherin expression was also observed in the DU145 cell line where the expression of pAKT was detected. Moreover, the expression of Snail and E-cadherin was also found to be inversely proportional in both MAH6 cells and the DU145 parental cell line. These results suggest that the small, E-cadherin-positive tumors formed by the MAH6 cell line are a result of the

selection and expansion of a rare cell population expressing a level of activated AKT low enough to permit the expression of E-cadherin. These results further suggest that a high level of Snail activity is required for significant repression of *E-cadherin* expression.

In chapter IV.5, *in vivo* extravasation and metastatic tumor colony formation analysis showed that fewer animals injected with MAH6 cells went onto form tumors than those injected with the DU145 parental cell line. Additionally, fewer metastatic tumor colonies formed in MAH6 injected animals and these tumor colonies were much smaller in size as compared to those found in animals injected with the DU145 parental cell line. The reduced tumor colony size observed in this assay is consistent with the reduced tumor size observed in the E-cadherin positive MAH6 tumors formed in the tumorigenesis assay of chapter IV.4. Taken together with the reduced number of tumor colonies formed overall in animals injected with MAH6 cells, these results lend further support to the idea that the formation of tumors by MAH6 cells occurs via the selection and expansion of a rare, E-cadherin positive MAH6 cell population.

To further explore the idea that MAH6 tumors are formed as a result of the selection and expansion of a rare E-cadherin positive cell population, future directions will focus on repeating these *in vivo* assays using the MAH7 cell line which is heterogeneous for cells expressing a high level of activated AKT. Given that MAH7 cells contain both E-cadherin positive and E-cadherin negative cells, the resulting MAH7 tumors would be expected to be much larger than those formed by the MAH6 cell line as the population of cells that express a low level of

activated AKT and a high level of E-cadherin is much less rare in the MAH7 cell line. Additionally, the inverse proportionality of E-cadherin and activated AKT expression would be expected to be observed in the MAH7 tumors. To further verify that the observed small MAH6 tumor size is specifically a result of the repression of *E-cadherin* expression and is not due to unrelated effects of activated AKT signaling, these *in vivo* assays will also be repeated using MAH6 cells in which the expression of E-cadherin has been re-introduced. If the observed results are specific to the repression of *E-cadherin* then this re-introduction of E-cadherin expression should rescue the mutant tumor phenotype and would be expected to result in tumor sizes that are comparable to those of parental DU145 cell line.

The multiple outputs of the PI3K/AKT signaling pathway may contribute to the progression of prostate cancer on various levels. The finding that the permanent loss of E-cadherin expression may be disadvantageous to the progression of prostate cancer, in addition to the observed sensitivity of E-cadherin expression to the level of activated AKT expression may therefore represent a means of regulating the inhibition of E-cadherin expression by the PI3K/AKT signaling pathway such that a certain threshold of PI3K/AKT signaling may be required for the repression of *E-cadherin*. This hypothesis that certain cellular outputs are dependent upon achieving a particular AKT signaling threshold is supported by the findings of Segrelles et al., who examined the ectodermal development of myrAkt transgenic mice displaying different levels of Akt kinase activity (Segrelles et al., 2008). Transgenic mice that displayed a high

level of Akt kinase activity had defects in ectodermally derived organs including hair, teeth, nails, and epidermal glands. However, these defects were not found in animals that expressed either wild-type Akt or a low level of myr-Akt — indicative of a low level of Akt kinase activity — suggesting that a certain threshold of Akt signaling is required in order to result in the observed developmental defects. Additionally, the concept of an Akt activity threshold is further supported in the study by the finding that the nuclear localization and overall expression of Foxo3a was dramatically reduced in the keratinocytes of animals expressing a high level of myr-Akt, but not in those expressing a low level of myr-Akt.

In the course of conducting the analysis described in this chapter, a study was published by Gan et al. in which EGFR-mediated induction of the Akt signaling pathway was examined in the DU145 cell line (Gan et al., 2010). Gan et al., demonstrated that treatment of DU145 cells with EGF resulted in EGFR activation as well as downstream pAKT expression, and the observation of mesenchymal morphological features suggestive of an EMT. Conversely, treatment of DU145 cells with EGF in the presence of a PI3K inhibitor resulted in diminished EMT characteristics, suggesting that the observed EMT was specifically a result of activated PI3K/AKT signaling. Further, cell border expression of E-cadherin was reduced in DU145 cells treated with EGF, but unaffected in cells treated with EGF in the presence of the PI3K inhibitor. Additionally, Western blot analysis showed that DU145 cells treated with EGF displayed an increase in GSK3β phosphorylation, indicative of the inactivation of

GSK3β, as well as an increase in Snail expression. This pattern of expression was not observed in DU145 cells treated with EGF in the presence of the PI3K inhibitor. siRNA knockdown of endogenous Snail expression in DU145 cells was shown to prevent the loss of E-cadherin expression in the presence of EGF treatment. Taken together these results suggest that the activation of PI3K/AKT signaling in DU145 cells results in a loss of E-cadherin expression in the presence of increased Snail expression. These results are consistent with the analysis presented in this chapter, thereby lending further support to the hypothesis that PI3K/AKT signaling may lead to the EMT-like transcriptional repression of *E-cadherin* via Snail in prostate cancer.

Interestingly, the results presented in this chapter suggest that PI3K/AKT signaling affects E-cadherin based adherens junctions at the level of E-cadherin expression, but does not affect DSG2 based desmosomes at the level of DSG2 expression. The *in vitro* analyses in chapters IV.2 and IV.3 show that the expression of *DSG2* was relatively unaffected by the homogenously high level of AKT expression and the nuclear accumulation of Snail. Further, the high level of DSG2 protein expression detected in MAH6 cells suggests that activated AKT expression similarly does not affect overall DSG2 protein expression. However, the reduced cell border localization of DSG2 in MAH6 cells suggests that activated AKT expression may impair desmosome formation. Taken together these results suggest that PI3K/AKT signaling may disrupt desmosome formation, though this disruption does not occur as a result of the loss of DSG2 expression. Future directions will focus on analyzing the expression of other

desmosomal proteins in the MAH6 cell line to determine if the disruption of desmosome formation occurs as a result of the loss of expression of these proteins.

The results of the *in vivo* analyses described in chapter IV.4 show that the cell border expression of DGS2 was observed in MAH6 tumors, and while this expression was most robust in areas with low or no activated AKT expression, a low level of DSG2 cell border expression could often be detected in areas of high activated AKT expression. The results presented in this chapter further suggest that PI3K/AKT signaling may affect desmosome formation, as DSG2 could not consistently be detected at the cell border of all activated AKT expressing cells, but taken together with the results of chapters IV.2 it is likely that this affect is not due to the loss of DSG2 expression. Taken together these results suggest that separate pathways may be involved in the regulation of E-cadherin and DSG2 expression in prostate cancer.

Chapter IV.7

Materials and Methods

Mice

Both the *in vivo* tumorigenesis and *in vivo* extravasation and metastatic tumor colony formation assays were performed on 5-6 week old male NOD.CB17-Prkdc^{Scid} mice purchased from Jackson Laboratories (The Jackson Laboratories, Bar Harbor, ME, USA). Animal use and care followed institutional

guidelines established by the Columbia University, Institutional Animal Care and Use Committee.

Antibodies

The anti-E-cadherin mouse monoclonal antibody was purchased from Invitrogen (Carlsbad, CA, USA) and used at a dilution of 1:400 for immunofluorescence analysis of fresh fixed cells and OCT-embedded frozen tissue sections; a dilution of 1:1000 was used for Western Blot analysis. The anti-DSG2 (DG3.10) mouse monoclonal antibody was purchased from Fitzgerald (Acton, MA, USA) and used at a dilution of 1:50 for immunofluorescence analysis of fresh fixed cells and OCT-embedded frozen tissue sections; a dilution of 1:500 was used for Western blot analysis. The β-actin rabbit monoclonal antibody was purchased from Sigma-Aldrich (St. Louis, MI, USA) and used at a dilution of 1:2000 for Western blot analysis. The HA-tag (C29F4) rabbit monoclonal antibody was purchased from Cell Signaling (Danvers, MA, USA) and used at a dilution of 1:400 on fresh fixed cells and OCT-embedded frozen tissue sections; a dilution of 1:400 was also used for Western blot analysis. The Snail rabbit polyclonal antibody was purchased from Abcam (Cambridge, MA, USA) and used at a dilution of 1:1000 on fresh fixed cells and OCT-embedded frozen tissue sections; a dilution of 1:1000 was also used for Western blot analysis. The Slug rabbit polyclonal antibody was purchased from Abcam (Cambridge, MA, USA) and used at a dilution of 1:500 on fresh-fixed cells. The Twist polyclonal rabbit antibody was purchased from Abcam (Cambridge, MA, USA) and used at a

dilution of 1:1000 on fresh fixed cells. The pAKT(Ser473) (clone 736E11) rabbit antibody was purchased from Cell Signaling (Danvers, MA, USA) and was used at a concentration of 1:50 on OCT-embedded frozen tissue sections.

Generation of Stable Myristoylated AKT HA-tagged (MAH) Cell Lines

A pLNCX retroviral construct containing myristoylated HA-tagged AKT1 was purchased from Addgene (Cambridge, MA, USA). One day prior to transfection, Phoenix2™-Ampho cells (Allele Biotechnology, San Diego, CA, USA) were plated in 10cm plates at a density of 1×10^6 in MEM media containing 10% FBS. On the day of transfection, 6µg of plasmid DNA and FuGENE 6® transfection reagent (Roche Applied Sciences, Indianapolis, IN, USA) were added to cells in serum-free culture medium according to the manufacturer's protocol. Two days after transfection, media from the target DU145 cell line was aspirated and the cells were infected once via a direct transfer of filtered media containing 10µg/mL Polybrene (Millipore, Billircia, MA, USA) from the transfected Phoenix2™-Ampho cells. This infection procedure was repeated twice the following day. The day after the final infection, cells were collected via trypsinization and split into 96-well plates. The culture media (MEM with 10% FBS) was changed two days after plating, and fresh media containing 600 µg/mL Geneticin (Invitrogen, Carlsbad, CA, USA) was added for selection. Surviving cell lines were maintained under selective conditions and used for further analysis.

RNA and Protein Isolation

RNA isolation was conducted as described in chapter II.5. Protein was isolated as described in chapter III.6

qRT-PCR

qRT-PCR was conducted as described in chapter II.5. Primers used for qRT-PCR analysis are shown in Table 1.

Table 1: RT-PCR Primers and qRT-PCR Primers

qRT-PCR Primers		
Transcript	Forward Primer	Reverse Primer
E-cadherin*	5-'CAGCACGTACACAGCCCTAA-3'	5'-ACCTGAGGCTTTGGATTCCT-3'
DSG2	5'-ATCAATGCAACAGATGCAGATGA-3'	5'-TGTCAAAGTGTAGCTGCTGTGT-3'
Snail*	5'- CTTCCAGCAGCCCTACGAC-3'	5'-CGGTGGGGTTGAGGATCT-3'
β-actin	5'-AAACTGGAACGGTGAAGGTG-3'	5'-GTGGCTTTTAGGATGGCAAG-3'

*E-cadherin and Snail primers designed as reported by Chen et al., 2010.

Immunofluorescence Analysis

Immunofluorescence analysis was conducted as described in chapter II.5.

Western Blot Analysis

Western blot analysis was conducted as described in chapter III.6.

In vivo Tumorigenesis Assay

In vivo tumorigenesis assays were conducted as described in chapter III.6.

In vivo Extravasation and Metastatic Tumor Colony Formation

In vivo extravasation and metastatic tumor colony formation assays were conducted as described in chapter III.6.

Statistical analysis

Experimental data is expressed as mean ± standard deviation; statistical analysis was performed using a Student's t-test. Fisher's exact test was used for the analysis of categorical data. Values were considered statistically significant at $P \leq 0.05$.

Chapter V

Examining the Role of E-cadherin, DSG2, pAKT, and Snail in Aggressive Prostate Cancer

Chapter V.1

Overview

As described in chapter I.8 the challenge of prostate cancer diagnosis and treatment lies in predicting the potential of a given cancer to be an aggressive cancer. To date, there are no established prognostic factors for prostate cancer beyond serum PSA determination. Therefore, there is a great need for prognostic biomarkers that can assist in estimating the likelihood of prostate cancer aggressiveness.

The overexpression of AKT and pAKT in prostate cancer has been described, and AKT/pAKT expression has been associated with biochemical recurrence in prostate cancer (Malik et al., 2002; Liao et al., 2003; Sun et al., 2001; Kreisberg et al., 2004; Li et al., 2009; Bedolla et al., 2007; Ayala et al., 2004). However, while the loss of E-cadherin expression has been described in prostate cancer, no large scale study has yet examined the association of E-cadherin expression and biochemical recurrence in prostate cancer (Rubin et al., 2001; Umbas et al., 1992). Additionally, the expression of DSG2 in prostate cancer has not been examined, to date.

The *in vitro* functional analysis performed in chapters IV.2 and IV.3 of this study demonstrated that activation of the PI3K/AKT signaling pathway can lead to the transcriptional repression of *E-cadherin* in prostate cancer, and suggested that this transcriptional repression may be mediated by the EMT-associated

transcription factor Snail. Additionally, the *in vivo* analysis performed in chapter IV.4 of this study demonstrated that the expression of E-cadherin is inversely proportional to that of both myristoylated-AKT and Snail, further supporting the hypothesis that PI3K/AKT and Snail are repressors of E-cadherin expression. Interestingly, while this pattern of expression could be observed for DSG2, it was observed to a lesser degree. Taken together with the *in vitro* analyses performed in chapters IV.2 and IV.3, these results suggest that the regulation of DSG2 expression may be separate from that of E-cadherin expression in the progression of prostate cancer.

Having performed these functional analyses I next sought to further examine the hypothesis that PI3K/AKT signaling may lead to the EMT-like transcriptional repression of *E-cadherin* via Snail in prostate cancer. I also wanted to examine the expression of DSG2 in human prostate cancer tissue samples to determine whether a loss of DSG2 expression similar to that described for E-cadherin could be observed. Additionally I wanted to determine whether the relationship between DSG2, activated AKT and Snail expression observed in chapter IV could also be observed in human prostate cancer tissue samples. Finally, I wanted to examine whether E-cadherin and DSG2 could serve as useful predictors of prostate cancer aggressiveness by determining whether their expression was associated with biochemical recurrence.

To accomplish these goals I examined the expression of E-cadherin, DSG2, pAKT, and Snail in a large cohort of patients with prostate cancer who underwent radical prostatectomy. Details of the cohort and the method by which

the expression of these proteins of interest were analyzed are described in chapter V.2. In chapter V.3 I describe the statistical analysis performed to determine the expression profiles of the individual proteins of interest in primary prostate cancer, the correlation between the expression of the proteins of interest themselves, the correlation between the expression of the proteins of interest and clinicopathological characteristics of prostate cancer, and the association of the proteins of interest with biochemical recurrence. I found that, similar to E-cadherin, there is a reduced expression of DSG2 in prostate cancer. Further there is a strong and statistically significant positive correlation between the expression of DSG2 and E-cadherin in prostate cancer, and the expression of these cadherins is negatively correlated with the clinicopathological features of prostate cancer examined. A weak correlation between the expression of E-cadherin, pAKT, and Snail as well as DSG2, pAKT, and Snail was also observed. Finally, the reduced expression of both E-cadherin and DSG2 were significantly associated with biochemical recurrence in prostate cancer. In chapter V.4 I discuss the results observed for the expression of these markers and the potential use of both E-cadherin and DSG2 as markers of aggressive prostate cancer. The materials utilized for this portion of the study are further described in chapter V.5.

Chapter V.2

Immunofluorescence analysis of E-cadherin, DSG2, pAKT, and Snail on Primary Prostate Cancer Tissue Microarrays and Descriptive Statistics of the Cohort

To examine the expression of E-cadherin, DSG2, pAKT, and Snail in primary prostate cancer I performed immunofluorescence analysis for these proteins of interest on tissue microarrays (TMAs). TMAs are built using tissue cores, small cylinders of tissue 0.6 μm in diameter extracted from formalin-fixed paraffin-embedded (FFPE) tissue blocks of patient samples. As many as 250 tissue cores embedded together in paraffin may be used to build a given TMA, thereby allowing for the analysis of a given protein of interest in many patient samples, simultaneously, in a single experiment.

The TMAs utilized in this study were built in the Cordon-Cardo laboratory, and were generated from 414 radical prostatectomy cases which were originally collected between September, 2000 to January, 2005 at the Henry Ford Health System in Detroit as part of the Gene-Environment Interaction Prostate Cancer Study (GECAP: NIH/NIES R01 ES11126-03). Follow-up data for these cases regarding evidence of biological recurrence was available for our study. To build the TMAs, tissue samples for each case were first reviewed by two pathologists in the lab to identify the areas of the sample that contained the highest density of tumor cells. Based on these reviews, tissue cores were extracted from the FFPE

tissue blocks for each patient sample. In this way, the representative cores for each patient sample were enriched for tumor cells. A minimum of three cores taken from the tumor rich regions of each patient sample were used to build the TMAs; therefore, each patient sample was represented in triplicate, at minimum, on the TMAs. TMAs including adjacent normal tissue for each patient were also built in the manner described. Once built, 5μm sections were cut from the TMA paraffin blocks and immunofluorescence analysis was performed for each protein of interest. The TMAs were then scored with Dr. Mireia Castillo-Martin, a pathologist in the Cordon-Cardo laboratory. The expression of the proteins of interest was scored by estimating the percentage of tumor cells with immunoreactivity per tissue core (Figure 1). The average values of the representative cores from each patient sample were then used for the statistical analyses described in chapter V.3. The clinical characteristics of the patients included in this study are shown in Table 1.

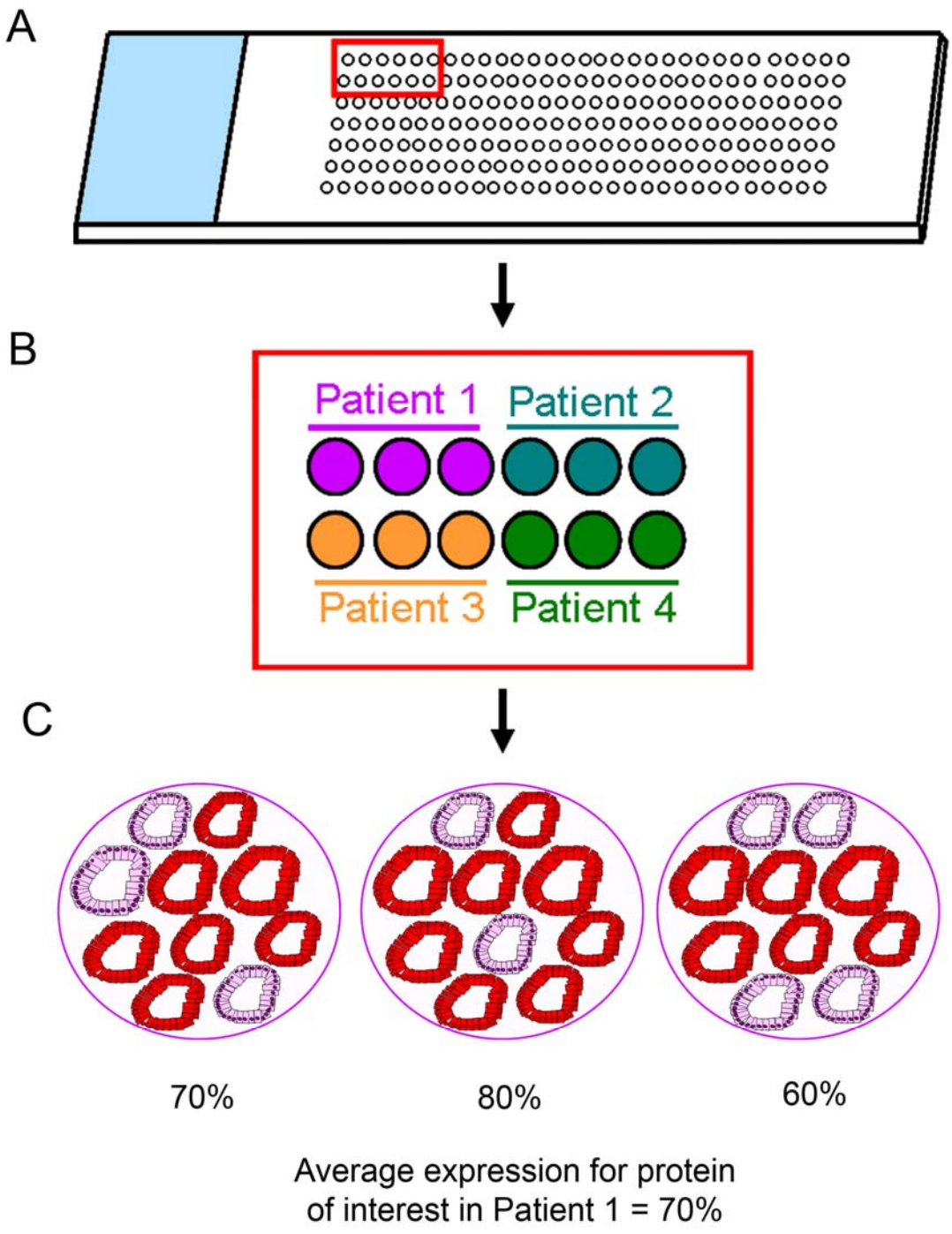

Figure 1: Schematic depiction of a TMA and TMA scoring. Up to 250 tissue cores may be used to build a TMA (A). Each patient case is represented by a minimum of three tissue cores (B). Immunofluorescence analysis (depicted here in red) is used to examine the expression of each protein of interest. Each tissue core is scored by estimating the percentage of tumor cells with immunoreactivity per tissue core. The final score for the marker of interest in a given patient sample is the average value of the representative cores for the patient (C).

Table 1: Clinical characteristics of patients with prostate cancer who underwent radical prostatectomy (*n* = 414)

Age at Diagnosis	
Mean	61
Range	41 - 74.7
≤50	36 (9%)
>50- ≤60	165 (40%)
>60-≤70	192 (46%)
>70	16 (4%)
Unavailable	5 (1%)
Race	
White	230 (56%)
African American	179 (43%)
Asian/Polynesian	1 (<1%)
Hispanic	2 (<1%)
Unknown	2 (<1%)
PSA at Diagnosis (ng/mL)	
Mean	7
Range	0.4 - 51.4
<4	72 (17%)
4-10	272 (66%)
>10	66 (16%)
Unavailable	4 (<1%)
Gleason Score	
<7	148 (36%)
7	177 (43%)
>7	77 (18%)
Unavailable	12 (3%)
TNM Stage	
T1, T2	329 (79%)
T3	73 (18%)
T4	10 (2%)
Unavailable	2 (<1%)
Resected at Margins	
Negative	268 (65%)
Positive	130 (31%)
Unavailable	16 (4%)
Angiolymphatic Invasion	
Negative	392 (95%)
Positive	11 (3%)
Unavailable	11 (3%)
Perineural Invasion	
Negative	135 (33%)
Positive	268 (65%)
Unavailable	11 (3%)
Biochemical Relapse	
Negative	316 (76%)
Positive	98 (24%)

Chapter V.3

Descriptive Statistics and Expression of E-cadherin, DSG2, pAKT, and Snail in Primary Prostate Cancer

To assess the expression of the proteins of interest in prostate cancer as compared to normal prostate tissue, I performed immunofluorescence analysis for each protein of interest on prostate cancer TMAs for the entire cohort (*n* = 414) as well as normal prostate TMAs for a subset of the cohort (*n* = 50, E-cadherin and DSG2; *n* = 91, pAKT and Snail) (Table 2; Figure 2). In addition to an antibody for the protein of interest, an antibody for CK8/18 — keratins found in both normal prostate luminal epithelial cells and adenocarcinoma cells — was also included on each TMA as a means of identifying the epithelial cells in each sample.

A significant decrease in the expression of E-cadherin was found in prostate cancer as compared to normal prostate, consistent with the reported reduced expression of E-cadherin in prostate cancer (Rubin et al., 2001; Umbas et al., 1992). While the cell border expression of E-cadherin was generally high in well differentiated areas of the tumor, this expression was often much lower in poorly differentiated areas of the tumor (Figure 3). Interestingly, there is also a significant decrease in the expression of DSG2 in prostate cancer as compared to normal prostate. Similar to the pattern of E-cadherin expression, the cell border expression of DSG2 was generally high in areas of the tumor that were well differentiated and often much lower in areas of the tumor that were poorly

differentiated (Figure 4). Conversely, a significant increase in pAKT expression was detected in prostate cancer as compared to normal prostate, a result that is consistent with the reported increase of pAKT expression in prostate cancer (Malik et al., 2002; Liao et al., 2003; Sun et al., 2001). This pAKT expression was detected in both the cytoplasm and the nucleus and was generally high in both well and poorly differentiated areas of the tumor (Figure 5). Additionally, there was a slight but significant increase in the nuclear expression of Snail in prostate cancer as opposed to normal prostate consistent with the reported increase of Snail in prostate cancer (Heeboll et al., 2009) (Figure 6).

Table 2: Expression of proteins of interest in prostate cancer as compared to normal prostate.

	Cancer	Normal	*P*-value*
E-cadherin			
Mean	69.2	87.2	0.0003
Standard Deviation	20.2	3.6	
Median	75	88	
Interquartile Range	60-83.3	85-90	
DSG2			
Mean	57.5	81.1	0.0002
Standard Deviation	25.7	9.9	
Median	66.7	84.5	
Interquartile Range	40-76.7	80-86.7	
pAKT			
Mean	28.8	8.2	<0.000
Standard Deviation	27.9	16.3	
Median	23.3	0	
Interquartile Range	0-53.3	0-9	
Snail			
Mean	8.9	7.1	0.04
Standard Deviation	18.2	14.4	
Median	0	0	
Interquartile Range	0-10	0-6.3	

**P*-value determined using Student's T-test

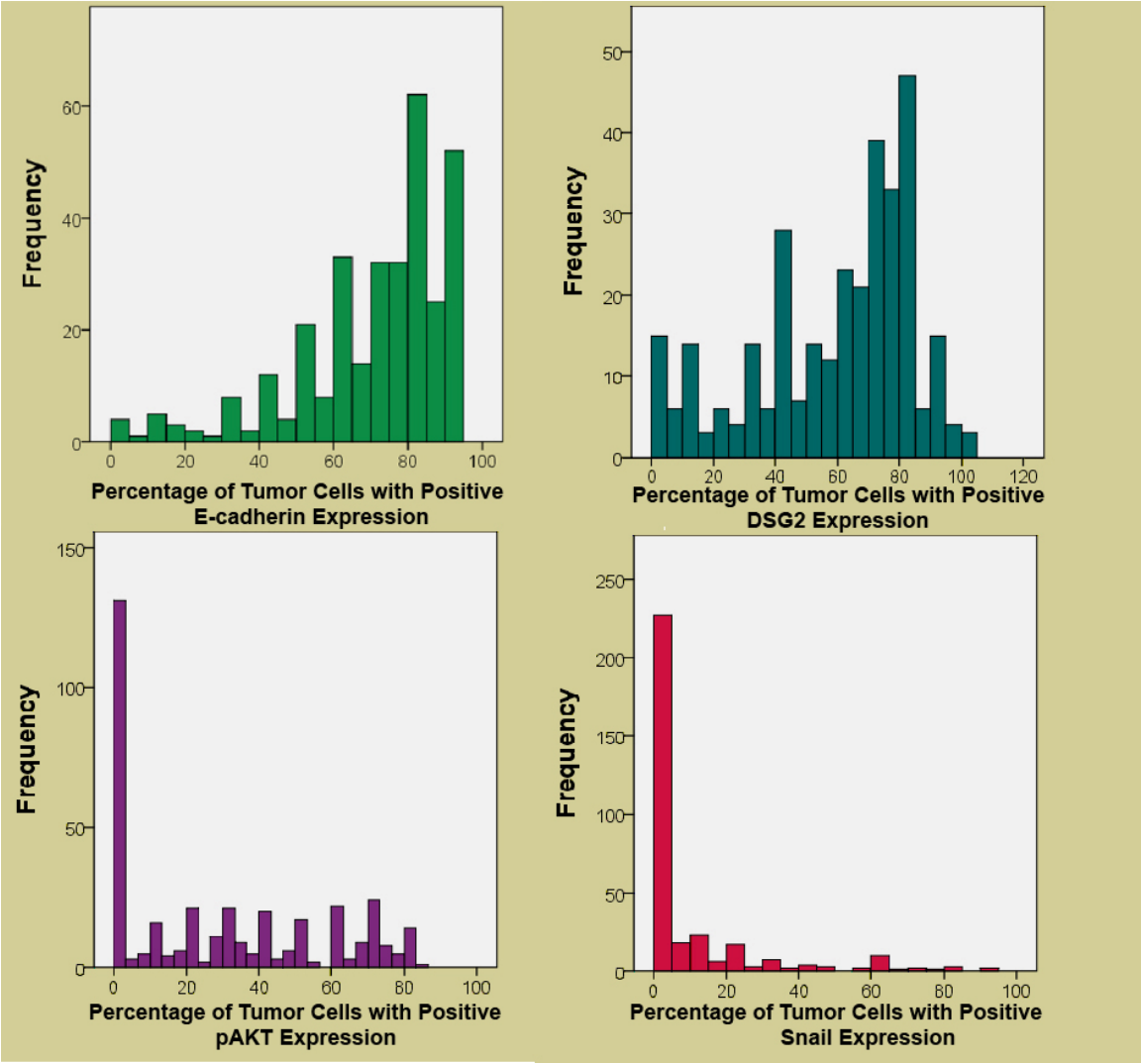

Figure 2: Histogram depicting the number of cases within the cohort (y-axis) with positive expression for the proteins of interest (x-axis) on primary prostate cancer TMAs.

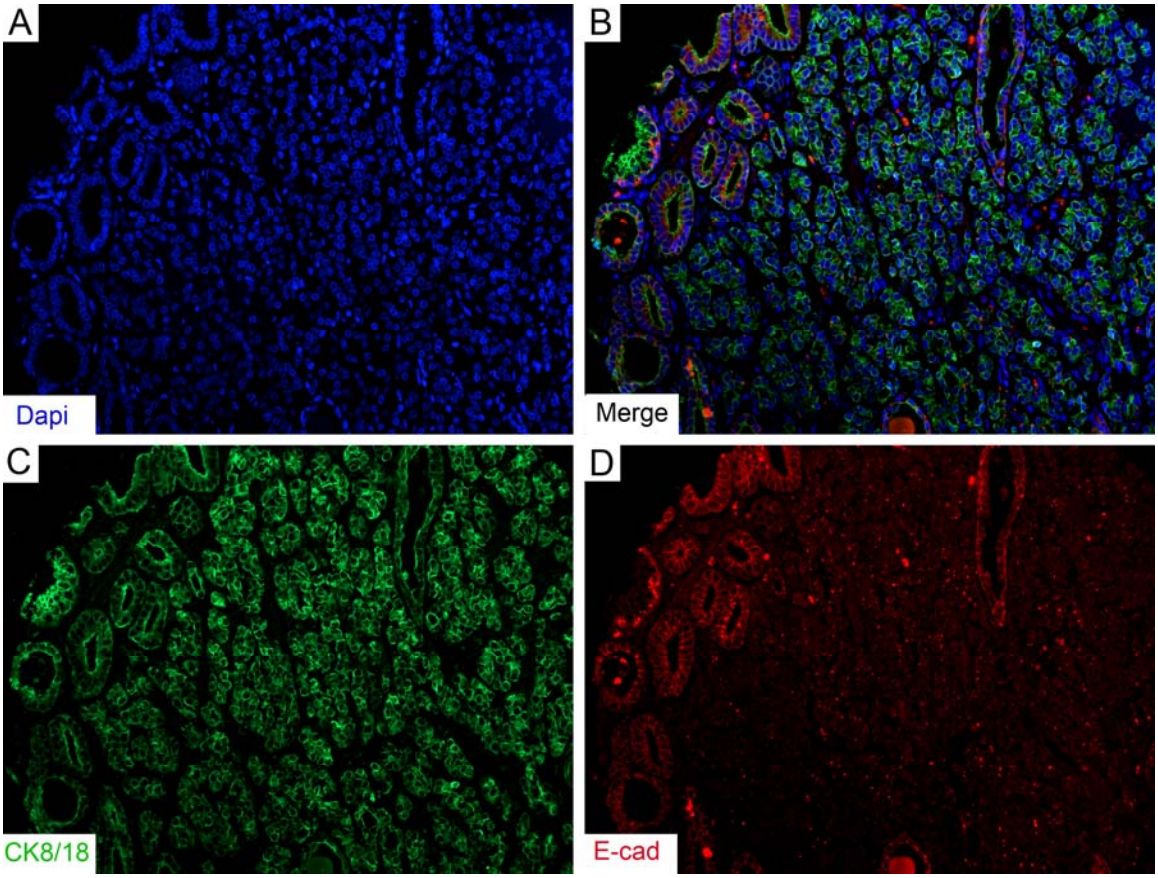

Figure 3: Immunofluorescence analysis of E-cadherin and CK8/18 in prostate cancer TMAs. The cell border expression of E-cadherin is high in well differentiated areas of the tumor and low in poorly differentiated areas of the tumor. E-cadherin is shown in red, CK8/18 is shown in green, and DAPI is shown in blue.

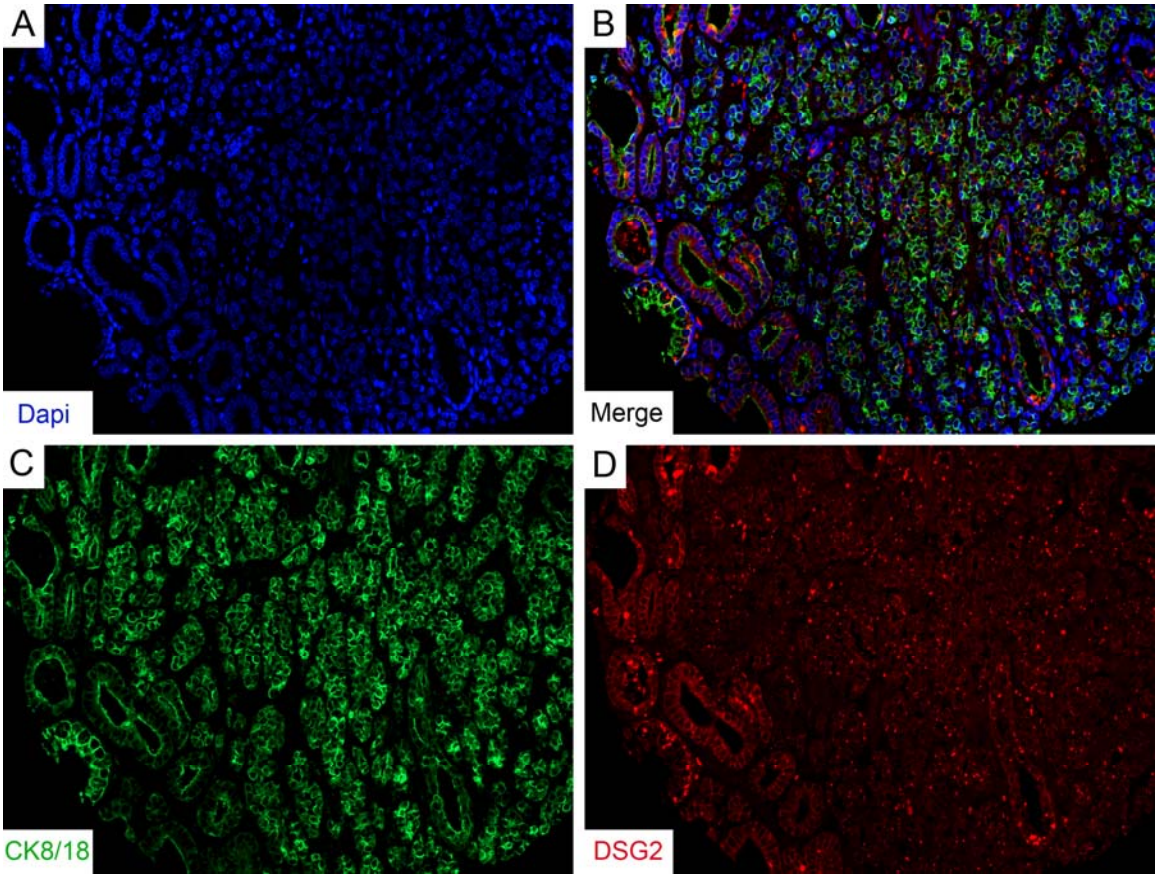

Figure 4: Immunofluorescence analysis of DSG2 and CK8/18 in prostate cancer TMAs. The cell border expression of DSG2 is high in well differentiated areas of the tumor and low in poorly differentiated areas of the tumor. DSG2 is shown in red, CK8/18 is shown in green, and DAPI is shown in blue.

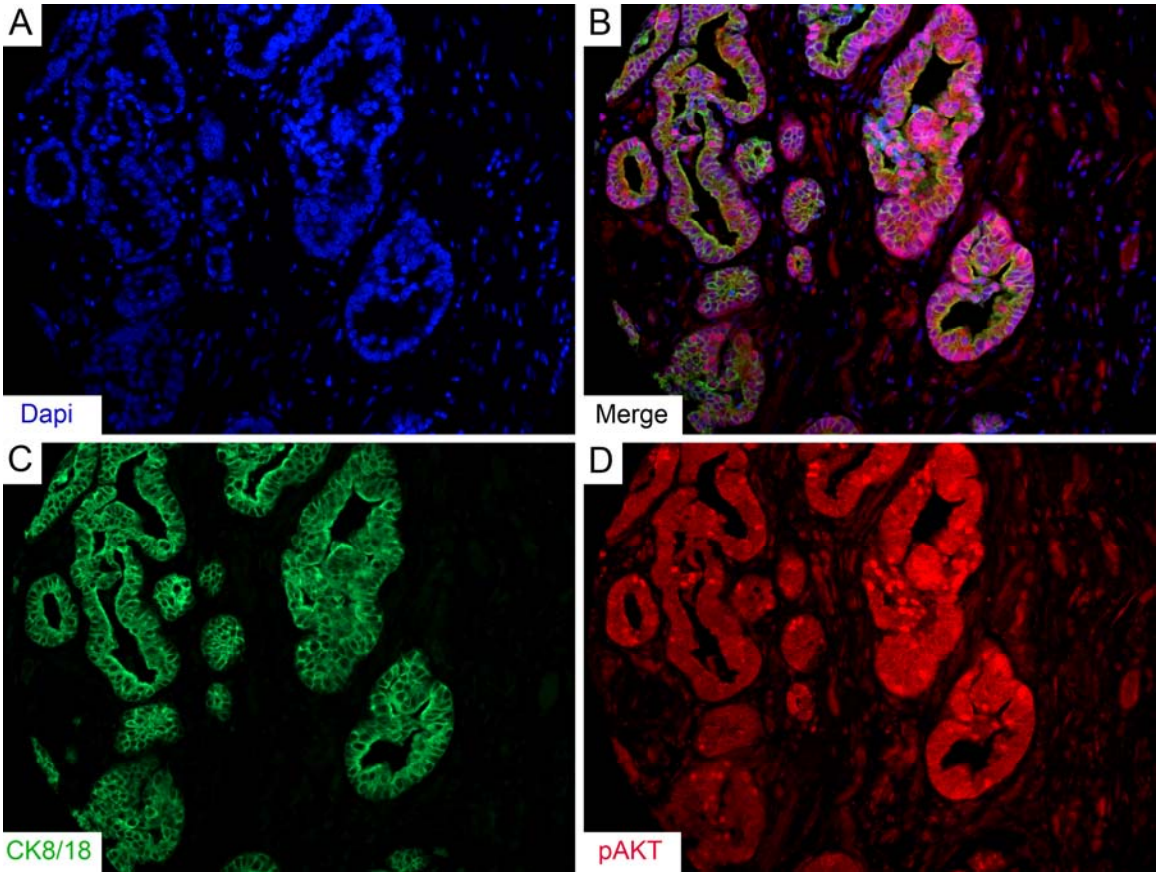

Figure 5: Immunofluorescence analysis of pAKT and CK8/18 in prostate cancer TMAs. The expression of pAKT can be detected in the nucleus and cytoplasm and is high in both well differentiated and poorly differentiated areas of the tumor. pAKT is shown in red, CK8/18 is shown in green, and DAPI is shown in blue.

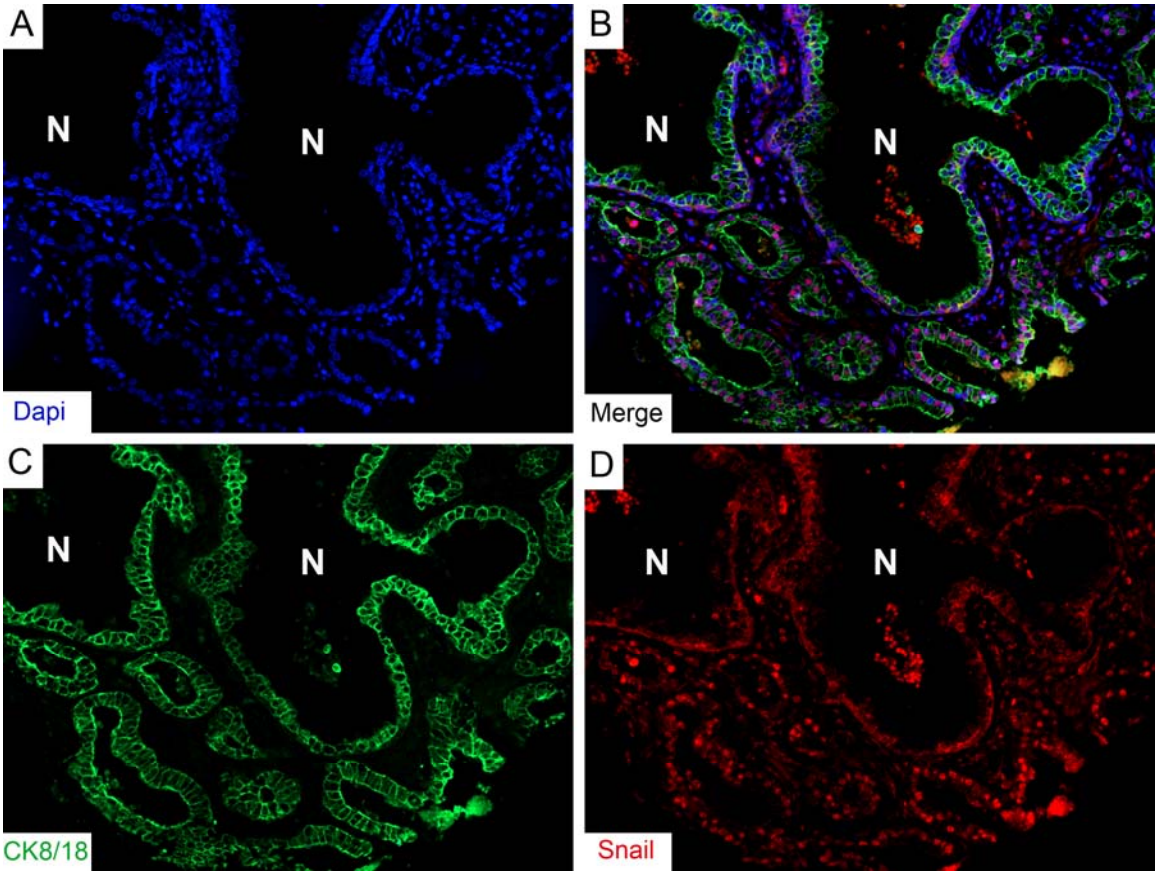

Figure 6: Immunofluorescence analysis of Snail and CK8/18 in prostate cancer TMAs. Here the nuclear expression of Snail is more often detected in cancer cells than in normal prostate epithelium (as indicated by the letter N). Snail is shown in red, CK8/18 is shown in green, and DAPI is shown in blue.

Correlation for the Expression of Proteins of Interest and Clinicopathological Characteristics of Prostate Cancer Patients

Having examined the expression of E-cadherin, DSG2, pAKT, and Snail in the cohort, I next wanted to determine whether there was a correlation between the expression of the proteins of interest themselves, as well as whether there was a correlation between the expression of the proteins of interest and clinicopathological characteristics most commonly associated with aggressive prostate cancer including serum PSA concentration, Gleason score, and pathological stage (Quinn et al., 2001) (Table 3). This analysis was performed using Spearman's rank correlation. Interestingly, there was a strong and significant positive correlation between the expression of E-cadherin and DSG2, therefore suggesting that as the expression of E-cadherin decreases in prostate cancer so too does the expression of DSG2.

A weak but significant positive correlation between the expression of pAKT and the expression of Snail was detected, suggesting that as the expression of pAKT increases so too does the nuclear expression of Snail. Contrary to the results of the *in vitro* and *in vivo* functional analysis performed in chapter IV, there was a weak but significant positive correlation between the expression of pAKT and the expression of E-cadherin. There was also very weak positive correlation between the expression of pAKT and DSG2, weaker than that of pAKT and E-cadherin; however, this correlation was not significant. These results suggest that the expression of E-cadherin and DSG2 increase as pAKT expression increases, as opposed to the results of the functional analyses

performed in chapter IV, which suggest the opposite relationship. There was also a very weak negative correlation between E-cadherin and Snail. Though this correlation was not significant, it was consistent with the reduced expression of *E-cadherin* detected in cells with high nuclear Snail expression observed in chapter IV.2, as well as the inverse expression pattern of E-cadherin and Snail observed in chapter IV.4. Additionally, there is a very weak positive correlation between DSG2 and Snail; though this correlation is not significant, it is consistent with observation in chapter IV.2 that there is no reduction in level of *DSG2* expression in cells with high nuclear Snail expression, further suggesting that the expression of Snail does not affect the expression of DSG2 in prostate cancer.

Interestingly, though not significant, there was a negative correlation between E-cadherin expression and all the clinicopathological features examined. A negative correlation was also observed for DSG2 expression and all the clinicopathological features examined. This correlation was significant for both serum PSA concentration and Gleason score, and slightly stronger that the correlation observed between E-cadherin and these same features. Taken together, these results suggest that the expression of both E-cadherin and DSG2 decrease as the level of serum PSA concentration increases, as well as in cases of prostate cancer with a high Gleason scores and advanced pathological stage.

		PSA	Gleason Score	TNM Stage	pAKT	E-cadherin	DSG2	Snail
PSA	Correlation	1.000	.312**	.256**	.111*	-.072	-.161**	-.071
	Sig. (2-tailed)	.	.000	.000	.034	.201	.004	.200
	N	410	400	410	364	317	316	327
Gleason Score	Correlation		1.000	.363**	.163**	-.109	-.160**	.032
	Sig. (2-tailed)		.	.000	.002	.054	.005	.566
	N		402	402	359	314	313	323
TNM Stage	Correlation			1.000	.109*	-.083	-.084	-.001
	Sig. (2-tailed)			.	.037	.139	.135	.979
	N			412	366	319	318	329
pAKT	Correlation				1.000	.134*	.053	.129*
	Sig. (2-tailed)				.	.017	.358	.021
	N				368	314	305	318
E-cadherin	Correlation					1.000	.498**	-.025
	Sig. (2-tailed)					.	.000	.669
	N					321	292	306
DSG2	Correlation						1.000	.033
	Sig. (2-tailed)						.	.578
	N						320	293
Snail	Correlation							1.000
	Sig. (2-tailed)							.
	N							331

**. Correlation is significant at the 0.01 level (2-tailed).

*. Correlation is significant at the 0.05 level (2-tailed).

Table 3: Examining the correlation between the proteins of interest and clinicopathological characteristics using Spearman's rank correlation. There is a strong and significant positive correlation between the expression of E-cadherin and DSG2 (ρ = 0.498**). There is a weak but significant positive correlation between the expression of pAKT and Snail (ρ = 0.129*). There is a weak but significant positive correlation between pAKT and E-cadherin (ρ = 0.134*), and a very weak positive correlation between pAKT and DSG2 which is not significant (ρ = 0.053). There is a very weak negative correlation between E-cadherin and Snail (ρ = -0.025) and a very weak positive correlation between DSG2 and Snail (ρ = 0.033), neither of which are significant. Interestingly there is a negative correlation between both DGS2 and E-cadherin and all clinicopathological features examined.

Clinical Implications of the Expression of Proteins of Interest

Having examined the correlation between the proteins of interest and clinicopathological features of prostate cancer, I next wished to determine whether these proteins of interest are associated with biochemical recurrence. This analysis was performed using the log-rank test, and Kaplan-Meier survival curves were plotted. To examine E-cadherin, I compared cases with high E-cadherin expression (≥ 70%) to those with low E-cadherin expression (<70%). A cut-off value of 70% E-cadherin expression was utilized as this was the

approximate mean expression value observed for E-cadherin in this prostate cancer cohort (Table 2). Importantly, <70% E-cadherin expression was not observed in the normal prostate cases examined thereby emphasizing the utility of this cut-off value (Table 3). Interestingly, patients expressing ≥70% E-cadherin had a higher rate of recurrence free survival than those expressing <70% E-cadherin and the difference between these two groups was statistically significant (Figure 7, $P = 0.043$). Patients with <70% E-cadherin expression had a median time to biochemical recurrence of 104 months, while those with ≥70% E-cadherin expression did not reach the median time to biochemical recurrence after a follow-up time of 120 months. To examine DSG2, I compared cases with high DSG2 expression (≥ 60%) to those with low DSG2 expression (<60%). A cut-off value of 60% was utilized as this was the approximate mean expression value observed for DSG2 in this prostate cancer cohort (Table 2). Importantly, <60% DSG2 expression was only observed in 2% of the normal prostate cases examined, thereby emphasizing the utility of this cut-off value (Table 3). Much like E-cadherin, patients expressing ≥ 60% DSG2 had a higher rate of recurrence free survival than those expressing < 60%, and the difference between these two groups was statistically significant (Figure 8, $P = 0.01$). Patients with <60% DSG2 expression had a median time to biochemical recurrence of 104 months, while those with ≥60% DSG2 expression did not reach the median time to biochemical recurrence after a follow-up time of 120 months. Taken together, these results indicate that reduced cadherin expression is associated with biochemical

recurrence in prostate cancer, therefore suggesting that E-cadherin and DSG2 may be useful prognostic markers of aggressiveness for prostate cancer.

To examine pAKT, I compared cases that did not express pAKT (and were therefore considered negative for pAKT expression) to those that did express pAKT (and were therefore considered positive for pAKT expression). Importantly, pAKT expression was observed in significantly fewer normal prostate cases (38%) as compared to prostate cancer cases (67%), thereby emphasizing the utility of this cut-off value (Table 3). Patients who were negative for pAKT expression had a higher rate of recurrence-free survival than those who were positive for pAKT expression, and the difference between these two groups was nearly statistically significant (Figure 9, $P = 0.078$). Patients who were positive for pAKT expression had a median time to biochemical recurrence of 106 months, while those who were negative for pAKT expression did not reach the median time to biochemical recurrence after a follow-up time of 120 months. To examine Snail, I compared cases that did not express Snail (and were therefore considered negative for Snail expression) to those that did express Snail (and were therefore considered positive for Snail expression). Though there was a slight but significant increase in the mean expression value for Snail in prostate cancer as compared to normal prostate, as shown in Table 2, a significant difference in positive Snail expression in normal prostate cases (40%) as compared to prostate cancer cases (36%) was not detected (Table3). Accordingly, while patients who were negative for Snail expression had a higher rate of recurrence-free survival than those who were positive for Snail

expression, there was not a significant difference between these two groups (Figure 10, *P* = 0.263). Patients who were positive for Snail expression had a median time to recurrence of 106 months, while those who were negative for Snail expression did not reach the median time to biochemical recurrence after a follow-up time of 120 months. Taken together these results suggest that pAKT expression is associated with biochemical recurrence in prostate cancer and that this association is very nearly statistically significant, indicating that pAKT may serve as a useful prognostic marker of aggressiveness in prostate cancer. Though taken as a whole, these results indicate that E-cadherin and DSG2 are the most useful markers of prostate cancer aggressiveness examined in this study.

Table 3: Cut-off values for biomarker expression in prostate cancer as compared to normal prostate

	Cancer	Normal	*P*-value*
E-cadherin			
≥70%	204 (64%)	46 (100%)	<0.001
<70%	117 (36%)	0 (0%)	
DSG2			
≥60%	191 (60%)	44 (98%)	<0.001
<60%	129 (40%)	1 (2%)	
pAKT			
No Expression	122 (33%)	51 (62%)	<0.001
Expression	246 (67%)	31 (38%)	
Snail			
No Expression	211 (64%)	49 (60%)	0.587
Expression	120 (36%)	32 (40%)	

**P*-value determined using $\chi 2$ test

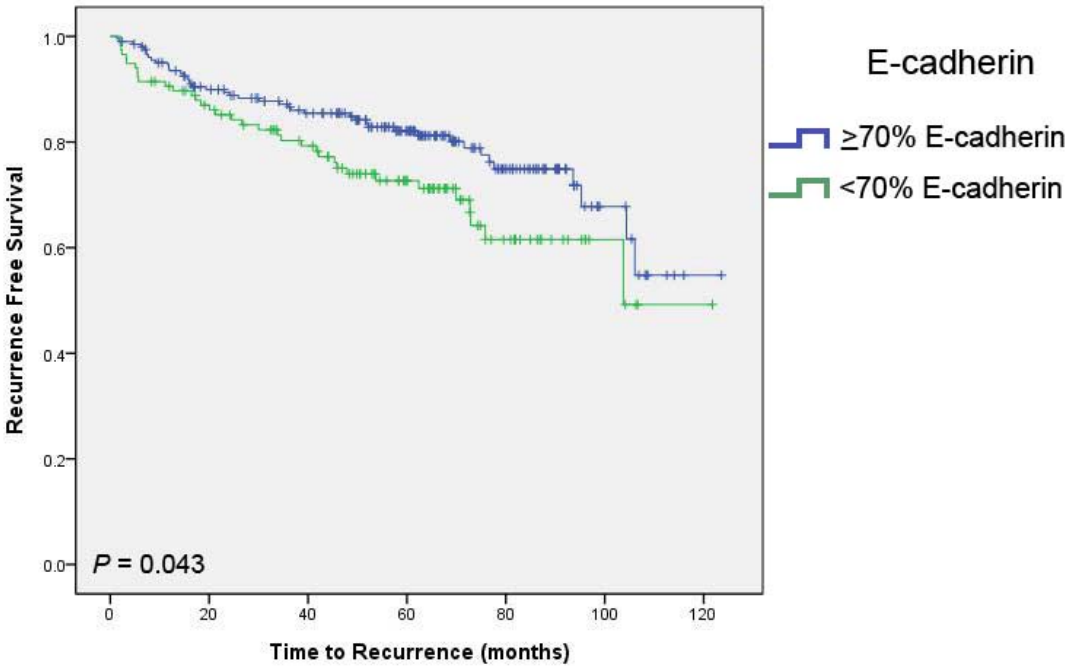

Figure 7: Kaplan-Meier survival curve for E-cadherin. Patients expressing ≥70% E-cadherin had a higher rate of recurrence free survival than those expressing <70% E-cadherin and the difference between these two groups is statistically significant.

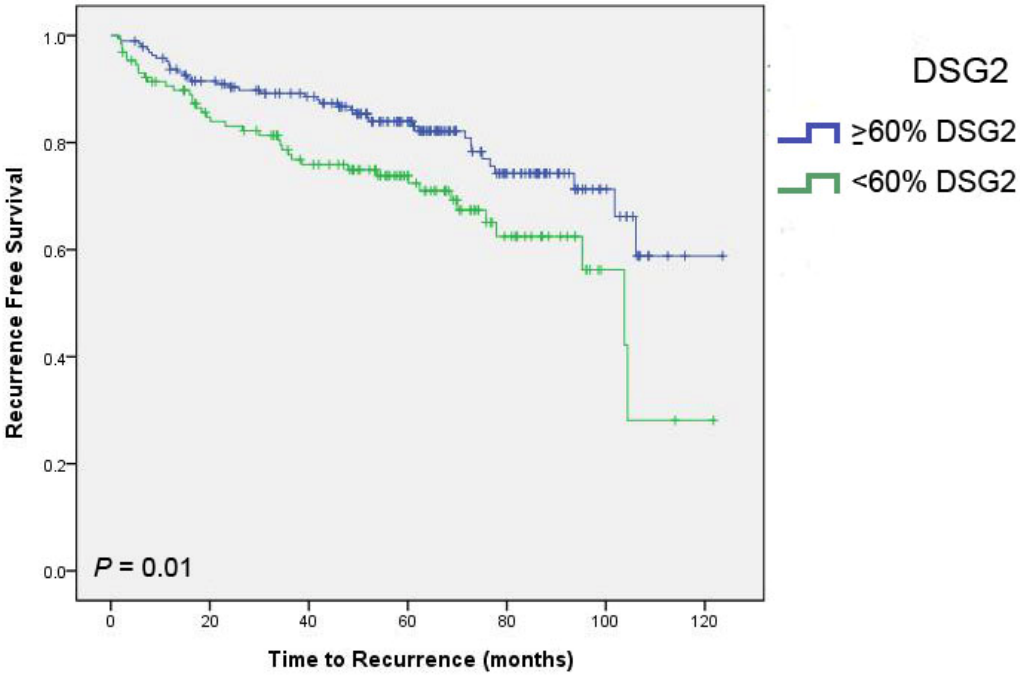

Figure 8: Kaplan-Meier survival curve for DSG2. Patients expressing ≥60% DSG2 had a higher rate of recurrence free survival than those expressing <60% DSG2 and the difference between these two groups is statistically significant.

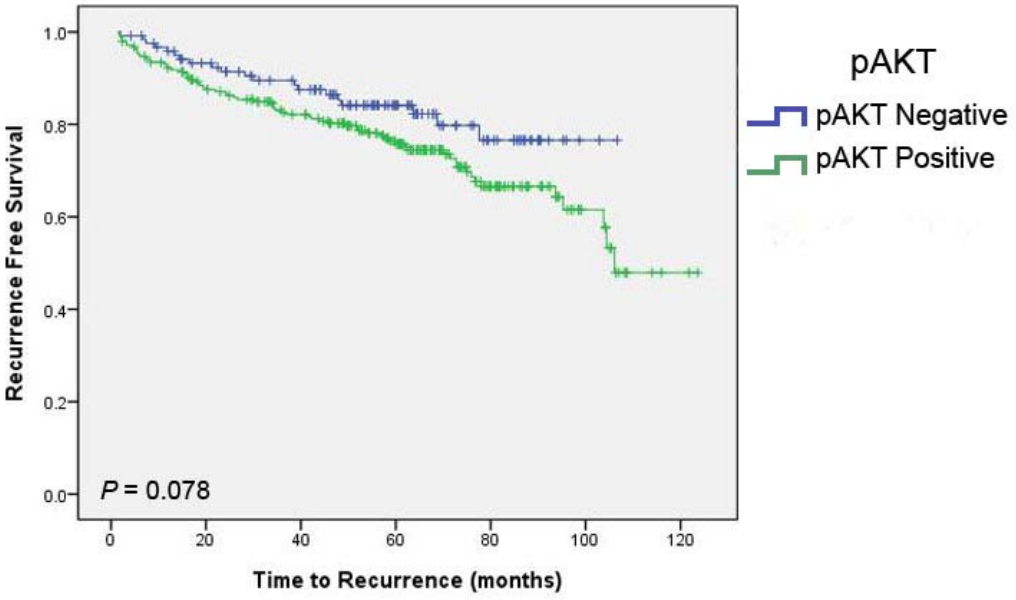

Figure 9: Kaplan-Meier survival curve for pAKT. Patients negative for pAKT expression had a higher rate of recurrence free survival than those with positive pAKT expression and the difference between these two groups is nearly statistically significant.

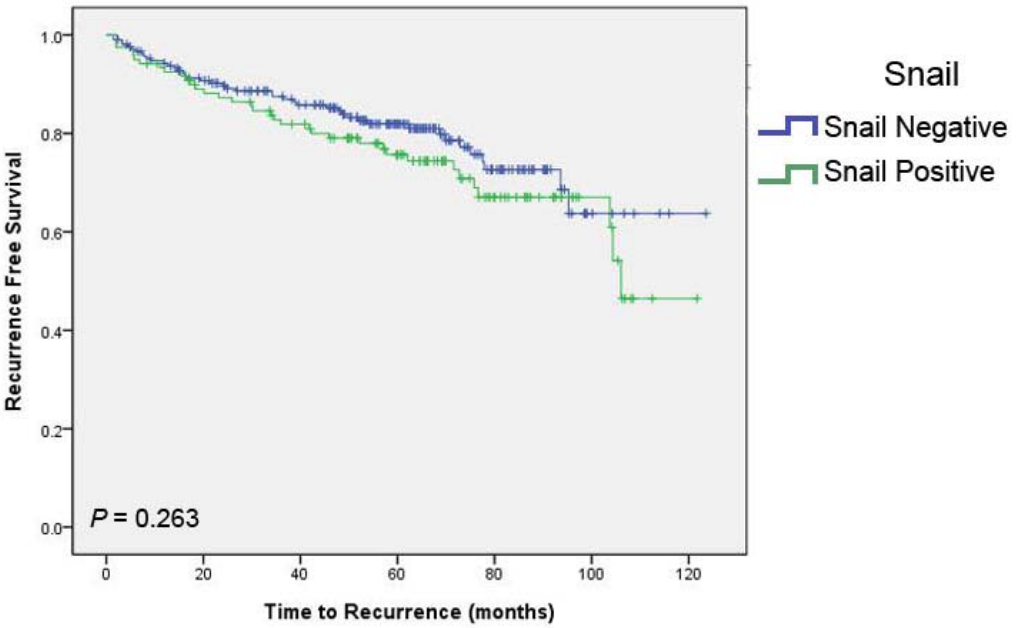

Figure 10: Kaplan-Meier survival curve for Snail. Patients negative for Snail expression had a higher rate of recurrence free survival than those with positive Snail expression, but the difference between these two groups is not statistically significant.

Chapter V.4

Discussion

The results of the analyses performed in chapter IV suggest that PI3K/AKT signaling may mediate the transcriptional repression of *E-cadherin* in prostate cancer via Snail. These results also suggest that the regulation of E-cadherin expression may be separate from that of DSG2 expression, as PI3K/AKT signaling does not appear to negatively affect the level of DSG2 expression. In chapter V.3, using Spearman's rank correlation a very weak negative correlation was observed for the expression of E-cadherin and Snail, while a weak positive correlation was observed for DSG2 and Snail. These results support the hypothesis that Snail may act as a transcriptional repressor of *E-cadherin* expression in prostate cancer, and that Snail is not involved in the repression of *DSG2* expression in prostate cancer. Though a weak but significant positive correlation was observed for the expression of pAKT and E-cadherin, contrary to what was predicted by my hypothesis, given the many potential roles of PI3K/AKT signaling in prostate cancer progression coupled with the various means by which the expression of E-cadherin may be inhibited, these results may imply that PI3K/AKT signaling is but one of a variety of mechanisms by which E-cadherin expression is inhibited in prostate cancer.

While the loss of E-cadherin expression has been previously reported in prostate cancer, a large scale analysis of the utility of this cadherin in predicting prostate cancer aggressiveness had not been performed. Additionally, prior to

this study, the expression of desmosomal cadherins in prostate cancer had not been examined. Given that both adherens junctions and desmosomes are involved in cell-cell adhesion in prostatic epithelium, an understanding of the expression of both classical cadherins and desmosomal cadherins would provide a deeper insight into the role of anchoring junctions in prostate cancer progression. Interestingly, DSG2 expression was significantly reduced in prostate cancer as opposed to normal prostate. Much like E-cadherin, the expression of DSG2 was generally high in well differentiated areas of the tumor and low in poorly differentiated areas of the tumor. Consistent with this observation, the results of the Spearman's rank correlation show that there is a strong positive correlation between the expression of E-cadherin and DSG2. Further, there is a negative correlation between the expression of these cadherins and serum PSA concentration, Gleason score, and pathological stage. Taken together these results suggest that cadherin expression is reduced in the poorly differentiated cells of primary prostate tumors. Taken together with the results of the Kaplan-Meier survival curves, these results further suggest that tumor cells with reduced cadherin expression are more likely to be aggressive and would therefore possess a greater potential for metastatic behavior than those cells with a high level of cadherin expression. These results highlight a potentially critical role for cadherin based cell-cell adhesion in the progression of prostate cancer, and demonstrate that both E-cadherin and DSG2 may be useful prognostic markers of aggressive prostate cancer.

Chapter V.5

Materials and Methods

Antibodies

The anti-E-cadherin mouse monoclonal antibody was purchased from Invitrogen (Carlsbad, CA, USA) and used at a dilution of 1:400 for immunofluorescence analysis of FFPE TMA sections. The anti-DSG2 (DG3.10) mouse monoclonal antibody was purchased from Fitzgerald (Acton, MA, USA) and used at a dilution of 1:20 for immunofluorescence analysis of FFPE TMA sections. The pAKT(Ser473) (clone 736E11) rabbit antibody was purchased from Cell Signaling (Danvers, MA, USA) and was used at a concentration of 1:50 for immunofluorescence analysis of FFPE TMA sections. The Snail rabbit polyclonal antibody was purchased from Abcam (Cambridge, MA, USA) and used at a dilution of 1:800 for immunofluorescence analysis of FFPE TMA sections. The CK8/18 guinea pig polyclonal antibody was purchased from Progen (Heidelberg, Germany) and used at a concentration of 1:100 for immunofluorescence analysis of FFPE TMA sections.

Immunofluorescence Analysis of FFPE TMA sections

TMAs were built as described in chapter V.2, and 5µm sections were cut from each TMA FFPE block for analysis. The slides were deparaffinized and rehydrated, and antigen retrieval was performed by heating slides in a steamer in citrate buffer, pH 6.0 for 15 minutes. Slides were allowed to come to room

temperature, washed under running tap water for 1 minute, and then washed once in 1X PBS. Slides were incubated in 0.1% Triton X-100/ 1% BSA/ 1X PBS block at room temperature for 1 hour. Block was then aspirated, primary antibody was added, and slides were incubated overnight at 4ºC. The following day, slides were washed in 1XPBS with agitation, then a 1:600 dilution of secondary antibody, either Alexa Fluor® 594 or Alexa Fluor® 488 (Invitrogen, Carlsbad, CA, USA), was added and slides were incubated at room temperature for 45 min. Slides were then washed three times in 1X PBS + 0.1% Triton with agitation, washed three times in 1X PBS to remove detergent, immersed briefly in water and mounted using VECTASHIELD® mounting medium with DAPI (Vector Laboratories, Burlingame, CA, USA). TMAs were then scored in the manner described in chapter V.2.

Statistical Analysis

Statistical analysis was conducted using SPSS v18.0 (SPSS Inc., Chicago, IL, USA). The Student's t-test was used to compare the expression of the proteins of interest in primary prostate cancer and normal prostate tissue. Spearman's rank correlation was used to analyze the correlations between proteins of interest and clinicopathological features. Biochemical recurrence was analyzed using Kaplan-Meier survival curves, and curves were compared using the log-rank test. A P-value ≤ 0.05 was considered statistically significant.

Chapter VI

General Discussion

General Discussion

The Role of Cell-Cell Adhesion in Aggressive Prostate Cancer

Adherens junctions and desmosomes play a crucial role in the development and maintenance of normal tissues, and the importance of these cell-cell junctions is underscored by the developmental aberrations and human diseases resulting from their disregulation. Desmosomes and desmosomal cadherins have been extensively examined in the epidermis and epidermal appendages, and aberrations of desmosomal cadherins are known to be associated with diseases of the skin, hair, and heart. However, little is known regarding the expression of desmosomal cadherins in other epithelial tissues. In the prostate, the presence of desmosomes has been described, though the expression profile of desmosomal cadherins had not been characterized prior to this study (Fisher and Jeffrey, 1965).

In chapter II, I examined the expression of desmosomal cadherins in normal human prostate and found that, though most desmosomal cadherins are expressed in the prostate at the RNA level, only DSG2, DSC2, and DSG4 expression can be detected in the prostate at the protein level. Further, the expression of DSG2 and DSG4 was found to be largely restricted to the luminal cells of the prostate. Interestingly, the expression of DSG2 was present in metastatic prostate cancer cell lines *in vitro,* while the expression of *DSG4* was absent in all cancer cell lines examined. Importantly, the retained expression of

DSG2 in most cancer cell lines examined may illustrate a requirement for desmosomal adhesion in metastatic prostate cancer cells.

In cancer, the role of E-cadherin as a tumor suppressor has been well established. The downregulation or loss of E-cadherin expression is a common occurrence in many types of cancer, and the role of E-cadherin as a suppressor of invasive behavior has been demonstrated both *in vitro* and *in vivo* (Berx and van Roy, 2009; Vleminckx et al., 1991; Perl et al., 1998). Conversely, the role of desmosomal cadherins in cancer is less well understood; the loss of expression, *de novo* expression, and overexpression of desmosomal cadherins has been reported in various types of cancer (Biedermann et al., 2005; Yashiro et al., 2006; Ramani et al., 2008; Oshiro et al., 2005; Khan et al., 2006; Kurzen et al., 2003; Chen et al., 2007). In prostate cancer, the reduced expression of E-cadherin has been reported, though the association of E-cadherin expression and biochemical recurrence had not been examined prior to this study (Rubin et al., 2001; Umbas et al., 1992). Additionally, the expression of desmosomal cadherins in prostate cancer had not been examined prior to this study.

In chapter V, I examined the expression of E-cadherin and DSG2 in primary tumors from a large cohort of patients with prostate cancer who underwent radical prostatectomy. Interestingly, much like the expression of E-cadherin, the expression of DSG2 was found to be significantly reduced in primary prostate cancer as compared to normal prostate tissue. Additionally, there was a strong and significant positive correlation between the expression of E-cadherin and the expression of DSG2, suggesting that as the expression of E-

cadherin decreases in primary prostate cancer, so too does the expression of DSG2. The expression of both cadherins was generally detected in well differentiated areas of the tumors, but was often reduced or lost in poorly differentiated areas of the tumors. Further, a negative correlation was found between the expression of E-cadherin and DSG2 and clinicopathological features of prostate cancer. These results suggest that cadherin expression is reduced in the poorly differentiated cells of primary prostate tumors.

Importantly, the reduced expression of both E-cadherin and DSG2 was found to be significantly associated with biochemical recurrence in prostate cancer. These results support the pre-established role of E-cadherin as a tumor suppressor in prostate cancer and also demonstrate for the first time a role for DSG2 as a tumor suppressor in prostate cancer. The significant association of reduced E-cadherin and DSG2 expression with biochemical recurrence suggests that these cadherins may serve as useful markers of aggressive prostate cancer. Taken together with the pattern of cadherin expression in prostate tumors, as well as the negative correlation of cadherin expression and clinicopathological features of prostate cancer, these results further suggest that tumor cells with reduced cadherin expression are more likely to be aggressive and would therefore possess a greater potential for metastatic behavior than tumor cells that have retained a high level of cadherin expression. These results highlight a potentially critical role for cadherin based cell-cell adhesion in the progression of primary prostate cancer to a metastatic state (Figure 1).

While the assembly of adherens junctions has been extensively studied, less is known regarding the assembly of desmosomes. Previous studies have demonstrated that the formation of adherens junctions precedes that of desmosomes both in early development as well as in the *de novo* assembly of cell-cell anchoring junctions; additionally, the formation of desmosomes is commonly believed to be dependent upon the prior formation of adherens junctions (Ohsugi et al., 1996; Jackson et al., 1980; Fleming et al., 1991; Vasioukhin et al., 2000). The strong and significant correlation between the reduced expression of E-cadherin and DSG2 in primary prostate cancer observed in this study coupled with the findings of previous studies examining adherens junction and desmosome assembly in development and *de novo* cell-cell anchoring junction formation, suggests that the reduced expression of DSG2 observed in primary prostate cancer may result from the prior loss of E-cadherin expression and therefore the loss of E-cadherin based adherens junctions.

In chapter III, I examined the hypothesis that the loss of E-cadherin based adherens junctions in prostate cancer results in the loss of desmosomal adhesion. Surprisingly, the loss of *E-cadherin* expression in prostate cancer cells *in vitro* did not alter the expression of DSG2, therefore suggesting that the loss of E-cadherin based adherens junctions in prostate cancer does not result in the reciprocal loss of desmosomes. This result also suggests that, while adherens junction assembly precedes that of desmosomes in early development as well as *de novo* anchoring junction formation, the formation of desmosomes does not strictly require the presence of adherens junctions.

Further, *in vivo* analysis of prostate tumor xenografts lacking the expression of E-cadherin revealed that the loss of E-cadherin based adherens junctions results in a dramatic reduction in the size of tumors formed, despite the retention of desmosomal adhesion. *In vivo* analysis of extravasation and metastatic tumor colony formation revealed that prostate cancer cells lacking the capacity to form E-cadherin based adherens junctions are able to form metastatic tumor colonies, therefore suggesting that extravasation is not impaired by the loss of E-cadherin. However, this analysis further showed that significantly fewer animals injected with cells lacking E-cadherin expression are able to form metastatic tumor colonies, and that the size of the metastatic tumor colonies that were able to form was significantly smaller than those formed by cells which retained E-cadherin expression. These results suggest that the loss of E-cadherin inhibits metastasis at the level of metastatic tumor colony formation.

While the results of the functional analyses performed in chapter III suggest that the formation of desmosomes is not dependent upon prior formation of adherens junctions, the positive correlation between the expression of E-cadherin and DSG2 discovered in chapter V raises the question: are adherens junctions affected by the loss of desmosomal adhesion in prostate cancer? The foremost future direction of this portion of the study is therefore to examine E-cadherin based adherens junctions in a prostate cancer environment lacking desmosomal adhesion. To accomplish this goal I will knockdown the expression of *DSG2* via the same approach utilized for the knockdown of *E-cadherin*, and then perform the *in vitro* and *in vivo* assays discussed in chapter III. The results

of this study will provide insight into whether the formation of adherens junctions is dependent upon the formation of desmosomes in prostate cancer. These results will also allow for a better understanding as to whether the role of DSG2 in prostate cancer is strictly that of a tumor suppressor, or whether DSG2 is associated with the same tumor promoting capabilities as E-cadherin. If tumorigenesis and metastatic tumor formation are unimpaired or enhanced in prostate cancer cells lacking DSG2 expression, these results would support the role of DSG2 in prostate cancer as strictly that of a tumor suppressor. If tumorigenesis and metastatic tumor formation are impaired in prostate cancer cells lacking DSG2 expression, then this would suggest that both E-cadherin and DSG2 have a dual role in the progression of prostate cancer in addition to their roles as tumor suppressors.

In summary, these findings shed a new light on the role of cell-cell anchoring junctions in prostate tumorigenesis and metastatic prostate tumor colony formation. The results of the analysis performed on human prostate cancer tissue samples in chapter V support the pre-established role of E-cadherin as a tumor suppressor in prostate cancer and introduce for the first time the role of DSG2 as a tumor suppressor in prostate cancer. While the role of DSG2 as a tumor suppressor is further supported by the results of the functional analyses presented in chapter III, these results also suggest a novel role for E-cadherin based adherens junctions in the promotion of primary and metastatic tumor formation. Taken together, these results show that E-cadherin and DSG2 are expressed in primary prostate tumors and suggest that expression of E-

cadherin may in fact be required for the initial formation of primary prostate tumors. The expression of E-cadherin and DSG2 is then reduced in tumor cells, quite possibly in tumor cells with the greatest potential for metastatic behavior, thereby allowing for the progression from a tumor mass confined to the prostate capsule to a metastatic cancer. Following extravasation, the expression of E-cadherin and DSG2 may then again increase to accommodate the formation of metastatic tumor colonies (Figure 1).

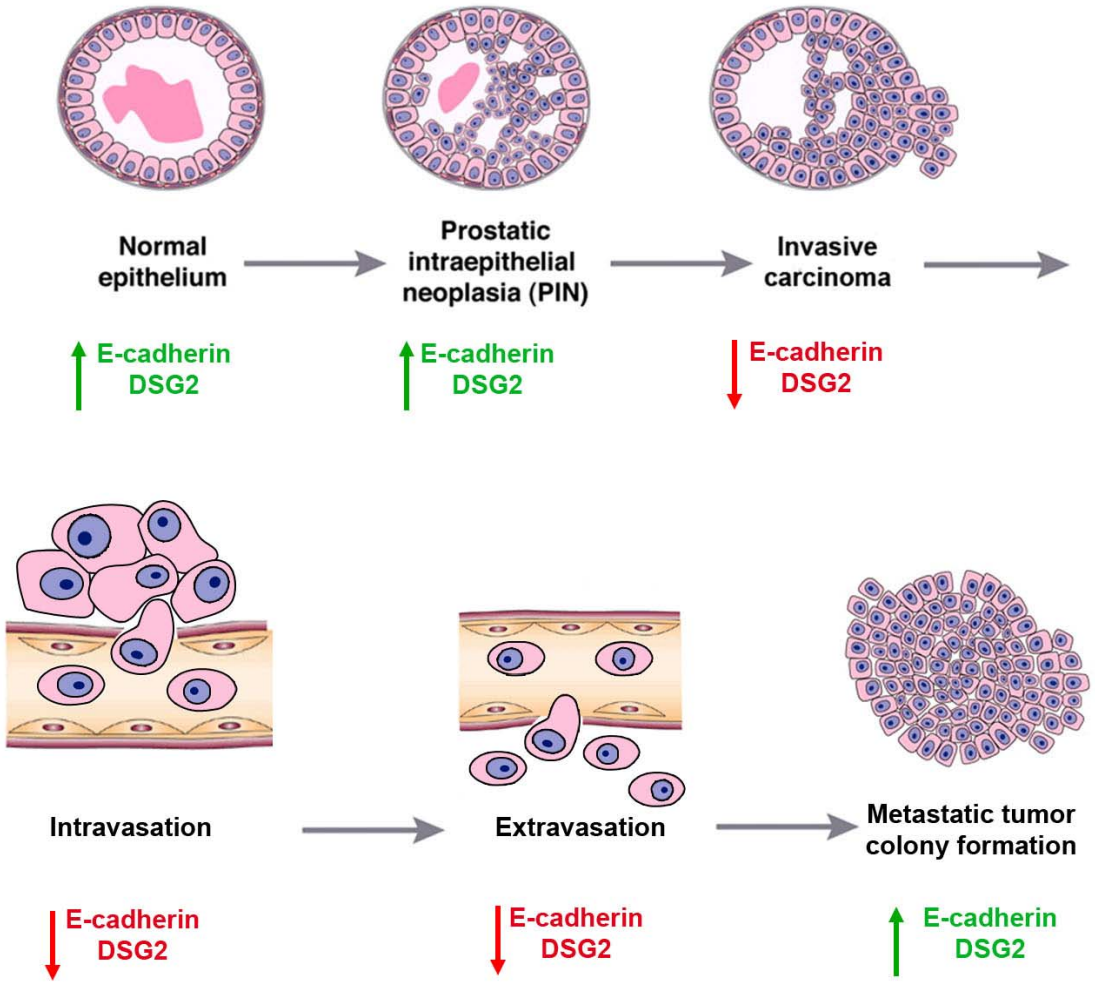

Figure 1: A model of the expression of E-cadherin and DSG2 in the progression of prostate cancer. (Adapted from Shen and Abate-Shen, 2010; Thiery et al., 2002)

The Regulation of Cell-Cell Adhesion in Aggressive Prostate Cancer

The dual role of E-cadherin in the suppression of invasive tumor cell behavior and promotion of primary and metastatic tumor formation suggests that the repression of E-cadherin expression in primary prostate tumors observed in chapter V may need to be a transient event. One such mechanism by which *E-cadherin* may be transiently repressed in cancer is via EMT, as hallmarks of EMT

include reversibility and the downregulation of *E-cadherin*. Towards this point, the expression of the EMT-associated transcription factor Snail has been associated with the downregulation of E-cadherin in breast and colorectal cancer while the transcriptional repression of *E-cadherin* via Snail has been demonstrated in a variety of cancer cell lines *in vitro* (Blanco et al., 2002; Cheng et al., 2001; Pena et al., 2005; Cano et al., 2000; Batlle et al., 2000). The potential requirement for transient repression of E-cadherin expression in the progression of prostate cancer coupled with the demonstrated significance of PI3K/AKT signaling in the progression of prostate cancer and the association of this signaling with EMT-like events in several other types of cancer, led me to hypothesize that PI3K/AKT signaling may lead to the EMT-like transcriptional repression of *E-cadherin* via Snail in prostate cancer (Di Cristofano, 1998; Di Cristofano 2001; Kim et al., 2002; Abate-Shen et al., 2003; Majumder et al., 2003; Irie et al., 2005; Ju et al., 2007; Grille et al., 2003; Grille et al., 2003; Zhou et al., 2004) .

In chapter IV the stable overexpression of activated AKT in a metastatic prostate cancer cell line *in vitro* was associated with a significant reduction in *E-cadherin* expression as well as a dramatic increase in the nuclear accumulation of Snail, an indication of increased Snail activity. Additionally, *in vivo* analysis of prostate tumor xenografts demonstrated that tumors formed by activated AKT expressing cells were significantly smaller than those formed by control cells, though these tumors were unexpectedly positive for the expression of E-cadherin. Further analysis revealed that there appears to be an inverse correlation between the expression of E-cadherin and that of activated AKT, such

that areas of the tumor with high levels of AKT expression generally showed low or no expression of E-cadherin. This inverse correlation could also be observed for the expression of Snail versus the expression of E-cadherin. Finally, *in vivo* analysis of extravasation and metastatic tumor colony formation showed that significantly fewer animals injected with activated AKT expressing cells formed metastatic tumor colonies as compared to the control animals, and those animals that did form tumors formed significantly fewer tumors than the control animals. In light of the observed small size of E-cadherin positive prostate tumor xenografts formed by activated AKT expressing cells, this result may suggest that that the formation of primary and metastatic tumors by activated AKT expressing cells occurs via the selection and expansion of a rare, E-cadherin positive cell population. Taken together, the results of the *in vitro* analysis and the inverse pattern of expression observed for E-cadherin and activated AKT as well as E-cadherin and Snail in prostate tumor xenografts support the hypothesis that PI3K/AKT signaling may lead to the EMT-like transcriptional repression of *E-cadherin* via Snail in prostate cancer. Additionally, the small size of both the prostate tumor xenografts and metastatic tumor colonies formed by activated AKT expressing cells further supports the concept that E-cadherin plays a positive role in the formation of primary and metastatic tumors.

In chapter V, the expression of pAKT was associated with biochemical recurrence in prostate cancer and this association was nearly significant. This result is consistent with the importance of PI3K/AKT signaling in aggressive prostate cancer indicated in previous studies (Kreisberg et al., 2004; Li et al.,

2009; Bedolla et al., 2007; Ayala et al., 2004). Though a very weak negative correlation was found between E-cadherin and Snail expression, a weak but significant positive correlation was observed for the expression of pAKT and E-cadherin. This finding is inconsistent with the hypothesis that PI3K/AKT mediated signaling may lead to the transcriptional repression of *E-cadherin*. However, taken together with the functional analyses performed in chapter IV, this result may suggest that while PI3K/AKT signaling can lead to the transcriptional repression of *E-cadherin* in prostate cancer, this repression may also be mediated either entirely or in part by other mechanisms.

Given the many potential roles of PI3K/AKT signaling in prostate cancer progression, coupled with the fact that the analysis of activated AKT expression performed in chapter IV was conducted in a prostate cancer cell line which, by its nature, contains many disregulated signaling pathways, it is possible that the observed transcriptional repression of E-cadherin by activated AKT is context-dependent insofar as it relies upon the joint activation of other pathways not identified in this study. One possibility is that the transcriptional repression of E-cadherin by activated AKT signaling in prostate cancer requires the joint activation of the Ras/MAPK signaling pathway. Activated RTKs can be bound by the SH2 domain adaptor protein GRB2, which in turn can bind to SOS. SOS acts as a guanine nucleotide exchange factor and therefore is an activator of Ras (Bar-Sagi, 1994). In this way, activated RTK signaling is coupled to the activation of the Ras/MAPK signaling pathway as well as the PI3K/AKT signaling pathway. Further, there is a direct link between the Ras/MAPK pathway and the PI3K/AKT

pathway as, in addition to activating the Ras/MAPK signaling pathway, activated Ras can also bind to PI3K and recruit it to the membrane thereby allowing for the activation of PI3K/AKT signaling (Rodriguez-Viciana et al., 1994). Importantly, there is evidence to suggest that the joint activation of the Ras/MAPK and PI3K/AKT signaling pathways is involved in EMT. The EMT-like loss of adherens junctions and cell scattering was observed in NBT-II rat bladder carcinoma cells treated with HGF/SF, and this loss of adherens junctions could be blocked by inhibitors of PI3K or dominant negative mutants of MAPK suggesting that the activation of both PI3K and MAPK are required for the loss of adherens junctions (Potempa et al., 1998).

The observed weak negative correlation between the expression of E-cadherin and Snail in primary prostate tumors could imply that EMT associated transcription factors other than Snail may be involved in the downregulation of E-cadherin expression. For example, the EMT associated transcription factors Slug and Twist have been associated with reduced expression of E-cadherin in cancer and have been shown to directly inhibit the expression of *E-cadherin in vitro* (Uchikado et al., 2005; Hajra et al., 2002; Bolos et al., 2002; Yang et al., 2004). While PI3K/AKT signaling has been associated with the activation of Snail, Slug and Twist, the activation of these transcription factors by other signaling pathways has also been demonstrated (Saegusa et al., 2009; Vichalkovski et al., 2010). This raises the possibility that the reduced expression of E-cadherin in primary prostate tumors observed in chapter V may be due the EMT-like

transient inhibition of E-cadherin expression by pathways other than the PI3K/AKT.

An example of such a pathway is the TGFβ signaling pathway which has been well characterized as an inducer of EMT. Activation of the TGFβ pathway has been shown to induce the expression of Snail, Slug, and Twist via the SMAD-mediated expression of HMGA2 (Zavadil et al., 2005; Thuault et al., 2006). Additionally, the Notch signaling pathway has also been implicated in the EMT-like repression of E-cadherin expression. *In vitro* analysis of the SKOV-3 ovarian cancer cell line demonstrated that the Notch signaling pathway is able to induce EMT via the direct upregulation of *Snail* by the Notch intracellular domain (NICD) resulting in reduced E-cadherin expression (Sahlgren et al., 2008). Moreover, the Hedgehog (Hh) signaling pathway has been implicated in the induction of EMT as upregulation of *Snail* expression in the presence the Hh pathway effector Gli has been demonstrated *in vitro* (Li et al., 2006). Finally, the Wnt signaling pathway is known to be involved in the positive regulation of EMT-associated transcription factors in two ways. First, β-catenin/TCF signaling leads to the direct upregulation of both *Twist* and *Snail* (Howe et al., 2003; Vallin et al., 2001; Conacci-Sorrell et al., 2003). Second, like the PI3K/AKT pathway, activated Wnt signaling inhibits GSK3B, an inhibitor of Snail, thereby allowing for Snail activation (Zhou et al., 2004). Much like the PI3K/AKT and Ras/MAPK pathways, crosstalk between the aforementioned signaling pathways has been implicated in EMT in cancer. For example, crosstalk between the TGFβ signaling pathway and the PI3K/AKT pathway, the Ras/MAPK pathway, the Notch

pathway, and the Wnt pathway has been observed (Bakin et al., 2000; Janda et al., 2002; Zavadil et al., 2004; Eger et al., 2004). Additionally, crosstalk between the Notch and Hh signaling pathways has also been demonstrated (Kasper et al., 2006). The variety of EMT-associated signaling pathways, as well as the many ways in which these pathways have been shown to communicate, illustrate the complexity of the regulation of EMT in cancer and suggest that it may be necessary to broaden the focus of EMT-mediated E-cadherin repression to include several signaling pathways and/or EMT associated transcription factors in addition to the PI3K/AKT signaling pathway and Snail.

It should also be noted that the downregulation of E-cadherin expression in primary prostate cancer may be due to processes unrelated to the transcriptional repression of *E-cadherin*. For example, the homeostasis of adherens junctions involves the recycling of E-cadherin via endocytosis which enables the movement of E-cadherin to new sites of cell-cell contact (Bryant and Stow, 2004). The activation of tyrosine kinases has been found to result in the phosphorylation of E-cadherin followed by the ubiquitination and degradation of E-cadherin mediated by the E3 ubiquitin ligase Hakai (Behrens et al., 1993; Fujita et al., 2002). Additionally, *in vitro* analysis of IGF2 signaling has been shown induce EMT in NBT-II cells whereby the loss of E-cadherin expression is due to the internalization of E-cadherin complexed with β-catenin and IGF1R followed by the lysosome mediated degradation of E-cadherin (Morali et al., 2001). Thus, the downregulation of E-cadherin in primary prostate cancer may be

due to the post-translational modification and subsequent degradation of E-cadherin.

Interestingly, the *in vitro* analysis of DSG2 in chapter IV.2 in addition to the very weak and insignificant positive correlation between DSG2 and pAKT expression observed in chapter V suggests that the reduced expression of DSG2 in primary prostate cancer is not associated with regulation by the PI3K/AKT signaling pathway. Given that the results of the analyses performed in chapter III demonstrate that the loss of E-cadherin based adherens junctions also has no effect on the expression of DSG2, these results further suggest that the reduced expression of E-cadherin and DSG2 observed in prostate cancer may be regulated separately. This then raises the question: what regulates the loss of DSG2 expression in prostate cancer? Given that the expression of DSG2 was reduced in primary prostate cancer yet found to be expressed at the cell border in most metastatic prostate cancer cell lines, it is likely that, much like E-cadherin, the downregulation of DSG2 in prostate cancer may need to be a transient event. Though Snail was found to have no effect on the expression of DSG2 in this study, it is still possible that the downregulation of DSG2 is mediated by EMT associated transcription factors. The most obvious candidate is Slug, as the overexpression of Slug in NBT-II cells has been shown to result in the disappearance of DP and DSG2 from sites of cell-cell contact (Savagner et al., 1997). Future studies will therefore focus on examining the correlation between Slug and DSG2 expression in primary prostate cancer.

Conclusion

Though both adherens junctions and desmosomes are required for the development and maintenance of normal tissues, and the loss of cell-cell adhesion is commonly observed in the progression of cancer, traditionally the study of cell-cell adhesion in cancer has focused solely on adherens junctions. This study is the first to examine the expression of desmosomal cadherins in both normal prostate tissue and prostate cancer. This is also the first study to examine the association of E-cadherin and DSG2 expression with biochemical recurrence in prostate cancer. Importantly, the results of this study illustrate that these cadherins may serve as useful markers of aggressive prostate cancer.

Further, this study provided evidence for a new role for E-cadherin in promoting the formation of primary and metastatic tumors. The dual role of E-cadherin as a both a tumor promoter and a tumor suppressor highlights a potential need for transient repression of E-cadherin expression in the progression of prostate cancer. The PI3K/AKT signaling pathway is one pathway that can mediate this transient repression of E-cadherin expression in prostate cancer as the functional analysis performed in this study demonstrated that the activation of AKT leads to a significant reduction of *E-cadherin* expression. Interestingly, neither the loss of E-cadherin based adherens junctions nor the activation of AKT affected the expression of DSG2, suggesting that the observed loss of E-cadherin and DSG2 expression in primary prostate cancer may be regulated by separate mechanisms. In conclusion, this study has provided an in depth analysis of the role of E-cadherin and DSG2 in prostate cancer, the regulation of E-cadherin

expression by the PI3K/AKT signaling pathway in prostate cancer, and has demonstrated the potential utility of E-cadherin and DSG2 as markers of aggressive prostate cancer.

References

Abate-Shen, C., Banach-Petrosky, W.A., Sun, X., Economides, K.D., Desai, N., Gregg, J.P., Borowsky, A.D., Cardiff, R.D., and Shen, M.M. (2003). Nkx3.1; Pten mutant mice develop invasive prostate adenocarcinoma and lymph node metastases. Cancer Res *63*, 3886-3890.

Abate-Shen, C., and Shen, M.M. (2000). Molecular genetics of prostate cancer. Genes Dev *14*, 2410-2434.

Abe, K., and Takeichi, M. (2008). EPLIN mediates linkage of the cadherin catenin complex to F-actin and stabilizes the circumferential actin belt. Proc Natl Acad Sci U S A *105*, 13-19.

Adams, C.L., Chen, Y.T., Smith, S.J., and Nelson, W.J. (1998). Mechanisms of epithelial cell-cell adhesion and cell compaction revealed by high-resolution tracking of E-cadherin-green fluorescent protein. J Cell Biol *142*, 1105-1119.

Adams, C.L., Nelson, W.J., and Smith, S.J. (1996). Quantitative analysis of cadherin-catenin-actin reorganization during development of cell-cell adhesion. J Cell Biol *135*, 1899-1911.

Amagai, M. (1999). Autoimmunity against desmosomal cadherins in pemphigus. J Dermatol Sci *20*, 92-102.

Awad, M.M., Dalal, D., Cho, E., Amat-Alarcon, N., James, C., Tichnell, C., Tucker, A., Russell, S.D., Bluemke, D.A., Dietz, H.C.*, et al.* (2006). DSG2 mutations contribute to arrhythmogenic right ventricular dysplasia/cardiomyopathy. Am J Hum Genet *79*, 136-142.

Ayala, G., Thompson, T., Yang, G., Frolov, A., Li, R., Scardino, P., Ohori, M., Wheeler, T., and Harper, W. (2004). High levels of phosphorylated form of Akt-1 in prostate cancer and non-neoplastic prostate tissues are strong predictors of biochemical recurrence. Clin Cancer Res *10*, 6572-6578.

Bakin, A.V., Tomlinson, A.K., Bhowmick, N.A., Moses, H.L., and Arteaga, C.L. (2000). Phosphatidylinositol 3-kinase function is required for transforming growth factor beta-mediated epithelial to mesenchymal transition and cell migration. J Biol Chem *275*, 36803-36810.

Barber, A.G., Wajid, M., Columbo, M., Lubetkin, J., and Christiano, A.M. (2007). Striate palmoplantar keratoderma resulting from a frameshift mutation in the desmoglein 1 gene. J Dermatol Sci *45*, 161-166.

Bar-Sagi, D. (1994). The Sos (Son of sevenless) protein. Trends Endocrinol Metab *5*, 165-169.

Batlle, E., Sancho, E., Franci, C., Dominguez, D., Monfar, M., Baulida, J., and Garcia De Herreros, A. (2000). The transcription factor snail is a repressor of E-cadherin gene expression in epithelial tumour cells. Nat Cell Biol *2*, 84-89.

Bazzi, H., Getz, A., Mahoney, M.G., Ishida-Yamamoto, A., Langbein, L., Wahl, J.K., 3rd, and Christiano, A.M. (2006). Desmoglein 4 is expressed in highly differentiated keratinocytes and trichocytes in human epidermis and hair follicle. Differentiation *74*, 129-140.

Becker, K.F., Atkinson, M.J., Reich, U., Becker, I., Nekarda, H., Siewert, J.R., and Hofler, H. (1994). E-cadherin gene mutations provide clues to diffuse type gastric carcinomas. Cancer Res *54*, 3845-3852.

Bedolla, R., Prihoda, T.J., Kreisberg, J.I., Malik, S.N., Krishnegowda, N.K., Troyer, D.A., and Ghosh, P.M. (2007). Determining risk of biochemical recurrence in prostate cancer by immunohistochemical detection of PTEN expression and Akt activation. Clin Cancer Res *13*, 3860-3867.

Behrens, J., Vakaet, L., Friis, R., Winterhager, E., Van Roy, F., Mareel, M.M., and Birchmeier, W. (1993). Loss of epithelial differentiation and gain of invasiveness correlates with tyrosine phosphorylation of the E-cadherin/beta-catenin complex in cells transformed with a temperature-sensitive v-SRC gene. J Cell Biol *120*, 757-766.

Bellairs, R. (1986). The primitive streak. Anat Embryol (Berl) *174*, 1-14.

Berx, G., Staes, K., van Hengel, J., Molemans, F., Bussemakers, M.J.G., van Bokhoven, A., and van Roy, F. (1995). Cloning and characterization of the human invasion suppressor gene E-cadherin (CDH1). Genomics *26*, 281-289.

Berx, G., and van Roy, F. (2009). Involvement of members of the cadherin superfamily in cancer. Cold Spring Harb Perspect Biol *1*, a003129.

Biedermann, K., Vogelsang, H., Becker, I., Plaschke, S., Siewert, J.R., Hofler, H., and Keller, G. (2005). Desmoglein 2 is expressed abnormally rather than mutated in familial and sporadic gastric cancer. J Pathol *207*, 199-206.

Blanco, M.J., Moreno-Bueno, G., Sarrio, D., Locascio, A., Cano, A., Palacios, J., and Nieto, M.A. (2002). Correlation of Snail expression with histological grade and lymph node status in breast carcinomas. Oncogene *21*, 3241-3246.

Bolos, V., Peinado, H., Perez-Moreno, M.A., Fraga, M.F., Esteller, M., and Cano, A. (2003). The transcription factor Slug represses E-cadherin expression and induces epithelial to mesenchymal transitions: a comparison with Snail and E47 repressors. J Cell Sci *116*, 499-511.

Bonkhoff, H., and Remberger, K. (1996). Differentiation pathways and histogenetic aspects of normal and abnormal prostatic growth: a stem cell model. Prostate *28*, 98-106.

Boormans, J.L., Korsten, H., Ziel-van der Made, A.C., van Leenders, G.J., Verhagen, P.C., and Trapman, J. (2010). E17K substitution in AKT1 in prostate cancer. Br J Cancer *102*, 1491-1494.

Bostwick, D.G., Amin, M.B., Dundore, P., Marsh, W., and Schultz, D.S. (1993). Architectural patterns of high-grade prostatic intraepithelial neoplasia. Hum Pathol *24*, 298-310.

Brawer, M.K. (1992). Prostatic intraepithelial neoplasia: a premalignant lesion. Hum Pathol *23*, 242-248.

Bryant, D.M., and Stow, J.L. (2004). The ins and outs of E-cadherin trafficking. Trends Cell Biol *14*, 427-434.

Bukholm, I.K., Nesland, J.M., and Borresen-Dale, A.L. (2000). Re-expression of E-cadherin, alpha-catenin and beta-catenin, but not of gamma-catenin, in metastatic tissue from breast cancer patients [seecomments]. J Pathol *190*, 15-19.

Burdsal, C.A., Damsky, C.H., and Pedersen, R.A. (1993). The role of E-cadherin and integrins in mesoderm differentiation and migration at the mammalian primitive streak. Development *118*, 829-844.

Burgering, B., Coffer, P. (1995). Protein kinase B (c-Akt) in phosphatidylinositol-3-OH kinase signal transduction. Nature *376*, 599-602.

Byun, D.S., Cho, K., Ryu, B.K., Lee, M.G., Park, J.I., Chae, K.S., Kim, H.J., and Chi, S.G. (2003). Frequent monoallelic deletion of PTEN and its reciprocal associatioin with PIK3CA amplification in gastric carcinoma. Int J Cancer *104*, 318-327.

Cairns, P., Okami, K., Halachmi, S., Halachmi, N., Esteller, M., Herman, J.G., Jen, J., Isaacs, W.B., Bova, G.S., and Sidransky, D. (1997). Frequent inactivation of PTEN/MMAC1 in primary prostate cancer. Cancer Res *57*, 4997-5000.

Cancer, A.J.C.o. (2010). AJCC Cancer Staging Manual, Seventh Edition (New York, Springer).

Cano, A., Perez-Moreno, M.A., Rodrigo, I., Locascio, A., Blanco, M.J., del Barrio, M.G., Portillo, F., and Nieto, M.A. (2000). The transcription factor snail controls epithelial-mesenchymal transitions by repressing E-cadherin expression. Nat Cell Biol *2*, 76-83.

Carpten, J.D., Faber, A.L., Horn, C., Donoho, G.P., Briggs, S.L., Robbins, C.M., Hostetter, G., Boguslawski, S., Moses, T.Y., Savage, S.*, et al.* (2007). A transforming mutation in the pleckstrin homology domain of AKT1 in cancer. Nature *448*, 439-444.

Carver, E.A., Jiang, R., Lan, Y., Oram, K.F., and Gridley, T. (2001). The mouse snail gene encodes a key regulator of the epithelial-mesenchymal transition. Mol Cell Biol *21*, 8184-8188.

Ceteci, F., Ceteci, S., Karreman, C., Kramer, B.W., Asan, E., Gotz, R., Rapp, U.R. (2007) Disruption of tumor cell adhesion promotes angiogenic switch and progression to micrometastasis in RAF-driven murine lung cancer. Cancer Cell *12*, 145-149.

Chen, M.L., Xu, P.Z., Peng, X.D., Chen, W.S., Guzman, G., Yang, X., Di Cristofano, A., Pandolfi, P.P., and Hay, N. (2006). The deficiency of Akt1 is sufficient to suppress tumor development in Pten+/- mice. Genes Dev *20*, 1569-1574.

Chen, Y.J., Chang, J.T., Lee, L., Wang, H.M., Liao, C.T., Chiu, C.C., Chen, P.J., and Cheng, A.J. (2007). DSG3 is overexpressed in head neck cancer and is a potential molecular target for inhibition of oncogenesis. Oncogene *26*, 467-476.

Chen, J., Imanaka, N., and Griffin, J.D. (2010). Hypoxia potentiates Notch signaling in breast cancer leading to decreased E-cadherin expression and increased cell migration and invasion. Br J Cancer *102*, 351-360.

Cheng, C.W., Wu, P.E., Yu, J.C., Huang, C.S., Yue, C.T., Wu, C.W., and Shen, C.Y. (2001). Mechanisms of inactivation of E-cadherin in breast carcinoma: modification of the two-hit hypothesis of tumor suppressor gene. Oncogene *20*, 3814-3823.

Chitaev, N.A., Leube, R.E., Troyanovsky, R.B., Eshkind, L.G., Franke, W.W., and Troyanovsky, S.M. (1996). The binding of plakoglobin to desmosomal cadherins: patterns of binding sites and topogenic potential. J Cell Biol *133*, 359-369.

Chitaev, N.A., and Troyanovsky, S.M. (1997). Direct Ca2+-dependent heterophilic interaction between desmosomal cadherins, desmoglein and desmocollin, contributes to cell-cell adhesion. J Cell Biol *138*, 193-201.

Ciruna, B., and Rossant, J. (2001). FGF signaling regulates mesoderm cell fate specification and morphogenetic movement at the primitive streak. Dev Cell *1*, 37-49.

Conacci-Sorrell, M., Simcha, I., Ben-Yedidia, T., Blechman, J., Savagner, P., and Ben-Ze'ev, A. (2003). Autoregulation of E-cadherin expression by cadherin-cadherin interactions: the roles of beta-catenin signaling, Slug, and MAPK. J Cell Biol *163*, 847-857.

Cully, M., You, H., Levine, A.J., and Mak, T.W. (2006). Beyond PTEN mutations: the PI3K pathway as an integrator of multiple inputs during tumorigenesis. Nat Rev Cancer *6*, 184-192.

Damjanov, I., Damjanov, A., and Damsky, C.H. (1986). Developmentally regulated expression of the cell-cell adhesion glycoprotein cell-CAM 120/80 in peri-implantation mouse embryos and extraembryonic membranes. Developmental Biology *116*, 194-202.

De Vries, W.N., Evsikov, A.V., Haac, B.E., Fancher, K.S., Holbrook, A.E., Kemler, R., Solter, D., and Knowles, B.B. (2004). Maternal beta-catenin and E-cadherin in mouse development. Development *131*, 4435-4445.

Delva, E., Tucker, D.K., and Kowalczyk, A.P. (2009). The desmosome. Cold Spring Harb Perspect Biol *1*, a002543.

Demlehner, M.P., Schafer, S., Grund, C., and Franke, W.W. (1995). Continual assembly of half-desmosomal structures in the absence of cell contacts and their frustrated endocytosis: a coordinated Sisyphus cycle. J Cell Biol *131*, 745-760.

Den, Z., Cheng, X., Merched-Sauvage, M., and Koch, P.J. (2006). Desmocollin 3 is required for pre-implantation development of the mouse embryo. J Cell Sci *119*, 482-489.

Deng, C.X., Wynshaw-Boris, A., Shen, M.M., Daugherty, C., Ornitz, D.M., and Leder, P. (1994). Murine FGFR-1 is required for early postimplantation growth and axial organization. Genes Dev *8*, 3045-3057.

Derksen D.W.B., Liu X., Saridin F., van der Gulden H., Zevenhoven, J., Evers, B., van Beijnum, J.R., Griffioen, A.W., Vink, J., Krimpenfort, P., Peterse, J.L., Cardiff, R.D., Berns, A., Jonkers, J. Somatic inactivation of E-cadherin and p53 in mice leads to metastatic lobular mammary carcinoma through induction of anoikis resistance and angiogenesis. (2006). Cancer Cell *10*, 437-449.

Di Cristofano, A., De Acetis, M., Koff, A., Cordon-Cardo, C., and Pandolfi, P.P. (2001). Pten and p27KIP1 cooperate in prostate cancer tumor suppression in the mouse. Nat Genet *27*, 222-224.

Di Cristofano, A., Pesce, B., Cordon-Cardo, C., and Pandolfi, P.P. (1998). Pten is essential for embryonic development and tumour suppression. Nat Genet *19*, 348-355.

Dobrosotskaya, I.Y., and James, G.L. (2000). MAGI-1 interacts with beta-catenin and is associated with cell-cell adhesion structures. Biochem Biophys Res Commun *270*, 903-909.

Duden, R., and Franke, W.W. (1988). Organization of desmosomal plaque proteins in cells growing at low calcium concentrations. J Cell Biol *107*, 1049-1063.

Eble JH, S.G., Epstein, JI, Sesterhenn IA. (2004). World Health Organization Classification of Tumors. Pathology and Genetics of Tumors of the Urinary System and Male Genital Organs. (Lyon, IARC Press).

Eger, A., Stockinger, A., Park, J., Langkopf, E., Mikula, M., Gotzmann, J., Mikulits, W., Beug, H., and Foisner, R. (2004). beta-Catenin and TGFbeta signalling cooperate to maintain a mesenchymal phenotype after FosER-induced epithelial to mesenchymal transition. Oncogene *23*, 2672-2680.

Elo, J.P., Harkonen, P., Kyllonen, A.P., Lukkarinen, O., Poutanen, M., Vihko, R., and Vihko, P. (1997). Loss of heterozygosity at 16q24.1-q24.2 is significantly associated with metastatic and aggressive behavior of prostate cancer. Cancer Res *57*, 3356-3359.

Engelman, J.A., Luo, J., and Cantley, L.C. (2006). The evolution of phosphatidylinositol 3-kinases as regulators of growth and metabolism. Nat Rev Genet *7*, 606-619.

Eshkind, L., Tian, Q., Schmidt, A., Franke, W.W., Windoffer, R., and Leube, R.E. (2002). Loss of desmoglein 2 suggests essential functions for early embryonic development and proliferation of embryonal stem cells. Eur J Cell Biol *81*, 592-598.

Feilotter, H.E., Coulon, V., McVeigh, J.L., Boag, A.H., Dorion-Bonnet, F., Duboue, B., Latham, W.C., Eng, C., Mulligan, L.M., and Longy, M. (1999). Analysis of the 10q23 chromosomal region and the PTEN gene in human sporadic breast carcinoma. Br J Cancer *79*, 718-723.

Fisher, E.R., and Jeffrey, W. (1965). Ultrastructure of Human Normal and Neoplastic Prostate; with Comments Relative to Prostatic Effects of Hormonal Stimulation in the Rabbit. Am J Clin Pathol *44*, 119-134.

Fleming, I.N., Gray, A., and Downes, C.P. (2000). Regulation of the Rac1-specific exchange factor Tiam1 involves both phosphoinositide 3-kinase-dependent and -independent components. Biochem J *351*, 173-182.

Fleming, T.P. (1987). A quantitative analysis of cell allocation to trophectoderm and inner cell mass in the mouse blastocyst. Dev Biol *119*, 520-531.

Fleming, T.P., Garrod, D.R., and Elsmore, A.J. (1991). Desmosome biogenesis in the mouse preimplantation embryo. Development *112*, 527-539.

Fuchs, E., Merrill, B.J., Jamora, C., and DasGupta, R. (2001). At the roots of a never-ending cycle. Dev Cell *1*, 13-25.

Fuchs, E., and Raghavan, S. (2002). Getting under the skin of epidermal morphogenesis. Nat Rev Genet *3*, 199-209.

Fujita, Y., Krause, G., Scheffner, M., Zechner, D., Leddy, H.E., Behrens, J., Sommer, T., and Birchmeier, W. (2002). Hakai, a c-Cbl-like protein, ubiquitinates and induces endocytosis of the E-cadherin complex. Nat Cell Biol *4*, 222-231.

Fukata, M., Kuroda, S., Nakagawa, M., Kawajiri, A., Itoh, N., Shoji, I., Matsuura, Y., Yonehara, S., Fujisawa, H., Kikuchi, A.*, et al.* (1999). Cdc42 and Rac1 regulate the interaction of IQGAP1 with beta-catenin. J Biol Chem *274*, 26044-26050.

Gallicano, G.I., Kouklis, P., Bauer, C., Yin, M., Vasioukhin, V., Degenstein, L., and Fuchs, E. (1998). Desmoplakin is required early in development for assembly of desmosomes and cytoskeletal linkage. J Cell Biol *143*, 2009-2022.

Gan, Y., Shi, C., Inge, L., Hibner, M., Balducci, J., and Huang, Y. (2010). Differential roles of ERK and Akt pathways in regulation of EGFR-mediated signaling and motility in prostate cancer cells. Oncogene *29*, 4947-4958.

Getsios, S., Huen, A.C., and Green, K.J. (2004). Working out the strength and flexibility of desmosomes. Nat Rev Mol Cell Biol *5*, 271-281.

Godsel, L.M., Hsieh, S.N., Amargo, E.V., Bass, A.E., Pascoe-McGillicuddy, L.T., Huen, A.C., Thorne, M.E., Gaudry, C.A., Park, J.K., Myung, K.*, et al.* (2005). Desmoplakin assembly dynamics in four dimensions: multiple phases differentially regulated by intermediate filaments and actin. J Cell Biol *171*, 1045-1059.

Gray, I.C., Phillips, S.M., Lee, S.J., Neoptolemos, J.P., Weissenbach, J., and Spurr, N.K. (1995). Loss of the chromosomal region 10q23-25 in prostate cancer. Cancer Res *55*, 4800-4803.

Grille, S.J., Bellacosa, A., Upson, J., Klein-Szanto, A.J., van Roy, F., Lee-Kwon, W., Donowitz, M., Tsichlis, P.N., and Larue, L. (2003). The protein kinase Akt induces epithelial mesenchymal transition and promotes enhanced motility and invasiveness of squamous cell carcinoma lines. Cancer Res *63*, 2172-2178.

Grunwald, V., DeGraffenried, L., Russel, D., Friedrichs, W.E., Ray, R.B., and Hidalgo, M. (2002). Inhibitors of mTOR reverse doxorubicin resistance conferred by PTEN status in prostate cancer cells. Cancer Res *62*, 6141-6145.

Guilford, P., Hopkins, J., Harraway, J., McLeod, M., McLeod, N., Harawira, P., Taite, H., Scoular, R., Miller, A., and Reeve, A.E. (1998). E-cadherin germline mutations in familial gastric cancer. Nature *392*, 402-405.

Hajra, K.M., Chen, D.Y., and Fearon, E.R. (2002). The SLUG zinc-finger protein represses E-cadherin in breast cancer. Cancer Res *62*, 1613-1618.

Hashimoto, K., Fujimoto, H., and Nakatsuji, N. (1987). An ECM substratum allows mouse mesodermal cells isolated from the primitive streak to exhibit motility similar to that inside the embryo and reveals a deficiency in the T/T mutant cells. Development *100*, 587-598.

Hashimoto, K., Nakatsuji, N. (1989). Formation of the primitive streak and mesoderm cells in mouse embryos—Detailed scanning electron microscopal study. Dev. Growth Differ. *31*, 209-218.

Hatta, K., Takagi, S., Fujisawa, H., and Takeichi, M. (1987). Spatial and temporal expression pattern of N-cadherin cell adhesion molecules correlated with morphogenetic processes of chicken embryos. Dev Biol *120*, 215-227.

Hayward, S.W., Dahiya, R., Cunha, G.R., Bartek, J., Deshpande, N., and Narayan, P. (1995). Establishment and characterization of an immortalized but non-transformed human prostate epithelial cell line: BPH-1. In Vitro Cell Dev Biol Anim *31*, 14-24.

Hedlund, T.E., Duke, R.C., and Miller, G.J. (1999). Three-dimensional spheroid cultures of human prostate cancer cell lines. Prostate *41*, 154-165.

Heeboll, S., Borre, M., Ottosen, P.D., Dyrskjot, L., Orntoft, T.F., and Torring, N. (2009). Snail1 is over-expressed in prostate cancer. APMIS *117*, 196-204.

Heuser, A., Plovie, E.R., Ellinor, P.T., Grossmann, K.S., Shin, J.T., Wichter, T., Basson, C.T., Lerman, B.B., Sasse-Klaassen, S., Thierfelder, L.*, et al.* (2006). Mutant desmocollin-2 causes arrhythmogenic right ventricular cardiomyopathy. Am J Hum Genet *79*, 1081-1088.

Hordijk, P.L., ten Klooster, J.P., van der Kammen, R.A., Michiels, F., Oomen, L.C., and Collard, J.G. (1997). Inhibition of invasion of epithelial cells by Tiam1-Rac signaling. Science *278*, 1464-1466.

Horoszewicz, J.S., Leong, S.S., Chu, T.M., Wajsman, Z.L., Friedman, M., Papsidero, L., Kim, U., Chai, L.S., Kakati, S., Arya, S.K.*, et al.* (1980). The LNCaP cell line--a new model for studies on human prostatic carcinoma. Prog Clin Biol Res *37*, 115-132.

Howe, L.R., Watanabe, O., Leonard, J., and Brown, A.M. (2003). Twist is up-regulated in response to Wnt1 and inhibits mouse mammary cell differentiation. Cancer Res *63*, 1906-1913.

Irie, H.Y., Pearline, R.V., Grueneberg, D., Hsia, M., Ravichandran, P., Kothari, N., Natesan, S., and Brugge, J.S. (2005). Distinct roles of Akt1 and Akt2 in regulating cell migration and epithelial-mesenchymal transition. J Cell Biol *171*, 1023-1034.

Ishida-Yamamoto, A., Takahashi, H., and Iizuka, H. (2002). Lessons from disorders of epidermal differentiation-associated keratins. Histol Histopathol *17*, 331-338.

Jackson, B.W., Grund, C., Schmid, E., Burki, K., Franke, W.W., and Illmensee, K. (1980). Formation of cytoskeletal elements during mouse embryogenesis. Intermediate filaments of the cytokeratin type and desmosomes in preimplantation embryos. Differentiation *17*, 161-179.

Janda, E., Lehmann, K., Killisch, I., Jechlinger, M., Herzig, M., Downward, J., Beug, H., and Grunert, S. (2002). Ras and TGF[beta] cooperatively regulate epithelial cell plasticity and metastasis: dissection of Ras signaling pathways. J Cell Biol *156*, 299-313.

Johnson, S.K., Ramani, V.C., Hennings, L., and Haun, R.S. (2007). Kallikrein 7 enhances pancreatic cancer cell invasion by shedding E-cadherin. Cancer *109*, 1811-1820.

Jou, T.S., and Nelson, W.J. (1998). Effects of regulated expression of mutant RhoA and Rac1 small GTPases on the development of epithelial (MDCK) cell polarity. J Cell Biol *142*, 85-100.

Ju, X., Katiyar, S., Wang, C., Liu, M., Jiao, X., Li, S., Zhou, J., Turner, J., Lisanti, M.P., Russell, R.G.*, et al.* (2007). Akt1 governs breast cancer progression in vivo. Proc Natl Acad Sci U S A *104*, 7438-7443.

Kaighn, M.E., Narayan, K.S., Ohnuki, Y., Lechner, J.F., and Jones, L.W. (1979). Establishment and characterization of a human prostatic carcinoma cell line (PC-3). Invest Urol *17*, 16-23.

Kanazawa, T., Watanabe, T., Kazama, S., Tada, T., Koketsu, S., and Nagawa, H. (2002). Poorly differentiated adenocarcinoma and mucinous carcinoma of the colon and rectum show higher rates of loss of heterozygosity and loss of E-cadherin expression due to methylation of promoter region. Int J Cancer *102*, 225-229.

Kanitakis, J. (2002). Anatomy, histology and immunohistochemistry of normal human skin. Eur J Dermatol *12*, 390-399; quiz 400-391.

Kasper, M., Schnidar, H., Neill, G.W., Hanneder, M., Klingler, S., Blaas, L., Schmid, C., Hauser-Kronberger, C., Regl, G., Philpott, M.P.*, et al.* (2006). Selective modulation of Hedgehog/GLI target gene expression by epidermal growth factor signaling in human keratinocytes. Mol Cell Biol *26*, 6283-6298.

Karkera, J.D., Ayache, S., Ransome, R.J., Jr., Jackson, M.A., Elsayem, A.F., Sridhar, R., Detera-Wadleigh, S.D., and Wadleigh, R.G. (2000). Refinement of regions with allelic loss on chromosome 18p11.2 and 18q12.2 in esophageal squamous cell carcinoma. Clin Cancer Res *6*, 3565-3569.

Khan, K., Hardy, R., Haq, A., Ogunbiyi, O., Morton, D., and Chidgey, M. (2006). Desmocollin switching in colorectal cancer. Br J Cancer *95*, 1367-1370.

Kim, M.J., Cardiff, R.D., Desai, N., Banach-Petrosky, W.A., Parsons, R., Shen, M.M., and Abate-Shen, C. (2002). Cooperativity of Nkx3.1 and Pten loss of function in a mouse model of prostate carcinogenesis. Proc Natl Acad Sci U S A *99*, 2884-2889.

Kim, S.H., Li, Z., and Sacks, D.B. (2000). E-cadherin-mediated cell-cell attachment activates Cdc42. J Biol Chem *275*, 36999-37005.

Kirkegaard, T., Witton, C.J., Edwards, J., Nielsen, K.V., Jensen, L.B., Campbell, F.M., Cooke, T.G., and Bartlett, J.M. (2010). Molecular alterations in AKT1, AKT2 and AKT3 detected in breast and prostatic cancer by FISH. Histopathology *56*, 203-211.

Kleer, C.G., van Golen, K.L., Braun, T., and Merajver, S.D. (2001). Persistent E-cadherin expression in inflammatory breast cancer. Mod Pathol *14*, 458-464.

Kljuic, A., Bazzi, H., Sundberg, J.P., Martinez-Mir, A., O'Shaughnessy, R., Mahoney, M.G., Levy, M., Montagutelli, X., Ahmad, W., Aita, V.M.*, et al.* (2003). Desmoglein 4 in hair follicle differentiation and epidermal adhesion: evidence from inherited hypotrichosis and acquired pemphigus vulgaris. Cell *113*, 249-260.

Kobielak, A., Pasolli, H.A., and Fuchs, E. (2004). Mammalian formin-1 participates in adherens junctions and polymerization of linear actin cables. Nat Cell Biol *6*, 21-30.

Kohn, A.D., Takeuchi, F., and Roth, R.A. (1996). Akt, a pleckstrin homology domain containing kinase, is activated primarily by phosphorylation. J Biol Chem *271*, 21920-21926.

Kotani, K., Yonezawa, K., Hara, K., Ueda, H., Kitamura, Y., Sakaue, H., Ando, A., Chavanieu, A., Calas, B., Grigorescu, F.*, et al.* (1994). Involvement of phosphoinositide 3-kinase in insulin- or IGF-1-induced membrane ruffling. EMBO J *13*, 2313-2321.

Kreisberg, J.I., Malik, S.N., Prihoda, T.J., Bedolla, R.G., Troyer, D.A., Kreisberg, S., and Ghosh, P.M. (2004). Phosphorylation of Akt (Ser473) is an excellent predictor of poor clinical outcome in prostate cancer. Cancer Res *64*, 5232-5236.

Kuroda, S., Fukata, M., Nakagawa, M., Fujii, K., Nakamura, T., Ookubo, T., Izawa, I., Nagase, T., Nomura, N., Tani, H.*, et al.* (1998). Role of IQGAP1, a target of the small GTPases Cdc42 and Rac1, in regulation of E-cadherin-mediated cell-cell adhesion. Science *281*, 832-835.

Kurzen, H., Moll, I., Moll, R., Schafer, S., Simics, E., Amagai, M., Wheelock, M.J., and Franke, W.W. (1998). Compositionally different desmosomes in the various compartments of the human hair follicle. Differentiation *63*, 295-304.

Kurzen, H., Munzing, I., and Hartschuh, W. (2003). Expression of desmosomal proteins in squamous cell carcinomas of the skin. J Cutan Pathol *30*, 621-630.

Lacombe, L., Orlow, I., Reuter, V.E., Fair, W.R., Dalbagni, G., Zhang, Z.F., and Cordon-Cardo, C. (1996). Microsatellite instability and deletion analysis of chromosome 10 in human prostate cancer. Int J Cancer *69*, 110-113.

Larue, L., Ohsugi, M., Hirchenhain, J., and Kemler, R. (1994). E-cadherin null mutant embryos fail to form a trophectoderm epithelium. Proc Natl Acad Sci U S A *91*, 8263-8267.

Latil, A., Cussenot, O., Fournier, G., Driouch, K., and Lidereau, R. (1997). Loss of heterozygosity at chromosome 16q in prostate adenocarcinoma: identification of three independent regions. Cancer Res *57*, 1058-1062.

Lewis, J.E., Wahl, J.K., 3rd, Sass, K.M., Jensen, P.J., Johnson, K.R., and Wheelock, M.J. (1997). Cross-talk between adherens junctions and desmosomes depends on plakoglobin. J Cell Biol *136*, 919-934.

Li, R., Dai, H., Wheeler, T.M., Sayeeduddin, M., Scardino, P.T., Frolov, A., and Ayala, G.E. (2009). Prognostic value of Akt-1 in human prostate cancer: a computerized quantitative assessment with quantum dot technology. Clin Cancer Res *15*, 3568-3573.

Li, X., Deng, W., Nail, C.D., Bailey, S.K., Kraus, M.H., Ruppert, J.M., and Lobo-Ruppert, S.M. (2006). Snail induction is an early response to Gli1 that determines the efficiency of epithelial transformation. Oncogene *25*, 609-621.

Li, J., Yen, C., Liaw, D., Podsypanina, K., Bose, S., Wang, S.I., Puc, J., Miliaresis, C., Rodgers, L., McCombie, R.*, et al.* (1997). PTEN, a putative protein tyrosine phosphatase gene mutated in human brain, breast, and prostate cancer. Science *275*, 1943-1947.

Liao, Y., Grobholz, R., Abel, U., Trojan, L., Michel, M.S., Angel, P., and Mayer, D. (2003). Increase of AKT/PKB expression correlates with gleason pattern in human prostate cancer. Int J Cancer *107*, 676-680.

Logothetis, C.J., and Lin, S.H. (2005). Osteoblasts in prostate cancer metastasis to bone. Nat Rev Cancer *5*, 21-28.

Machado, J.C., Oliveira, C., Carvalho, R., Soares, P., Berx, G., Caldas, C., Seruca, R., Carneiro, F., and Sobrinho-Simoes, M. (2001). E-cadherin gene (CDH1) promoter methylation as the second hit in sporadic diffuse gastric carcinoma. Oncogene *20*, 1525-1528.

Maehama, T., and Dixon, J.E. (1998). The tumor suppressor, PTEN/MMAC1, dephosphorylates the lipid second messenger, phosphatidylinositol 3,4,5-trisphosphate. J Biol Chem *273*, 13375-13378.

Majumder, P.K., Yeh, J.J., George, D.J., Febbo, P.G., Kum, J., Xue, Q., Bikoff, R., Ma, H., Kantoff, P.W., Golub, T.R.*, et al.* (2003). Prostate intraepithelial neoplasia induced by prostate restricted Akt activation: the MPAKT model. Proc Natl Acad Sci U S A *100*, 7841-7846.

Malanga, D., Scrima, M., De Marco, C., Fabiani, F., De Rosa, N., De Gisi, S., Malara, N., Savino, R., Rocco, G., Chiappetta, G.*, et al.* (2008). Activating E17K mutation in the gene encoding the protein kinase AKT1 in a subset of squamous cell carcinoma of the lung. Cell Cycle *7*, 665-669.

Malik, S.N., Brattain, M., Ghosh, P.M., Troyer, D.A., Prihoda, T., Bedolla, R., and Kreisberg, J.I. (2002). Immunohistochemical demonstration of phospho-Akt in high Gleason grade prostate cancer. Clin Cancer Res *8*, 1168-1171.

Martin, T.A., Goyal, A., Watkins, G., and Jiang, W.G. (2005). Expression of the transcription factors snail, slug, and twist and their clinical significance in human breast cancer. Ann Surg Oncol *12*, 488-496.

Meng, W., and Takeichi, M. (2009). Adherens junction: molecular architecture and regulation. Cold Spring Harb Perspect Biol *1*, a002899.

Michiels, F., Habets, G.G., Stam, J.C., van der Kammen, R.A., and Collard, J.G. (1995). A role for Rac in Tiam1-induced membrane ruffling and invasion. Nature *375*, 338-340.

Mitchell, S., Abel, P., Ware, M., Stamp, G., and Lalani, E. (2000). Phenotypic and genotypic characterization of commonly used human prostatic cell lines. BJU Int *85*, 932-944.

Moody, S.E., Perez, D., Pan, T.C., Sarkisian, C.J., Portocarrero, C.P., Sterner, C.J., Notorfrancesco, K.L., Cardiff, R.D., and Chodosh, L.A. (2005). The transcriptional repressor Snail promotes mammary tumor recurrence. Cancer Cell *8*, 197-209.

Morali, O.G., Delmas, V., Moore, R., Jeanney, C., Thiery, J.P., and Larue, L. (2001). IGF-II induces rapid beta-catenin relocation to the nucleus during epithelium to mesenchyme transition. Oncogene *20*, 4942-4950.

Nagafuchi, A., Shirayoshi, Y., Okazaki, K., Yasuda, K., and Takeichi, M. (1987). Transformation of cell adhesion properties by exogenously introduced E-cadherin cDNA. Nature *329*, 341-343.

Nakagawa, M., Fukata, M., Yamaga, M., Itoh, N., and Kaibuchi, K. (2001). Recruitment and activation of Rac1 by the formation of E-cadherin-mediated cell-cell adhesion sites. J Cell Sci *114*, 1829-1838.

Nguyen, D.X., Bos, P.D., and Massague, J. (2009). Metastasis: from dissemination to organ-specific colonization. Nat Rev Cancer *9*, 274-284.

Niemann, C., and Watt, F.M. (2002). Designer skin: lineage commitment in postnatal epidermis. Trends Cell Biol *12*, 185-192.

Nieto, M.A. (2002). The snail superfamily of zinc-finger transcription factors. Nat Rev Mol Cell Biol *3*, 155-166.

Nose, A., Nagafuchi, A., and Takeichi, M. (1987). Isolation of placental cadherin cDNA: identification of a novel gene family of cell-cell adhesion molecules. EMBO J *6*, 3655-3661.

Ohsugi, M., Hwang, S.Y., Butz, S., Knowles, B.B., Solter, D., and Kemler, R. (1996). Expression and cell membrane localization of catenins during mouse preimplantation development. Dev Dyn *206*, 391-402.

Ohsugi, M., Larue, L., Schwarz, H., and Kemler, R. (1997). Cell-junctional and cytoskeletal organization in mouse blastocysts lacking E-cadherin. Dev Biol *185*, 261-271.

Oshiro, M.M., Kim, C.J., Wozniak, R.J., Junk, D.J., Munoz-Rodriguez, J.L., Burr, J.A., Fitzgerald, M., Pawar, S.C., Cress, A.E., Domann, F.E.*, et al.* (2005). Epigenetic silencing of DSC3 is a common event in human breast cancer. Breast Cancer Res *7*, R669-680.

Pece, S., Chiariello, M., Murga, C., and Gutkind, J.S. (1999). Activation of the protein kinase Akt/PKB by the formation of E-cadherin-mediated cell-cell junctions. Evidence for the association of phosphatidylinositol 3-kinase with the E-cadherin adhesion complex. J Biol Chem *274*, 19347-19351.

Pena, C., Garcia, J.M., Silva, J., Garcia, V., Rodriguez, R., Alonso, I., Millan, I., Salas, C., de Herreros, A.G., Munoz, A.*, et al.* (2005). E-cadherin and vitamin D receptor regulation by SNAIL and ZEB1 in colon cancer: clinicopathological correlations. Hum Mol Genet *14*, 3361-3370.

Perez, T.D., Tamada, M., Sheetz, M.P., and Nelson, W.J. (2008). Immediate-early signaling induced by E-cadherin engagement and adhesion. J Biol Chem *283*, 5014-5022.

Perez-Moreno, M., and Fuchs, E. (2006). Catenins: keeping cells from getting their signals crossed. Dev Cell *11*, 601-612.

Perl, A.K., Wilgenbus, P., Dahl, U., Semb, H., and Christofori, G. (1998). A causal role for E-cadherin in the transition from adenoma to carcinoma. Nature *392*, 190-193.

Pilichou, K., Nava, A., Basso, C., Beffagna, G., Bauce, B., Lorenzon, A., Frigo, G., Vettori, A., Valente, M., Towbin, J.*, et al.* (2006). Mutations in desmoglein-2 gene are associated with arrhythmogenic right ventricular cardiomyopathy. Circulation *113*, 1171-1179.

Pollard, T.D., and Borisy, G.G. (2003). Cellular motility driven by assembly and disassembly of actin filaments. Cell *112*, 453-465.

Potempa, S., and Ridley, A.J. (1998). Activation of both MAP kinase and phosphatidylinositide 3-kinase by Ras is required for hepatocyte growth factor/scatter factor-induced adherens junction disassembly. Mol Biol Cell *9*, 2185-2200.

Quinn, D.I., Henshall, S.M., Haynes, A.M., Brenner, P.C., Kooner, R., Golovsky, D., Mathews, J., O'Neill, G.F., Turner, J.J., Delprado, W.*, et al.* (2001). Prognostic significance of pathologic features in localized prostate cancer treated with radical prostatectomy: implications for staging systems and predictive models. J Clin Oncol *19*, 3692-3705.

Ramani, V.C., Hennings, L., and Haun, R.S. (2008). Desmoglein 2 is a substrate of kallikrein 7 in pancreatic cancer. BMC Cancer *8*, 373.

Rameh, L.E., Arvidsson, A., Carraway, K.L., 3rd, Couvillon, A.D., Rathbun, G., Crompton, A., VanRenterghem, B., Czech, M.P., Ravichandran, K.S., Burakoff, S.J.*, et al.* (1997). A comparative analysis of the phosphoinositide binding specificity of pleckstrin homology domains. J Biol Chem *272*, 22059-22066.

Reifenberger, J., Wolter, M., Bostrom, J., Buschges, R., Schulte, K.W., Megahed, M., Ruzicka, T., and Reifenberger, G. (2000). Allelic losses on chromosome arm 10q and mutation of the PTEN (MMAC1) tumour suppressor gene in primary and metastatic malignant melanomas. Virchows Arch *436*, 487-493.

Rickman, L., Simrak, D., Stevens, H.P., Hunt, D.M., King, I.A., Bryant, S.P., Eady, R.A., Leigh, I.M., Arnemann, J., Magee, A.I.*, et al.* (1999). N-terminal deletion in a desmosomal cadherin causes the autosomal dominant skin disease striate palmoplantar keratoderma. Hum Mol Genet *8*, 971-976.

Ringel, M.D., Hayre, N., Saito, J., Saunier, B., Schuppert, F., Burch, H., Bernet, V., Burman, K.D., Kohn, L.D., and Saji, M. (2001). Overexpression and overactivation of Akt in thyroid carcinoma. Cancer Res *61*, 6105-6111.

Rodriguez-Viciana, P., Warne, P.H., Dhand, R., Vanhaesebroeck, B., Gout, I., Fry, M.J., Waterfield, M.D., and Downward, J. (1994). Phosphatidylinositol-3-OH kinase as a direct target of Ras. Nature *370*, 527-532.

Rohatgi, R., Ho, H.Y., and Kirschner, M.W. (2000). Mechanism of N-WASP activation by CDC42 and phosphatidylinositol 4, 5-bisphosphate. J Cell Biol *150*, 1299-1310.

Rohatgi, R., Ma, L., Miki, H., Lopez, M., Kirchhausen, T., Takenawa, T., and Kirschner, M.W. (1999). The interaction between N-WASP and the Arp2/3 complex links Cdc42-dependent signals to actin assembly. Cell *97*, 221-231.

Rubin, M.A., Mucci, N.R., Figurski, J., Fecko, A., Pienta, K.J., and Day, M.L. (2001). E-cadherin expression in prostate cancer: a broad survey using high-density tissue microarray technology. Hum Pathol *32*, 690-697.

Saegusa, M., Hashimura, M., Kuwata, T., and Okayasu, I. (2009). Requirement of the Akt/(beta)-Catenin Pathway for Uterine Carcinosarcoma Genesis, Modulating E-Cadherin Expression Through the Transactivation of Slug. Am J Pathol *174*, 2107-2115.

Sahlgren, C., Gustafsson, M., Jin, S., Poellinger, L., Lendahl, U. (2008). Notch signaling mediates hypoxia-induced tumor cell migration and invasion. Proc Natl Acad Sci *105*, 6392-6397.

Sarbassov, D.D., Guertin, D.A., Ali, S.M., and Sabatini, D.M. (2005). Phosphorylation and regulation of Akt/PKB by the rictor-mTOR complex. Science *307*, 1098-1101.

Savagner, P., Yamada, K.M., and Thiery, J.P. (1997). The zinc-finger protein slug causes desmosome dissociation, an initial and necessary step for growth factor-induced epithelial-mesenchymal transition. J Cell Biol *137*, 1403-1419.

Schaffer, J.V., Bazzi, H., Vitebsky, A., Witkiewicz, A., Kovich, O.I., Kamino, H., Shapiro, L.S., Amin, S.P., Orlow, S.J., and Christiano, A.M. (2006). Mutations in the desmoglein 4 gene underlie localized autosomal recessive hypotrichosis with monilethrix hairs and congenital scalp erosions. J Invest Dermatol *126*, 1286-1291.

Schafer, S., Stumpp, S., and Franke, W.W. (1996). Immunological identification and characterization of the desmosomal cadherin Dsg2 in coupled and uncoupled epithelial cells and in human tissues. Differentiation *60*, 99-108.

Scheid, M.P., and Woodgett, J.R. (2001). PKB/AKT: functional insights from genetic models. Nat Rev Mol Cell Biol *2*, 760-768.

Schweizer, J. (2006). More than one gene involved in monilethrix: intracellular but also extracellular players. J Invest Dermatol *126*, 1216-1219.

Segrelles, C., Moral, M., Lorz, C., Santos, M., Lu, J., Cascallana, J.L., Lara, M.F., Carbajal, S., Martinez-Cruz, A.B., Garcia-Escudero, R.*, et al.* (2008).

Constitutively active Akt induces ectodermal defects and impaired bone morphogenetic protein signaling. Mol Biol Cell *19*, 137-149.

Shen, M.M., and Abate-Shen, C. (2010). Molecular genetics of prostate cancer: new prospects for old challenges. Genes Dev *24*, 1967-2000.

Shih, J.Y., Tsai, M.F., Chang, T.H., Chang, Y.L., Yuan, A., Yu, C.J., Lin, S.B., Liou, G.Y., Lee, M.L., Chen, J.J.*, et al.* (2005). Transcription repressor slug promotes carcinoma invasion and predicts outcome of patients with lung adenocarcinoma. Clin Cancer Res *11*, 8070-8078.

Shimomura, Y., Sakamoto, F., Kariya, N., Matsunaga, K., and Ito, M. (2006). Mutations in the desmoglein 4 gene are associated with monilethrix-like congenital hypotrichosis. J Invest Dermatol *126*, 1281-1285.

Shioiri, M., Shida, T., Koda, K., Oda, K., Seike, K., Nishimura, M., Takano, S., and Miyazaki, M. (2006). Slug expression is an independent prognostic parameter for poor survival in colorectal carcinoma patients. Br J Cancer *94*, 1816-1822.

Simpson, M.A., Mansour, S., Ahnood, D., Kalidas, K., Patton, M.A., McKenna, W.J., Behr, E.R., and Crosby, A.H. (2009). Homozygous mutation of desmocollin-2 in arrhythmogenic right ventricular cardiomyopathy with mild palmoplantar keratoderma and woolly hair. Cardiology *113*, 28-34.

Society, A.C. (2009). Cancer Facts and Figures 2009. (Atlanta, American Cancer Society).

Songyang, Z., Fanning, A.S., Fu, C., Xu, J., Marfatia, S.M., Chishti, A.H., Crompton, A., Chan, A.C., Anderson, J.M., and Cantley, L.C. (1997). Recognition of unique carboxyl-terminal motifs by distinct PDZ domains. Science *275*, 73-77.

Staal, S.P. (1987). Molecular cloning of the akt oncogene and its human homologues AKT1 and AKT2: amplification of AKT1 in a primary human gastric adenocarcinoma. Proc Natl Acad Sci U S A *84*, 5034-5037.

Stepniak, E., Radice, G.L., and Vasioukhin, V. (2009). Adhesive and signaling functions of cadherins and catenins in vertebrate development. Cold Spring Harb Perspect Biol *1*, a002949.

Stone, K.R., Mickey, D.D., Wunderli, H., Mickey, G.H., and Paulson, D.F. (1978). Isolation of a human prostate carcinoma cell line (DU 145). Int J Cancer *21*, 274-281.

Strathdee, G. (2002). Epigenetic versus genetic alterations in the inactivation of E-cadherin. Semin Cancer Biol *12*, 373-379.

Sun, M., Wang, G., Paciga, J.E., Feldman, R.I., Yuan, Z.Q., Ma, X.L., Shelley, S.A., Jove, R., Tsichlis, P.N., Nicosia, S.V.*, et al.* (2001). AKT1/PKBalpha kinase is frequently elevated in human cancers and its constitutive activation is required for oncogenic transformation in NIH3T3 cells. Am J Pathol *159*, 431-437.

Sundfeldt, K., Piontkewitz, Y., Ivarsson, K., Nilsson, O., Hellberg, P., Brannstrom, M., Janson, P.O., Enerback, S., and Hedin, L. (1997). E-cadherin expression in human epithelial ovarian cancer and normal ovary. Int J Cancer *74*, 275-280.

Syed, S.E., Trinnaman, B., Martin, S., Major, S., Hutchinson, J., and Magee, A.I. (2002). Molecular interactions between desmosomal cadherins. Biochem J *362*, 317-327.

Syrris, P., Ward, D., Asimaki, A., Evans, A., Sen-Chowdhry, S., Hughes, S.E., and McKenna, W.J. (2007). Desmoglein-2 mutations in arrhythmogenic right ventricular cardiomyopathy: a genotype-phenotype characterization of familial disease. Eur Heart J *28*, 581-588.

Taddei, I., Piazzini, M., Bartoletti, R., Dal Canto, M., and Sardi, I. (2000). Molecular alterations of E-cadherin gene: possible role in human bladder carcinogenesis. Int J Mol Med *6*, 201-208.

Takaishi, K., Sasaki, T., Kotani, H., Nishioka, H., and Takai, Y. (1997). Regulation of cell-cell adhesion by rac and rho small G proteins in MDCK cells. J Cell Biol *139*, 1047-1059.

Takebayashi, S., Ogawa, T., Jung, K.Y., Muallem, A., Mineta, H., Fisher, S.G., Grenman, R., and Carey, T.E. (2000). Identification of new minimally lost regions on 18q in head and neck squamous cell carcinoma. Cancer Res *60*, 3397-3403.

Tam, P.P., and Beddington, R.S. (1987). The formation of mesodermal tissues in the mouse embryo during gastrulation and early organogenesis. Development *99*, 109-126.

Tam, P.P.L., and Behringer, R.R. (1997). Mouse gastrulation: the formation of a mammalian body plan. Mechanisms of Development *68*, 3-25.

Taylor, B.S., Schultz, N., Hieronymus, H., Gopalan, A., Xiao, Y., Carver, B.S., Arora, V.K., Kaushik, P., Cerami, E., Reva, B., Antipin, Y., Mitsiades, N., Landers, T., Dolgalev, I., Major, J.E., Wilson, M., Socci, N.D., Lash, A.E., Heguy, A., Eastham, J.A., Scher, H.I., Reuter, V.E., Scardino, P.T., Sander, C., Sawyers, C.L., Gerald, W.L. (2010) Integrative genomic profiling of human prostate cancer. Cell *18*, 1-12.

Thiery, J.P. (2002). Epithelial-mesenchymal transitions in tumour progression. Nat Rev Cancer *2*, 442-454.

Thuault, S., Valcourt, U., Petersen, M., Manfioletti, G., Heldin, C.H., and Moustakas, A. (2006). Transforming growth factor-beta employs HMGA2 to elicit epithelial-mesenchymal transition. J Cell Biol *174*, 175-183.

Tinkle, C.L., Lechler, T., Pasolli, H.A., and Fuchs, E. (2004). Conditional targeting of E-cadherin in skin: insights into hyperproliferative and degenerative responses. Proc Natl Acad Sci U S A *101*, 552-557.

Tinkle, C.L., Pasolli, H.A., Stokes, N., and Fuchs, E. (2008). New insights into cadherin function in epidermal sheet formation and maintenance of tissue integrity. Proc Natl Acad Sci U S A *105*, 15405-15410.

Tselepis, C., Chidgey, M., North, A., and Garrod, D. (1998). Desmosomal adhesion inhibits invasive behavior. Proc Natl Acad Sci U S A *95*, 8064-8069.

Uchikado, Y., Natsugoe, S., Okumura, H., Setoyama, T., Matsumoto, M., Ishigami, S., and Aikou, T. (2005). Slug Expression in the E-cadherin preserved tumors is related to prognosis in patients with esophageal squamous cell carcinoma. Clin Cancer Res *11*, 1174-1180.

Umbas, R., Schalken, J.A., Aalders, T.W., Carter, B.S., Karthaus, H.F., Schaafsma, H.E., Debruyne, F.M., and Isaacs, W.B. (1992). Expression of the cellular adhesion molecule E-cadherin is reduced or absent in high-grade prostate cancer. Cancer Res *52*, 5104-5109.

Vallin, J., Thuret, R., Giacomello, E., Faraldo, M.M., Thiery, J.P., and Broders, F. (2001). Cloning and characterization of three Xenopus slug promoters reveal direct regulation by Lef/beta-catenin signaling. J Biol Chem *276*, 30350-30358.

Vanhaesebroeck, B., Guillermet-Guibert, J., Graupera, M., and Bilanges, B. (2010). The emerging mechanisms of isoform-specific PI3K signalling. Nat Rev Mol Cell Biol *11*, 329-341.

Vasioukhin, V., Bauer, C., Yin, M., and Fuchs, E. (2000). Directed actin polymerization is the driving force for epithelial cell-cell adhesion. Cell *100*, 209-219.

Vichalkovski, A., Gresko, E., Hess, D., Restuccia, D.F., and Hemmings, B.A. (2010). PKB/AKT phosphorylation of the transcription factor Twist-1 at Ser42 inhibits p53 activity in response to DNA damage. Oncogene *29*, 3554-3565.

Vleminckx, K., Vakaet, L., Jr., Mareel, M., Fiers, W., and van Roy, F. (1991). Genetic manipulation of E-cadherin expression by epithelial tumor cells reveals an invasion suppressor role. Cell *66*, 107-119.

Wahl, J.K., 3rd (2002). Generation of monoclonal antibodies specific for desmoglein family members. Hybrid Hybridomics *21*, 37-44.

Wahl, J.K., 3rd (2005). A role for plakophilin-1 in the initiation of desmosome assembly. J Cell Biochem *96*, 390-403.

Watabe-Uchida, M., Uchida, N., Imamura, Y., Nagafuchi, A., Fujimoto, K., Uemura, T., Vermeulen, S., van Roy, F., Adamson, E.D., and Takeichi, M. (1998). alpha-Catenin-vinculin interaction functions to organize the apical junctional complex in epithelial cells. J Cell Biol *142*, 847-857.

Watanabe, T., Sato, K., and Kaibuchi, K. (2009). Cadherin-mediated intercellular adhesion and signaling cascades involving small GTPases. Cold Spring Harb Perspect Biol *1*, a003020.

Whittock, N.V., and Bower, C. (2003). Genetic evidence for a novel human desmosomal cadherin, desmoglein 4. J Invest Dermatol *120*, 523-530.

Wilcox, G., Soh, S., Chakraborty, S., Scardino, P.T., and Wheeler, T.M. (1998). Patterns of high-grade prostatic intraepithelial neoplasia associated with clinically aggressive prostate cancer. Hum Pathol *29*, 1119-1123.

Yang, J., Mani, S.A., Donaher, J.L., Ramaswamy, S., Itzykson, R.A., Come, C., Savagner, P., Gitelman, I., Richardson, A., and Weinberg, R.A. (2004). Twist, a master regulator of morphogenesis, plays an essential role in tumor metastasis. Cell *117*, 927-939.

Yang, J., and Weinberg, R.A. (2008). Epithelial-mesenchymal transition: at the crossroads of development and tumor metastasis. Dev Cell *14*, 818-829.

Yashiro, M., Nishioka, N., and Hirakawa, K. (2006). Decreased expression of the adhesion molecule desmoglein-2 is associated with diffuse-type gastric carcinoma. Eur J Cancer *42*, 2397-2403.

Yin, T., and Green, K.J. (2004). Regulation of desmosome assembly and adhesion. Semin Cell Dev Biol *15*, 665-677.

Yonemura, S., Itoh, M., Nagafuchi, A., and Tsukita, S. (1995). Cell-to-cell adherens junction formation and actin filament organization: similarities and differences between non-polarized fibroblasts and polarized epithelial cells. J Cell Sci *108 (Pt 1)*, 127-142.

Yoshiura, K., Kanai, Y., Ochiai, A., Shimoyama, Y., Sugimura, T., and Hirohashi, S. (1995). Silencing of the E-cadherin invasion-suppressor gene by CpG methylation in human carcinomas. Proc Natl Acad Sci U S A *92*, 7416-7419.

Zavadil, J., and Bottinger, E.P. (2005). TGF-beta and epithelial-to-mesenchymal transitions. Oncogene *24*, 5764-5774.

Zavadil, J., Cermak, L., Soto-Nieves, N., and Bottinger, E.P. (2004). Integration of TGF-beta/Smad and Jagged1/Notch signalling in epithelial-to-mesenchymal transition. EMBO J *23*, 1155-1165.

Zhou, B.P., Deng, J., Xia, W., Xu, J., Li, Y.M., Gunduz, M., and Hung, M.C. (2004). Dual regulation of Snail by GSK-3beta-mediated phosphorylation in control of epithelial-mesenchymal transition. Nat Cell Biol *6*, 931-940.

Zlotogorski, A., Marek, D., Horev, L., Abu, A., Ben-Amitai, D., Gerad, L., Ingber, A., Frydman, M., Reznik-Wolf, H., Vardy, D.A.*, et al.* (2006). An autosomal recessive form of monilethrix is caused by mutations in DSG4: clinical overlap with localized autosomal recessive hypotrichosis. J Invest Dermatol *126*, 1292-1296.